Study of the molecular mechanisms of boron toxicity in plants
-Characterization of *Arabidopsis thaliana* mutants hypersensitive to excess boron-

（植物におけるホウ素毒性の分子機構の研究

-ホウ素過剰超感受性シロイヌナズナ変異株の解析-）

Takuya Sakamoto

坂本　卓也

Ph.D thesis

The University of Tokyo

CONTENTS

List of figures and tables 4
List of abbreviation in the present thesis 6
Declaration 7
List of primers used in the present thesis 8
List of plasmids used in the present thesis 12
ABSTRACT 13
INTRODUCTION 18

Chapter 1 Condensin II alleviates DNA damage and is essential for excess boron tolerance in *Arabidopsis thaliana* 21
1.1 Abstract 21
1.2 Introduction 21
1.3 Materials and Methods 22
1.3.1 Plant materials and growth conditions 22
1.3.2 Positional mapping of the *HEB* genes 23
1.3.3 Determination of B contents 23
1.3.4 Observation of root morphology 23
1.3.5 Gene expression analyses 23
1.3.6 Sensitivity to genotoxic and oxidative stresses 24
1.3.7 Comet assay 24
1.3.8 Cell ploidy analysis 24
1.3.9 GUS activity assay 25
1.3.10 *CAP-G2* and *CAP-H2* cloning for complementation analysis 25
1.4 Results 26
1.4.1 The *heb* mutants are hypersensitive to excess B but not to other mineral stresses 26
1.4.2 *HEB1* and *HEB2* encode different subunits of a chromosomal protein complex, condensin II 27
1.4.3 Roots of the *heb* mutants showed severe defects in meristematic organization and morphology under the excess B condition 28
1.4.4 The *heb* mutants are sensitive to induction of DSBs 29
1.4.5 Excess B induces DSBs in root tip cells 30
1.4.6 *atr* mutant but not *atm* mutant was sensitive to excess B 30

1.4.7 Simultaneous induction of DSBs and replication blocks mimicked the effect of excess B on root growth in the *heb* mutants 31
1.4.8 B toxicity affects cell cycle progression in roots 32
1.4.9 Effect of excess B and condensin II on expression of cell cycle-related genes 33
1.4.10 Expression of condensins responds to B toxicity 33
1.4.11 Condensin II is required for alleviation of DNA damage caused by UV-C in shoots 34
1.5 Discussion 34
1.5.1 *A. thaliana* has a mechanism to tolerate excess B concentration in cells 35
1.5.2 DNA damages are major causes of B toxicity in roots of *A. thaliana* 35
1.5.3 B toxicity-induced DNA damage has a special character 36
1.5.4 Excess B affects cell cycle progression 37
1.5.5 *A. thaliana* condensin II has a role in reducing DNA damage 38
1.5.6 Requirement of *A. thaliana* condensin II in progression of G2 phase 39

Chapter 2 Involvement of 26S proteasome in excess B tolerance in *Arabidopsis thaliana*-Identification of possible targets involved in excess B tolerance- 54
2.1 Abstract 54
2.2 Introduction 54
2.3 Materials and methods 56
2.3.1 Plant materials and growth conditions 56
2.3.2 Positional mapping of the *HEB* genes 56
2.3.3 Observation of root morphology 57
2.3.4 Sensitivity to L-canavanin 57
2.3.5 Accumulation of poly-ubiquitinated proteins 57
2.3.6 Proteome analysis of poly-ubiquitinated proteins 57
2.3.7 Screening for revartants of *rpt5a-6* under the excess B condition 58
2.4 Results 58
2.4.1 *HEB3*, *HEB6* and *HEB7* encode subunits of 26S proteasome 58
2.4.2 RPN8a and RPT5a mutants show short-root phenotype under moderate levels of excess B and are not hypersensitive to other mineral stresses. 59
2.4.3 Root morphology of *rpn8a* and *rpt5a* mutants were severely altered by excess B treatment 60
2.4.4 Four 19S regulatory particle subunits are identified to be essential for excess B tolerance 61

2.4.5 *rpt5a* mutants are reduced in ubiquitin-dependent proteolytic activity in roots 61
2.4.6 Screening of subunits specific substrates of 26SP in response to excess B 62
2.4.7 Screening and isolation of revartants of *rpt5a-6* under the excess B condition 63
2.5 Discussion 63

Chapter 3 *Arabidopsis thaliana* 26S proteasome subunits RPT2a and RPT5a are crucial for Zinc deficiency-tolerance 76
3.1 Abstract 76
3.2 Introduction 76
3.3 Materials and Methods 77
3.3.1 Plant materials and growth conditions 77
3.3.2 Measurement of metal contents in plant tissues 77
3.3.3 Gene expression analyses 78
3.3.4 Evaluation of levels of oxidative effects in plant tissue 78
3.3.5 Analysis of proteasome activity 78
3.4 Results 79
3.4.1 Sensitivity of 26S proteasome mutants, *rpt2a-2* and *rpt5a-4*, to Zn deficiency 79
3.4.2 Response of *RPT2a* and *RPT5a* genes to Zn deficiency 79
3.4.3 Measurement of metal concentrations in *rpt2a-2* and *rpt5a-4* under the Zn-deficient condition 80
3.4.4 Expression patterns of Zn deficiency-responsive genes in *rpt2a-2* and *rpt5a-4* under the Zn-deficient condition 80
3.4.5 Evaluation of oxidative stress in *rpt2a-2* and *rpt5a-4a* under the Zn-deficient condition 81
3.4.6 Evaluation of 26S proteasome activities in *rpt2a-2* and *rpt5a-4* under the Zn-deficient condition 81
3.5 Discussion 82

CONCLUSION 90
REFERENCES 91
ACKNOWLEDGMENTS 105

List of figures and tables

Figure 1-1 Hyper sensitivity and specificity of *heb1-1* and *heb2-1* to excess B 41
Figure 1-2 Sensitivity of Col-0, *heb1-1* and *heb2-1* to oxidative stress 42
Figure 1-3 Mapping of *heb1* and *heb2* mutations 43
Figure 1-4 Molecular characterization of *HEB1* and *HEB2* 44
Figure 1-5 Complementation analysis of *heb1-1* and *heb2-1* 45
Figure 1-6 Effects of excess B on root morphology of condensin II mutants 46
Figure 1-7 Effects of excess B on length of meristematic zone 47
Figure 1-8 Sensitivity of the *heb* mutants to induction of DSBs in root growth 48
Figure 1-9 Elevated DSBs in the *heb* mutants and induction of DSBs by excess B in roots 49
Figure 1-10 Comparison of sensitivity of the *heb* mutants to combined DNA stress with that to excess B in root growth 50
Figure 1-11 Effects of excess B on mitotic activities in the roots of condensin II mutants 51
Figure 1-12 Responsiveness of condensin genes to excess B 52
Figure 1-13 DNA damage by UV-C in the shoots of condensin II mutants 53

Figure 2-1 Characterization of *HEB3*, *HEB6* and *HEB7* 67
Figure 2-2 Hypersensitivity and specificity of *rpn8a* and *rpt5a* mutants to excess B 68
Figure 2-3 Effect of excess B on root morphology of *rpn8a* and *rpt5a* mutants 69
Figure 2-4 Elucidation of the involvements of other subunits of 19S regulatory particle in excess B-tolerance 70
Figure 2-5 Elucidation of activity of poly-ubiquitin dependent proteolysis in *rpt5a* mutants 71
Figure 2-6 Purification and enrichment of poly-ubiquitinated proteins 72
Figure 2-7 Candidates of revertant of *rpt5a-6* showing moderate root growth under the excess B condition 73
Table 2-1 List of 19S prteasome subunits and mutatns used in the present thesis .. 74
Table 2-2 List of poly-ubiquitinated proteins identified and quantified 75

Figure 3-1 Characterization of *rpt2a-2* and *rpt5a-4* mutants and their sensitivity to Zn deficiency 85
Figure 3-2 Metal concentrations in *rpt2a-2* and *rpt5a-4* under the Zn-deficient condition 86

Figure 3-3 Response of Zn transporters and SOD-related genes in r*pt2a-2* and *rpt5a-4* under the Zn-deficient condition..... 87
Figure 3-4 Oxidative stress levels in *rpt2a-2* and *rpt5a-4* under the Zn-deficient condition.. 88
Figure 3-5 20S proteasome activities and protein ubiqutination in r*pt2a-2* and *rpt5a-4* under the Zn-deficient condition 89

Appendix Figure 1-1 The expression of genes of condensin complex during the mitotic cell cycle..... 102
Appendix Figure 1-2 Relationship between DSBs level and root elongation property in *A. thaliana* 103
Appendix Figure 3-1 A T-DNA inserted mutant of *RPT2b* and *RPT5b* 104

List of abbreviation in the present thesis

20S	20S proteasome
26SP	26S proteasome
cDNA	complementary DNA
CAP	chromosomal associated protein
DSB	DNA double strand break
EMS	ethyl methanesulfonate
GFP	green florescent protein
GUS	β-glucuronidase
HEB	hypersensitive to excess boron
ICP-MS	inductive coupled plasma-mass spectrometry
iTRAQ	isobaric tag for relative and absolute quantification
LB	left border
LC−MS/MS	liquid chromatography-mass spectrometry/ mass spectrometry
PCR	polymerase chain reaction
RAM	root apical meristem
ROS	reactive oxygen species
RP	19S regulatory particle
RPN	regulatory particle non-ATPase
RPT	regulatory particle triple-A-ATPase
RT	reverse transcription
T-DNA	transferred DNA
Ub	ubiquitin

Declaration

I declare that the experiments included in the present thesis were performed by Takuya Sakamoto, the author of the present thesis, unless otherwise stated.

Table I Primers used in the present thesis

Experiment	Gene		Primer sequence (5' to 3')	Product size	Reference
T-DNA insertion	SALK (pROK2) LB	LBb1 (provided)	GATGGCCCACTACGTGAACCAT		
	SAIL collection LB	LB (provided)	TTCATAACCAATCTCGATACAC		
(Chapter 1)	SALK_049790 (*heb1-2)*	genomic forward	GGTTGCAAATTCAAATGTTCG	1164	
		genomic reverse	TTCCAATGAGGTCACAAAAGG		
	SALK_059304 (*heb2-2*)	genomic forward	TTTCCGCTCTCTTCAACAGTC	985	
		genomic reverse	AAAAAGATTGGATGGAGCATTAC		
	SALK_032841 (*atr-2*)	genomic forward	GCTACGGAGAAAAGTTGCGAAAG		
(Chapter 2 and 3)	SALK_088636 (*rpn2a-1*)	genomic forward	TTCTCATTCCTTTGTCAACCG	1041	
		genomic reverse	AGCATGCATAATGGCATTAGC		
	SALK_135609 (*rpn2a-2*)	genomic forward	AATCGTGTTTGTTTGTTCATACAC	1045	
		genomic reverse	AGCTCAAACAATCCAAATCCC		
	SALK_024347 (*rpn2b*)	genomic forward	TGAAGGTTGTCCAGGTTTCAG	1003	
		genomic reverse	ACAAATTTTCCGCATCATGAC		
	SALK_117415 (*rpn3b-1*)	genomic forward	CTGCAAAAACATTGAAAAGGG	1067	
		genomic reverse	AGACTCCGACACAACGTGATC		
	SALK_088176 (*rpn3b-2*)	genomic forward	ACGAAACAAAACAAAATCCCC	1083	
		genomic reverse	TCGGCACAAAAGAAGAGAGAC		
	SALK_134671 (*rpn5b-1*)	genomic forward	GGCTCCGGCTGATATACCTAC	1248	
		genomic reverse	ACCGGGTTCTCAAGCTCTTAG		
	SALK_133892 (*rpn5b-2*)	genomic forward	AAACCCAGAACAATGGATTCC	1000	
		genomic reverse	GCCTGAAAGATTCTTTCCACC		
	SALK_127791 (*rpn5b-3*)	genomic forward	CCCTTCTGTAAAGGAAAACCC	1015	
		genomic reverse	GCCTGAAAGATTCTTTCCACC		
	SALK_151595 (*rpn8a-3*)	genomic forward	TTGCTCAGGGATGTGAAAGAC	1094	
		genomic reverse	GGCCTAAGCCTAACGAACTTG		
	SALK_009871 (*rpn8b*)	genomic forward	AGAAGCTTTGCGACTTAAGGC	1043	
		genomic reverse	TTTATGTTCGCACAGGGTTTC		
	SALK_043310 (*rpn9b*)	genomic forward	TTGGATCTTCCAACTTTCGTG	1224	
		genomic reverse	TTCGATCTTGTATCGGTTTGG		
	SALK_009616 (*rpn10-2)*	genomic forward	GTTGCTAGATCAGGCAATTGC	1144	
		genomic reverse	AAAACTACAGCTCGCATGTGG		

Table I Primers used in the present thesis (continued)

Experiment	Gene		Primer sequence (5' to 3')	Product size	Reference
	SALK_005596 (*rpt2a-2*)	genomic forward	GGAATTGTTTTACCGGAGGAG	1172	
		genomic reverse	GCGAGAAATTTGTTCTCATGG		
	SALK_043450 (*rpt2b-1*)	genomic forward	ACCGCAAAGTAAAAATGATGG	1267	
		genomic reverse	TTCGGAACTGTTGGAGATGAG		
	SALK_046321 (*rpn5a-4)*	genomic forward	ATGATGCTGAGGAAGATGGTG	1117	
		genomic reverse	TTCATCGCTACTGAATCCGTC		
	SAIL_293_H08 (*rpt5b-3*)	genomic forward	AACCACACTTTGAAGGGGTTC	979	
		genomic reverse	TGAGATTGACGCAATAGGGAC		
Complementation	*HEB1* genomic	forward	**CACC**TCGTTCTCTTGCTCACCAGG	7300	
		reverse	TTCTTCTTCCTCATCCATCATGTG		
	HEB2 genomic	forward	**CACC**AGATCATTAAGCTTGAGGTC	6220	
		reverse	CAATTTCCCCAAAGATTTTTCGATTGAAGC		
GUS	*HEB2* promoter	forward	**CACC**AGATCATTAAGCTTGAGGTC	2991	
		reverse	TCTCGGTGAAGACTCACGGAATTTAAG		
RT-PCR (Condensins)	*HEB1* (At1g64960)	forward	TTTCGCTCGTTACAGGTTGC	125	
		reverse	TGTTTGTCAAGCAGAGTATC		
	HEB2 (At3g16730)	forward	AAGATGGGCAAATTCCTGTG	147	
		reverse	GACTGTTCCTGGTCTCTTTG		
	HEB2 for semi-qRT-PCR	forward	TCACACCTGGATGCTCTTCTCGC	669	Fujimoto et al (2006)
		reverse	CTACACAATCTAATTTGAGTAGTCACAAT		
	CAP-D3 (At4g15890)	forward	ACTCTTTTCAAGTTCCTGTG	148	
		reverse	CAAACTGCCGCAAGCTAATG		
	CAP-G (At5g37630)	forward	TCCATCTTTGAAATACTCGG	136	
		reverse	CAGAGGATGTTTCTTCAATC		
	CAP-H (At2g32590)	forward	TCCAATTCAGGATGAGGAAC	128	
		reverse	AACATAGATGTGGTGAGATG		
	CAP-D2 (At3g57060)	forward	ACAATGTGGGGAAGAAGGCG	141	
		reverse	AGCAACTTGAACAGACATTC		
(RPTs)	*RPT2a* (At4g29040)	forward	GGAACTTCTGAACCAGCTTG	521	
		reverse	ATTGTTTTACCGGAGGAGAT		
	RPT2b (At2g20140)	forward	GAGATTGATGCTGTTGGCAC	550	
		reverse	TAAGCAGAGAGTGAAAACAG		
	RPT5a (At3g05530)	forward	AAGTCAGCGGAGACAGGGAA	538	
		reverse	TAGATGATCCTGATTCGAAAAC		
	RPT5b (At1g09100)	forward	CATCGGAGATGGAGCAAAAC	1132	
		reverse	ATTCTATTCATCCATCAGACCA		

Table I Primers used in the present thesis (continued)

Experiment	Gene		Primer sequence (5' to 3')	Product size	Reference
(DNA damage-inducible)	*BRCA1* (At4g21070)	forward	CCATGTATTTTGCAATGCGTG	105	Inagaki et al (2006)
		reverse	TGTGGAGCACCTCGAATCTCT		
	RAD51 (At5g20850)	forward	CGAGGAAGGATCTCTTGCAG	109	Inagaki et al (2006)
		reverse	GCACTAGTGAACCCCAGAGG		
	GR1 (At3g52115)	forward	GAAGGAGCAGACAAAGTGAG	104	Inagaki et al (2006)
		reverse	GGTGAGATGGAAGTGATAGG		
	PARP1 (At4g02390)	forward	GCTTTGGGAGACATGAATGAAC	147	Ricaud et al (2007)
		reverse	AAGTGGAACAACAACACCGTCT		
(Cell cycle-related)	*CYCA1;1* (At1g44110)	forward	TCGAGTTCCATGGTCGTCTTG	95	Inagaki et al (2006)
		reverse	CACTATGCTCTCTCATTCTCC		
	CYCA2;1 (At5g25380)	forward	TAAGGCTTGCAAGCGAGGTGG	107	Inagaki et al (2006)
		reverse	TAATCTTTGACAAATCTTCTG		
	CYCA2;2 (At5g11300)	forward	TGTATGTGTTGGCCGTAATG	91	Yoshizumi et ai (2006)
		reverse	TGGTGTCTCTTGCATGCTTA		
	CYCA2;3 (At1g15570)	forward	CTCTATGCCCCTGAAATCCA	136	Yoshizumi et ai (2006)
		reverse	ACCTCCACAAGCCAATCAAC		
	CYCA2;4 (At1g80370)	forward	CAAAGCCTCCGATCTCAAAG	152	Yoshizumi et ai (2006)
		reverse	CTTGTCCGGTAGCTCTCCAG		
	CYCB1;1 (At4g37490)	forward	TAAGCAGATTCAGTTCCGGTCAAC	96	Inagaki et al (2006)
		reverse	GGGAGCTTTACGAAAGAAATACTCC		
	CDKA1 (At3g48750)	forward	CTGAGTTCGTTTCCTACTTATATTC	105	Inagaki et al (2006)
		reverse	GATACAAGAAACTGATCTCAAAAGC		
	CDKB2;1 (At1g76540)	forward	AATCTTCAGTTAGTATCTTTCCAAG	108	Inagaki et al (2006)
		reverse	GCTAAAGAAAGGATGATTCATAGAGG		
(Zinc transporter)	*ZIP4* (At1g10970)	forward	AGCAAGAGAGGAATCAGGCTG	144	
		reverse	GCACGAATGCCGACAATGTG		
	ZIP9 (At4g33020)	forward	CATCACTACTCCGATCGGTG	156	
		reverse	AAATCCGCAGCGATCAAATCC		
(SOD-related)	*CSD1* (At1g08830)	forward	GTTGCTTGCGGCATCATTGG	125	
		reverse	GCCACACACCAGAAGATACAC		
	CSD2 (At2g28190)	forward	TCGGAAAGGGTGGCCATGAG	102	
		reverse	GCTTAGCCTCTGACTTAGAGCGG		
	CCS1 (At1g12520)	forward	GCACAGAGCCATTGGGAGAC	126	
		reverse	GTCTTGTACACCACGACGGC		
(Reference)	*Actin8* (At1g49240)	forward	GCCAGATCTTCATCGTCGTG	160	Ohtsu et al (2004)
		reverse	TCTCCAGCGAATCCAACCTT		

Table II Primers used in the present thesis (for mapping of *HEB* genes)

Line	Marker name	Type		Primer Sequence (5' to 3')	Restrectio n Enzyme	Product size Col-0	Ler
heb1	F24O1	SSLP	forward	TGTATTGTCACAAAAATGCAACA		202	185
			reverse	ACTCGGACCCGTTACAAGAA			
	T22E19	SSLP	forward	TGTTTTGCTTGTCCGTTTTT		224	202
			reverse	CATTGAGACGGGACGTTTTT			
	F2K11	SSLP	forward	TGGTCGTCACTCTCGTTCAG		198	140
			reverse	CAGATGAGACAATTCAGGGAGA			
	F22C12	SSLP	forward	GATTTCGCCGGTGATGTTAC		221	207
			reverse	AGCCGGGCATCTTATGACTT			
	F13O11a	SSLP	forward	CCGCTTAAGGCTATTGCTGT		223	220
			reverse	TGGCTATGGCCAACATACAC			
	F13O11b	1 base subsitiution	forward	GTCTAAATGTGCAAGAAATCCACAG		G	T
			reverse	CATTTGGCTTCATTTCTCTTCC			
	F13O11c	1 base subsitiution	forward	TGCTTCTGTTTATAAGTCCACTTGC		A	T
			reverse	GGACACAAAAACTATCTTGCTCGT			
	F16G16	SSLP	forward	AAAATCGACACATCACTAAGTCG		234	224
			reverse	TGATTTCGCAAAAACGAATG			
	T8F5	SSLP	forward	TGGTCTGAGCTGTGAAGTGG		237	225
			reverse	CCCACCATTTCCTGTCCTAA			
	F12P19	SSLP	forward	TGCAGTGCTTGGTTCTGAAG		248	222
			reverse	CCTGTGTTGCTGTGGAGTGT			
heb2	MDC16	SSLP	forward	ACTCTTTTGGCTCGGACAAG		233	199
			reverse	CGTTGTAATCGGGAAAATGC			
	MXL8	SSLP	forward	AAGTAGCCCAAAGCCGTACA		201	172
			reverse	GCAGGGACAATCCGTAAAGA			
	MSJ11	SSLP	forward	CACACATCGTGTTTTTGTCCA		234	213
			reverse	GGAAGTTGAGATGGCTGCAT			
	MDC8	SSLP	forward	GTGTATCGTACGCCCCACTC		211	172
			reverse	TGTCGTCGTTTAGTGGATGTG			
	MGL6a	SSLP	forward	TGCTCCCAATTTTATCCCTCT		239	186
			reverse	CCCTTCATAACTAATTCCACACA			
	MGL6b	CAPS	forward	AAAACACAATCCAATGGTCATAA	Hind III	388	699
			reverse	TCACGCATACGTCTTAACAGAAA		311	
	MGL6c	SSLP	forward	CAAACTCGGAGCTGAAGACC		182	179
			reverse	TGAGCAAAGCAATGTGAAGG			
	MGL6d	SSLP	forward	AGGTTTTTACCGTCGCATTG		243	221
			reverse	CAAGTTAGGAACCCCTGTTTGA			
	MUH15	SSLP	forward	TGAGGCTGTTTAGGGTTTTG		209	197
			reverse	CTTTGTGCACCGTGTGATTC			
	K14A17	SSLP	forward	CGCAAATTTTAATCGGTGAAG		182	153
			reverse	CTTTGTTTGAAGTCGCATCG			

Table II Primers used in the present thesis (for mapping of *HEB* genes)

Line	Marker name	Type		Primer Sequence (5' to 3')	Restrection Enzyme	Product size Col-0	Ler
heb3	T32M21	SSLP	forward	GAGAACCAGATGATCCAAGTCC		193	183
			reverse	ATCCACCAATGCTACGTTCC			
	NHFD	SSLP	forward	AAAAACCCAAACTTTCTATTTATAC		124	113
			reverse	ACTTCGCTTCAAGTAAAGAGG			
	F8L15	SSLP	forward	AAAAATCAGCATTGTTGTGGTT		240	196
			reverse	GCTTGACTCCGGTGTTGACT			
	K18I23	SSLP	forward	TTGCTACAACTTGCGATTCC		213	223
			reverse	TTAAAGGTTTCCGGTGTACG			
	MOP10	SSLP	forward	CTTGCACTACATGTCCATAGAACC		248	259
			reverse	ATCGTGAGCCTTATCAACTTGC			
	MJJ3a	SSLP	forward	TGCCAAAAGACAGAAACGAA		145	112
			reverse	ATTGATTTGCAAAATGAGTATCC			
	MJJ3b	SSLP	forward	GGATCCAGGGTCTGACTCAA		177	168
			reverse	GAACCAGCAGCAAGTGAACA			
	MJJ3c	SSLP	forward	CCTCTCCCTTGGTTCTTTCTTC		222	234
			reverse	CTGACTTCAGCTTTGGGTAAGG			
heb7	nga172	SSLP	forward	CATCCGAATGCCATTGTTC		162	136
			reverse	AGCTGCTTCCTTATAGCGTCC			
	T12H1	SSLP	forward	AGGTTAGCGATTGAAGTTTCG		246	233
			reverse	AAAAGCAGTGTTGGGGAAGA			
	F22F7a	SSLP	forward	TTGTCACCACATTAATTCCAAG		242	177
			reverse	GAACCCCTGAACTCTGCAAC			
	F22F7b	SSLP	forward	CAATGCCAGCTGCAAAGTTA		220	203
			reverse	CGCCGTTAGTTTACCCAAAA			
	F18C1a	SSLP	forward	ACTGCTGCTCCTAACCAGTCTC		210	200
			reverse	GCAGTTGAACAATACCCTCCTC			
	F18C1b	SSLP	forward	CCGGTGGAGAAAAGAACAAA		165	161
			reverse	GGAAATCCGGCTAGTGAGAA			
	F18C1c	SSLP	forward	TTTGTGCTGGGTTTCAATCA		157	149
			reverse	TGTGTGATGGAATCAATTTGG			

Table III Plasmids used in the present thesis

Experiment	Name	Vector	Construct
Complementation	CAP-G2-G-GFP	pMDC107	CAP-G2 promoter CAP-G2 genomic sequence-GFP
	CAP-H2-G-GFP	pMDC107	CAP-H2 promoter CAP-H2 genomic sequence-GFP
GUS	CAP-H2-P-GUS	pMDC163	CAP-H2 promoter-GUS

ABSTRACT

The molecular mechanisms of boron (B) toxicity are not well-understood. In order to obtain insights into the molecular mechanisms of B toxicity, seven *Arabidopsis thaliana* mutants hypersensitive to excess B (*heb*) were studied. Through the analysis of the mutants, I first identified six genes involved in B toxicity-tolerance. These genes represent the first identification of genes essential for B toxicity-tolerance in plants.

Boron (B) is an essential element for plants. It can also become toxic when it exists in soils at excessive levels. Limitation of crop yield and quality caused by B toxicity is an agricultural problem in the world especially in semi arid areas.

To understand B toxicity mechanisms and breed excess-B tolerant crops, isolation of genes involved in B toxicity and/or tolerance has been attempted. Recently, overexpression of B transport molecules BOR4 and TIP5;1 were revealed to improve excess-B tolerance in plants, although the biological functions of these molecules in B toxicity have remained unclear. These studies established that regulations of molecules function in efflux and uptake of B are major mechanisms for excess-B tolerances in plants. On the other hand, at the molecular level, mechanisms of excess-B toxicity are still unknown. Other than B transport molecules, several *A. thaliana* proteins involved in transcription, RNA process and anti-oxidative system are shown to provide B tolerance to yeast. However, their functions in B toxicity-tolerance are not revealed yet. Moreover, it has not been elucidated whether these genes are essential for B toxicity-tolerance in plants. Isolation and identification of novel plant genes involved in B toxicity and/or tolerance is expected to provide us new insights into molecular mechanisms of B toxicity in plants.

For this purpose, I focused on genetic approach using EMS mutagenized *Arabidopsis thaliana* (ectype Col-0). I studied seven recessive mutants, *hypersensitive to excess B* (*heb*). The *heb* mutants showed extremely shorter relative root length than the wild-type under the toxic B condition (3 mM boric acid), although they showed slightly reduced root elongation under the control condition (0.03 mM boric acid), indicating their hypersensitivity to excess B. In the present thesis, I identified the genes that are essential for B toxicity-tolerance in plants using the *heb* mutants and characterized their functions in B toxicity-tolerance. Through the analyses, I established new aspects of two protein complexes, condensin II and 26S proteasome.

Chapter 1 Condensin II alleviates DNA damage and is essential for excess boron tolerance in *Arabidopsis thaliana*

First I investigated the mineral specificity of the short-root phenotype of *heb1-1* and *heb2-1.* The root growth of *heb1-1* and *heb2-1* were not sensitive to B deficiency, arsenite toxicity and salinity stress, indicating that short-root phenotype of *heb1-1* and *heb2-1* are specific to excess B among mineral stresses tested.

Genetic mapping and sequence analysis revealed that *heb1-1* carried two mutations in At1g64960 which encodes chromosomal associated protein-G2 (CAP-G2) and that *heb2-1* carried a mutation in At3g16730 encoding CAP-H2. Introduction of GFP-fused CAP-G2 and CAP-H2 into the respective *heb* mutants complemented their excess-B dependent phenotype, confirming that these are responsible genes for the *heb* phenotype. Both proteins are subunits of chromosomal protein complex condensin II, suggesting that the function of condensin II complex is crucial for excess B tolerance in *A. thaliana*.

Condensin II is composed of two core subunits CAP-C and CAP-E and three regulatory subunits HEB1/CAP-G2, HEB2/CAP-H2 and CAP-D3. In human cells, condensin II is well known to have a role in mitotic chromosomal condensation in concert with another type of condensin, condensin I. In human cells, in addition to the mitotic function, condensins are known to be involved in DNA damage repair during interphase. To investigate whether *A. thaliana* condensin II is involved in DNA damage response as is the case in animal cells, I examined the sensitivity of *HEB1*/*CAP-G2* and *HEB2*/*CAP-H2* mutants to reagents/conditions that induce DNA double strand breaks (DSBs) or replication block. The root growth of both *heb1-1* and *heb2-1* were sensitive to DSBs-inducible and replication block reagents compared to the wild-type, suggesting the involvement of condensin II in DNA damage repair and/or in resistance to genotoxicity.

To examine whether excess B causes DNA damage, I investigated the expression of DSBs-inducible genes and the levels of DSBs in the root tip cells treated with excess B. RT-PCR revealed that expressions of DSBs-inducible genes such as *BRCA1* and *PARP1* were up-regulated by excess B treatment in both the wild-type and the mutants. Transcripts of these genes were higher in the *heb* mutants than in the wild-type both under the control and the excess B conditions. Comet assay revealed that the *heb* mutants highly accumulated DSBs compared to the wild-type under the control and the excess B conditions. The levels of DSBs in both the wild-type and the *heb* mutants were elevated by the excess B treatment. In addition, simultaneous treatment of a DSBs-inducible regent and a replication block reagent mimicked the extent of root growth inhibition induced by excess B treatment in the *heb* mutants. Taken together, these results demonstrate that excess B causes DNA damages in root tip cells and *A. thaliana* condensin II has a role in the

alleviation of DNA damages.

In conclusion, I demonstrated that involvement of DNA damages in B toxicity and a novel function of plant condensin II in repairing damaged DNA and/or protecting genome from genotoxic stresses especially under the excess B condition.

Chapter 2 Involvement of 26S proteasome in excess B tolerance in *Arabidopsis thaliana*-Identification of possible targets involved in excess B tolerance-

Genetic mapping and sequence analysis revealed that *heb3* carries a mutation in At5g05780 which encodes regulatory particle non-ATPase 8a (RPN8a) and *heb6-2* in At3g05530 which encodes regulatory particle triple-A-ATPase 5a (RPT5a). Another mutant line, *heb6-1,* had a mutation in RPT5a at a different site from *heb6-2*. These mutants were not much sensitive to B deficiency, cadmium, arsenite and sodium chloride toxicity as compared to excess B, indicating the specificity of the mutants to excess B tolerance. To avoid confusion, I renamed *heb3*, *heb6-1* and *heb6-2* as *rpn8a-2*, r*pt5a-5* and *rpt5a-6*, respectively.

RPN8a and RPT5a are subunits of 19S regulatory particle (RP) of 26S proteasome (26SP), a large proteolytic device. RP functions in recognition and unfolding of target proteins which are mostly modified by ubiquitin (Ub). In *A. thaliana*, most of the RP subunits were encoded by two genes, suggesting a diverse subunit combination of 26SP is present, which may expand the target specificity and functions. Among T-DNA inserted RP mutants I examined, *rpn2a* and *rpt2a* mutants were also hypersensitive to excess B, but *rpn2b*, *rpn8b*, *rpt2b* and *rpt5b* mutants were not. This suggests the existence of specific combination of RP subunits and specific targets in response to B toxicity.

I elucidated whether the Ub-dependent proteolysis activity is reduced in the *rpt5a* mutants. The *rpt5a* mutants were sensitive to treatment with amino acid analogue which induces accumulation of misfolded proteins. Misfolded proteins are known to be degraded through the Ub-26SP pathway. This suggests that the reduced total Ub-dependent activity in the *rpt5a* mutants and that excess B may cause protein misfolding. On the other hand, the levels of accumulated poly-ubiquitinated proteins in the *rpt5a* mutants were not higher than those in the wild-type under the normal condition. This indicates that the accumulation of poly-ubiquitinated proteins does not reflect the reduced total Ub-dependent activity in the *rpt5a* mutants. Interestingly, the accumulations of poly-ubiquitinated proteins were increased by excess B in the *rpt5a* mutants, but not in the wild-type. Taken together, these data suggest that RPT5a contained 26SP is involved in the degradation of those proteins induced by excess B.

To investigate whether the subunit specific poly-ubiquitinated proteins in response

to excess B are present, I conducted proteome analysis of poly-ubiquitinated proteins. Poly-ubiquitinated proteins were purified from the root extracts of the wild-type and *rpt5a-6* and were analyzed by isobaric tag for relative and absolute quantification (iTRAQ) LC−MS/MS. As a result, 30 of 57 identified proteins were relatively quantified. Accumulations of 21 of 30 proteins were higher in *rpt5a-6* than in the wild-type irrespective of B condition and were elevated by excess B treatment, suggesting that those proteins are degraded through a system that requires RPT5a. Some of the identified proteins were known to be associated with stress response and cell morphogenesis. One possibility is that these proteins undegraded are cause of excess B sensitivity.

As another approach to elucidate molecular mechanisms of RPT5a involvement in excess B tolerance, several revertants carries *rpt5a-6* mutation and can elongate roots under the excess B condition were isolated. The revertants are expected to provide molecular information on the function of RPT5a in tolerance to excess B.

In conclusion, in this chapter, I demonstrated the requirements of RPN2a, RPN8a, RPT2a and RPT5a for B toxicity-tolerance. I propose that among a variety of compositions of 26SP, those containing RPN2a, RPN8a, RPT2a and/or RPT5a are crucial for excess B tolerance. These sets of 26SP may have essential function in B toxicity-tolerance through Ub-dependent proteolysis of certain proteins with negative effects on root growth.

Chapter 3 *Arabidopsis thaliana* 26S proteasome subunits RPT2a and RPT5a are crucial for Zinc deficiency-tolerance

Through the analysis of nutritional response of RP mutants, I found that the shoot growth of *rpt2a* and *rpt5a* mutants were more sensitive to zinc (Zn) deficiency compared to the wild-type.

I first speculated that the *rpt* mutants are defective in the regulation of Zn uptake. However, in the *rpt* mutants, shoot Zn contents were similar to that of the wild-type. On the other hand, transcripts of Zn deficiency-inducible genes, *ZIP4* and *ZIP9* were highly accumulated in the *rpt* mutants, suggesting the possibility that the *rpt* mutants are suffering from various Zn deficiency symptoms although Zn levels are not reduced.

Indeed, lipid peroxidation levels, known to be increased under Zn deficiency, were higher in the *rpt* mutants than in the wild-type, suggesting that ROS accumulation in the *rpt* mutants are higher than in the wild-type.

It has been known that up-regulation of 26SP subunit genes reflects the decrease in Ub-dependent 26SP activity in plants. Zn deficiency induced expression of both *RPT2a* and *RPT5a* genes, and the extents of induction of these genes were much higher in the *rpt* mutants, suggesting the reduced activities of Ub-dependent proteolysis under Zn deficiency,

especially in the *rpt* mutants. Indeed, poly-ubiquitinated proteins were accumulated upon exposure to Zn deficiency, especially in the *rpt* mutants.

Overall, my analysis established that RPT2a and RPT5a are involved in Zn deficiency response, possibly through alleviation of oxidative stresses and/or processing of poly-ubiquitinated proteins.

Conclusion

Through the characterization of *heb* mutants, I identified six genes required for B toxicity-tolerance in plants and established novel aspects and mechanisms of B toxicity at the molecular level. In addition, the present thesis also provides novel aspects of condensin II and 26S proteasome function in nutritional responses.

Reference

Sakamoto T, Kamiya T, Sako K, Yamaguchi J, Yamagami M and Fujiwara. *Arabidopsis thaliana* 26S proteasome subunits RPT2a and RPT5a are crucial for Zinc deficiency-tolerance. *Bioscience, Biotechnology, and Biochemistry* ***in press***

INTRODUCTION

1. Physiological roles of boron in plants

Boron (B), a metalloid, is established as essential for normal growth and development of higher plans as early as 1923 by Warington. Thus, B availability in soil and irrigation water is an important determinant of yield and quality of crop products (Tanaka and Fujiwara 2008). Several physiological defects caused by B deficiency implies that B is involved in very diverse physiological processes such as cell elongation, membrane integrity, carbon and nitrogen fixation, secondary metabolism, nucleic acid synthesis, and regulation of gene expression in plants (Cakmak and Ro¨mheld 1997; Blevins and Lukaszewski 1998; Brown et al. 2002; Wimmer et al., 2009). However, up to the present date, the only physiological function of B proven at the molecular level in plants is only in maintaining of cell wall structure through crosslinkking two rhamnogalacturonan II (RG-II) monomers in the cell wall into an RG-II dimer, a component of cell wall pectic polysaccharides (O'Neill et al. 1996; Kobayashi et al. 1996). The essentiality of B for intracellular processes is still unknown.

2. Excess boron in agriculture

Excess levels of B also damages both crop yield and quality (Nable et al., 1997). Typical visual symptoms of B toxicity in crops include yellowing, necrosis, and chlorosis of the tips and margins of the older leaves (Roessner et al., 2006). Soils with excess B are often seen in alkaline and saline soil areas where a rainfall and a leaching are scarce. In agricultural areas of Southern Australia, North Africa, and West Asia, naturally B-excess soils are present in addition to artificially high-B contaminated soils by over-B-fertilization and/or irrigation of high B containing water (Nable et al., 1997; Rashid and Ryan, 2004). Thus, management of B levels is especially important in agricultures in such B rich regions. At the same time, it is expected to establish plant species, cultivars and also genetically-engineered plants that tolerate to toxic levels of B in soils. To archive this, a number of researchers have been focused on the mechanisms of B toxicity and tolerance in plants.

3. Physiological effects of excess boron on plants

To understand mechanisms of B toxicity, much biochemical and physiological data has been accumulated and it has been demonstrated that negative impacts of excess B involves many developmental/biochemical processes in plants such as altered metabolism (Loomis and Durst, 1992; Lukaszewski et al., 1992; Roessner et al., 2006; Cervilla et al., 2009), reduced activity in photosynthetic process (Han et al., 2009), reduced root cell division (Liu

et al., 2000; Konuk et al., 2007), reduced shoot cell wall expansion (Loomis and Durst, 1992) and generation of reactive oxygen species (ROS) followed by oxidative damage (Gunes et al., 2006; Molassiotis et al. 2006; Cervilla et al., 2007). Reid et al (2004) also demonstrated that excess B impairs the tolerance to photo-oxidative stress. However, to my knowledge, limited information is available at the molecular level about how B toxicity develops in plants and how plants respond to the B toxicity.

4. Genes and loci involved in the tolerance to excess boron in plants

Excess-B tolerant plant species or genus represented by a single variety have been reported more than 70 years ago. More recent investigations have demonstrated that there are a lot of varieties in response to excess B among a number of crop cultivars such as bread wheat (*Triticum aestivum*), barley (*Hordeum vulgare*), rice (*Oryza sativa*) (Nable *et al*., 1997). Using the variation in susceptibility to B toxicity among crop cultivars, quantitative trait locus (QTL) analyses have been conducted to isolate the genes involved in B toxicity-tolerance to understand B toxicity mechanisms and breed excess-B tolerant crops.

In bread wheat, at least three chromosomal regions named *Bo1*, *Bo2* and *Bo3* are known to additively control yield and tissue B concentrations under excess B condition (Paull et al., 1991). In rice, a major region for B toxicity-tolerance in terms of shoot length was found in chromosomal 4 (Ochiai et al., 2008). In these two crops, however, positional cloning of genes responsible for observed QTL was not succeeded yet. In barley, four QTL associated with B toxicity-tolerance were detected on chromosomes 2H, 3H, 4H and 6H (Jefferies et al. 1999). B transporter HvBot1 was included in a B toxicity-tolerance QTL on chromosome 4H (Reid et al., 2007; Sutton et al., 2007) and this protein appeared to have the ability to provide excess B tolerance to plant and yeast (Sutton et al., 2007). In addition, an aquaporin form the nodulin-26-like intrinsic protein family, HvNIP2;1 was isolated from chromosome 6H QTL (Schnurbusch et al., 2010). Moreover, Hassan et al (2010) found that chromosome 2H QTL region encoding an S-adenosylmethionine decarboxylase precursor (SAMDC), involved in antioxidative response, and that yeast overexpressing barley SAMDC was able to grow on excess B medium.

Using other genetic and molecular techniques, further genes involved in excess B tolerance have been identified. The manipulation of B transport molecules of *A. thaliana* BOR4 and TIP5;1 (Miwa et al., 2007; Pang et al., 2010) improved plant and yeast growths under excess levels of B. Overexpression of *A. thaliana* proteins associated with transcription (MYB13 and MYB68) and RNA-dependent process (PAB2, RPS20B and RBP47c') conferred yeast B toxicity-tolerance (Nozawa et al., 2006). Microarray analysis using *A. thaliana* revealed that several genes such as MATE type are induced in response to

excess B in both shoots and roots (Kasajima and Fujiwara 2007).

The identified B transport molecules are suggested to exclude excess B or to regulate B homeostasis to avoid B toxicity, however, the transporters are unlikely to provide insights into the molecular mechanisms of excess-B toxicity. Furthermore, as to the proteins other than B transporter molecules described above, their functions in the process of B toxicity and/or tolerance are not revealed yet, and more importantly it has not been elucidated their essentiality for B toxicity-tolerance in plants.

5. Isolation of *Arabidopsis thaliana* mutants hypersensitive to excess boron

To identify novel genes involved in B toxicity and/or tolerance, Y. Kawara in our laboratory conducted a new genetic approach. The idea behind was that mutants with defects in genes important for B toxicity-tolerance, are likely to show growth defects only under excess levels of B. The strategy was to isolate plants that grow normally under the normal condition (0.03 mM boric acid), and o which root growth are severely restricted in moderate level of B toxicity (3 mM boric acid), which leads to much less damage in wild-type plants. About 20,000 ethyl methanesulfonate (EMS) mutagenized M2 seeds of *A*. *thaliana* (ecotype Col-0) were grown under the B toxic condition. After 2 weeks, plants showed short-root were transferred to the normal condition. Then, M3 seeds were collected from recovered plants and were subjected to second screening in the same way. Reselected plants were crossed with Col-0 for the segregation test. Finally, seven recessive mutants named *hypersensitive to excess B* (*heb1-heb6*) were isolated. Most of the *heb* mutants showed slightly reduced root elongation under the normal condition. But all mutants showed extremely short-root compared to the wild-type under the excess B condition, indicating their hypersensitivity to excess B.

It is expected that *heb* mutants carry mutations in genes essential for B toxicity-tolerance and that characterization of these genes provides new insights into the molecular mechanisms for B toxicity in plants. In the present thesis, I identified several genes responsible for the phenotype of the *heb* mutants and discussed their function in B toxicity-tolerance.

Chapter 1 Condensin II alleviates DNA damage and is essential for excess boron tolerance in *Arabidopsis thaliana*

1.1 Abstract

Excess boron (B) negatively affect growth of organisms including plants and animals, but its molecular mechanism of toxicity is unknown. We characterized two *Arabidopsis thaliana* mutants that are hypersensitive to excess boron (*heb1* and *heb2*). *HEB1* and *HEB2* encode CAP-G2 and CAP-H2, respectively, subunits of a chromosomal protein complex, condensin II. Condensin II functions in chromosome condensation during mitosis. Expressions of condensin II subunit genes were induced under the excess B condition. Simultaneous treatment of zeocin, a DNA double strand breaks (DSBs)-inducible reagent, and aphidicolin, a replication block reagent, mimicked the effect of excess B on root growth in the *heb* mutants. Transcripts of DSBs-inducible genes and levels of DSBs were increased both by excess B treatment and by the *heb* mutations, suggesting that DSBs are a cause of B toxicity and that condensin II reduces DSBs. *atr-2, a* T-DNA insertion mutant sensitive to replication blocking reagents, was sensitive to excess B. Taken together these data suggest involvements of DSBs and replication blocks in B toxicity and roles of plant condensin II in repairing DNA damage and/or protecting genome from genotoxic stresses especially under the excess B condition.

1.2 Introduction

To obtain new insights into the molecular mechanisms for B toxicity, seven *A. thaliana* mutants, which are hypersensitive to excess B (*heb*) were isolated by Ms. Kawara. The *heb* mutants showed extremely short-root phenotype under excess B condition but moderate root growth under normal B condition (Sakamoto et al., 2009). It is expected that *heb* mutants carry mutations in genes essential for B toxicity-tolerance and that characterization of these genes helps us to understand the B toxicity mechanisms in plants. Through the characterization of *heb1* and *heb2* mutants, I found that *HEB1* and *HEB2* encode subunit of protein complex condensin II, chromosomal associated protein-G2 (CAP-G2) and CAP-H2, respectively.

Condensin II is composed by two structural maintenance of chromosome (SMC) subunits and three non-SMC subunits including CAP-D3, CAP-G2 and CAP-H2. Higher eukaryotes have two types of condensin, condensin I and II. These condensins share two SMC subunits, CAP-C (SMC2) and CAP-E (SMC4), and have unique sets of non-SMC subunits (Hirano, 2005). Animal condensins are well-known to be localized to chromosomes during mitosis and play important roles in restructuring chromosomes to

achieve proper chromosomal condensation and segregation (Ono et al., 2003; Hirota et al., 2004; Ono et al., 2004). During interphase, condensin I and II show different sub-cellular localizations: condensin I is present in the cytoplasm, whereas condensin II is localized to the nucleolus (Ono et al., 2004). The roles of interphase animal condensins have been reported; condensin I is involved in DNA single strand breaks repair (Heale et al., 2006) and transcriptional silencing (Cobbe et al., 2003), and condensin II is required for DNA double strand breaks (DSBs) repair (Wood et al., 2008). In addition, the similar dual roles of condensin during mitosis and interphase are also reported in yeast which has only type I condensin (Aono et al., 2002; Chen et al., 2004).

Several studies of plant condensins have been reported. AtCAP-E complemented the yeast *smc2-Δ6* mutant which is defective in chromosomal condensation and segregation (Siddiqui et al., 2003). In addition, the sub-cellular localization of condensins has been reported. *A. thaliana* non-SMC subunits, AtCAP-H and AtCAP-H2 expressed in BY-2 tobacco cultured cells showed similar sub-cellular localization patterns as animal cells described above (Fujimoto et al., 2005). These suggest that plant condensins have similar function for condensation and segregation. Takeda et al (2004) analyzed *A. thaliana* SMC2$^{+/-}$ mutant and demonstrated that condensin I and/or II are important for transcriptional silencing. To my knowledge, these are the only experimental evidences for the function of condensins in plants.

In this chapter 1, I established a novel function of *A. thaliana* condensin II in repairing DNA damages and/or protecting genome from genotoxicity derived from abiotic stresses. I also propose that B toxicity induces DSBs and possibly replication blocks and that the repair and/or prevention of the DNA damages by condensin II are required for B toxicity-tolerance in plants.

1.3 Materials and Methods

1.3.1 Plant materials and growth conditions

The *heb1-1* and *heb2-1* mutants of *A. thaliana* (ecotype Col-0) were isolated as described previously (Sakamoto et al., 2009). T-DNA insertion mutants of *HEB1*, *heb1-2* (SALK_049790; ecotype Col-0) and *HEB2*, *heb2-2* (SALK_059304; ecotype Col-0), and *atr-2* (SALK_032841; ecotype Col-0) were obtained from the ABRC. Lines carrying T-DNA in the homozygote were established, and the presence of T-DNA was determined by PCR using the primers sets listed in Table I. The *atm-2* (ecotype Col-0) was kindly derived by Anne Britt of Department of Plant Biology, University of California, Davis.

In all experiments, plant seeds were sown on the plates containing MGRL solution (Fujiwara et al., 1992), 1% (w/v) sucrose and 1.5% (w/v) Gellan gum. Boric acid was used

for the adjustment of B concentrations in the medium. After 3d incubation at 4°C, the plates were placed vertically in the growth chamber until analyzed (16-h light/8-h dark cycle, 22°C).

1.3.2 Positional mapping of the *HEB* genes

heb1-1 and *heb2-1* mutants (M3 generation) (Col-0 background) were crossed with Ler wild-type plants. DNA was extracted from 1152 (for *heb1-1*) and 1134 (for *heb2-1*) F2 plants and were analyzed using simple sequence length polymorphism and cleaved-amplified polymorphic sequence markers (Table II), which were generated based on Cereon Arabidopsis Polymorphism Collection (http://www.Arabidopsis.org/Cereon). F3 progeny of F2 recombinants were grown on excess B condition and short-root phenotype was used to map the *heb* mutations.

1.3.3 Determination of B contents

Whole roots and shoots of 14d-old-seedlings were harvested from individual plant at 0.03 mM B condition and 3 - 5 plants at 3 mM B condition, respectively. After the drying at 60°C for 2d, the samples were digested with concentrated nitric acid (13 M, Wako, Osaka, Japan) and the B contents were measured using ICP-MS (SPQ-9700) (Seiko Instrument Inc., Chiba, Japan) as described (Nozawa et al., 2006).

1.3.4 Observation of root morphology

The root morphologies were observed and imaged using stereomicroscope SZH10 (Olympus, Tokyo, Japan) equipped with the digital camera (Olympus) after excess B and bleomycin treatment (see below). To observe the root tip structures, 14d-seedlings roots were stained with propidium iodide (10 μg/ml) (Molecular Probes, Eugene, OR, USA) for 5 to 10 min. Then images were captured using confocal microscope FV-1000 (Olympus) with 619 nm excitation and 559 nm emission. At least 10 plants per line were observed.

1.3.5 Gene expression analyses

Total RNA was extracted using RNeasy plant mini kit (Qiagen, Valencia, CA, USA), and treated with the RNase-free Dnase set (Qiagen) to remove the contaminated DNA. cDNA was synthesized from 500 ng of total RNA using PrimeScript RT reagent kit (Takara, Ohtsu, Japan) and was subjected to the following analyses. The *Actin8* mRNA was used as loading reference for semi-quantitative RT-PCR. Transcript levels of *HEB1*, *HEB2*, *CAP-D3* and *Actin8* were PCR amplified with optimum cycles for each gene by corresponding primer sets listed in Table I.

Quantitative real time RT-PCR was performed with SYBER premix ex*Taq*® II (Takara) on a Thermal Cycler Dice® Real Time System (Takara). Ct values were calculated by second derivative maximum method and the calculation of relative transcript levels were based on a standard curve generated with a serial dilutions of cDNA. The primer sets of cell cycle-related genes, DSBs-inducible genes and condensin genes were listed in Table I. *Actin8* were used for the normalization.

1.3.6 Sensitivity to genotoxic and oxidative stresses

Plants were pre-incubated vertically on MGRL plates for 5d. To test the sensitivity of plants to zeocin (Invitrogen, Carlsbad, CA, USA), bleomycin (Wako), aphidicolin (Wako) and HU (Wako), 5d-old-seedlings were transferred to the plates containing different concentrations of each DNA-damaging reagent, and root tip position of each plant was recorded that is to recognize the new root growth. After the additional 4d-incubation, the length of newly elongated primary roots were measured using ImageJ software (http://rsb.info.nih.gov/ij/).

UV-C treatment was conducted in a clean bench PCV-800TPG (Hitachi, Tokyo, Japan) equipped with UV-C lamp GL15 (Hitachi). Five-day-old-seedlings were exposed to UV-C on the opened plates as follows; Plates were placed vertically at a point that is 40 cm distant from UV-C lamp and incubated for several time durations with UV-C light, and non-treated plates were also placed at same position and incubated for 2 h without UV-C light. Plants were then incubated in a normal light condition for recovery. After the additional 4d incubation, the shoot fresh weights were measured for the examination of plant UV-C sensitivity.

1.3.7 Comet assay

For the detection of DSBs, comet assay (N/N protocol) was performed as described (Menke et al., 2001). Images of ethidium bromide-stained comets were captured by digital CCD camera (Olympus) equipped to fluorescent microscope BX50WI (Olympus). The comets were analyzed using CASP software (http://www.casp.of.pl/). We used “olive tail moment” as an index of DNA damage as described (Olive et al., 1990). For the assessment of DSBs induced by excess B and UV-C treatment, 50 root tips and 10 aerial parts were collected per sample, respectively.

1.3.8 Cell ploidy analysis

2 to 3 mm-long-root tips from 50 plants were protoplasted according to the method optimized for roots (Birnbaum et al., 2005). After the cell wall digestion, protoplasts were collected by centrifuging 500g for 2 min at room temperature. The supernatant was

carefully removed, and then prepared protoplasts were used for flow cytometric analysis as described (Yoshizumi et al., 2006).

1.3.9 GUS activity assay

A 2.45 kb region upstream of the *CAP-H2*/*HEB2*/At3g16730 start codon was amplified from Col-0 genomic DNA by PCR with the primers listed in Table I. The amplified DNA fragment were purified with a gel extraction kit (Qiagen, Valencia, CA, USA) and then subcloned into pENTR-D/TOPO vector based on manufacturer's protocol (Invitrogen). The accuracy of promoter sequence was confirmed by sequencing. The cloned promoter fragment was subsequently subcloned into Gateway plant transformation destination vector pMDC162 (Curtis and Grossniklaus, 2003) containing the GUS gene by a LR recombination reaction. The construct was mobilized into *Agrobacterium* (GV3101) and used to transform Col-0 plants by the floral dip method (Clough and Bent, 1998). Transformants were selected on half strength Murashige and Skoog (MS) plates containing 2% sucrose and 20 μg/ml hygromycin. T3 transformants which have T-DNA homozygously was used for the histochemical assay. Seedlings were stained with the solution containing 100 mM Na_2HPO_4 pH 7, 0.1% Triton X-100, 2 mM $K_3Fe[CN]_6$, 2 mM $K_4Fe[CN]_6$ and 0.5 mg ml^{-1} 5-bromo-4-chloro-3-indolyl-b-D-glucronic acid for 1h at 37°C. To clear the GUS-stained seedlings, 70% and 99.5% ethanol were primary treated. Just before the microscopy, seedlings were embedded in clearing solution.

1.3.10 *CAP-G2* and *CAP-H2* cloning for complementation analysis

Genomic region of *CAP-G2*/*HEB1*/At1g64960 and *CAP-H2*/*HEB2*/At3g16730 were amplified from Col-0 genomic DNA by PCR with the primers listed in Table I. These fragments contain 2 and 2.5 kb upstream region of the start codon of *HEB1*/At1g64960 and *HEB2*/At3g16730, respectively. The amplified DNA fragments were purified with a gel extraction kit (Qiagen, Valencia, CA, USA) and then subcloned into pENTR-D/TOPO vector based on manufacturer's protocol (Invitrogen, Carlsbad, CA, USA). The accuracy of sequence was confirmed by sequencing. The cloned genomic fragments were subsequently subcloned into Gateway plant transformation destination vector pMDC107 (Curtis and Grossniklaus, 2003) containing the GFP gene by a LR recombination reaction. The constructs were mobilized into *Agrobacterium* (GV3101) and used to transform Col-0 plants by the floral dip method (Clough and Bent, 1998). Transformants were selected on half strength Murashige and Skoog (MS) plates containing 2% sucrose and 20 μg/ml hygromycin. T3 transformants which have T-DNA homozygously was used for the complementation analysis. GFP fluorescence was observed using confocal microscopy FV-1000 (Olympus).

1.4 Results

1.4.1 The *heb* mutants are hypersensitive to excess B but not to other mineral stresses

A genetic screen was performed to identify mutants defective in excess B tolerance using 20,000 ethyl methanesulfornate (EMS) mutagenized Col-0 (Sakamoto et al., 2009). Candidates were screened based on relative root lengths under the excess B condition, 3 mM boric acid in this study, in the media. This B concentration was sufficient to cause moderate root growth inhibition in Col-0 plants (Figure 1-1 A and B). Seven recessive mutants were isolated from this screen (Sakamoto et al., 2009) and the mutants were named *heb* (*hypersensitive to excess boron*). Among seven *heb* mutants, *heb1-1* and *heb2-1* were selected for this study. The mutants were backcrossed to Col-0 for three times and were then used for the subsequent studies.

I first examined the growth property of the mutants under various B conditions. Under the control condition (0.03 mM B), the roots of *heb1-1* and *heb2-1* mutants were about 30% shorter than that of Col-0 (Figure. 1-1 A). The roots of the *heb* mutants were only about 10% of that of Col-0 under the excess B condition (3 mM B, Figure 1-1 A). The root growths of *heb1-1* and *heb2-1* were reduced in a dose-dependent manner in the presence of 1 mM or higher concentration of B, whereas that of Col-0 was not affected up to 2 mM B (Figure 1-1 B). Moreover, extents of root length reduction in both mutants under 1, 2 and 3 mM B were much severer than that of Col-0 (Figure 1-1 B). As observed in the case of root growth, the growth of shoots of *heb1-1* and *heb2-1* were also more reduced than those of Col-0 under high B treatments (Figure 1-1 C). These results established that *heb1-1* and *heb2-1* are sensitive to excess B in both terms of B concentration required for growth inhibition and the extents of growth inhibition.

To examine whether the phenotypes of *heb1-1 and heb2-1* are specific to B toxicity, growth of the mutants were tested under other mineral stresses conditions. Low B supply (Koshiba et al., 2009), arsenite (As) treatment (Verbrugge et al., 2009) and salinity stress (Mahajan et al., 2008) are well known to generate reactive oxygen species (ROS) as is the case of B toxicity (Gunes et al., 2006; Molassiotis et al., 2006; Cervilla et al., 2007). If the high sensitivity of *heb* mutants to high B conditions is due to increased sensitivity to ROS, treatments that generate ROS would severely inhibit root growth of the *heb* mutants. These mineral stresses reduced root lengths of both Col-0 and the *heb* mutants in a similar manner, except for the case of low B treatment where root elongation of *heb1-1* was roughly 90% of Col-0. Considering that the root elongation of the mutant plants is reduced by

about 90% under 3 mM boric acid condition, these results suggest that *heb1-1* phenotype is specific to excess B (Figure 1-1 D) among the treatments examined. Overall, these results suggest that *heb1-1* and *heb2-1* are hypersensitive to excess B and that it is not likely that ROS is involved in hypersensitivity of the mutants. I also examined sensitivity of the mutants to reagents generating ROS, hydrogen peroxides and methyl viologen, and found that these reagents reduce root length of the mutants and the wild-type similarly (Figure 1-2 A and B). This further supports the hypothesis that ROS is not likely to be involved in the hypersensitivity of the mutants to excess B.

Plants control B uptake and its internal distribution in response to B availability in soils through regulation of B transporters in roots to avoid over-accumulation of B (Miwa and Fujiwara, 2010). It was possible that the specific sensitivity to excess B of the *heb* mutants was caused by misregulation of B transporters and subsequent over accumulation of B in roots. I determined B contents in *heb1-1* and *heb2-1* in shoots and roots and found that they were about 60-80% and 30% of those in Col-0 under the 0.03 mM and 3 mM B treatments, respectively (Figure 1-1 E). The reduced B contents in the mutants cannot be the reason for the growth defects of the *heb* mutants under the excess B condition.

1.4.2 *HEB1* and *HEB2* encode different subunits of a chromosomal protein complex, condensin II

Genetic mapping limited the *heb1* and *heb2* loci to about 70 and 12 kb regions containing At1g64960 and At3g16730, respectively (Figure 1-3 A and B). The mutations in the DNA regions containing *heb* loci were identified (Figure 1-4 A and B). *heb1-1* possessed single base substitution and a 4 bp-insertion, which resulted in a sense and a frameshift mutation, respectively. The 4 bp insertion generated an aberrant stop codon at the amino acid residue 470 of *HEB1* (At1g64960). *heb2-1* possessed a nonsense mutation at the predicted ninth exon of *HEB2* (At3g16730). From the collection of T-DNA mutant of SALK institute (Alonso et al., 2003), I identified new T-DNA inserted mutant alleles, *heb1-2* (SALK_049790) and *heb2-2* (SALK_059304) (Figure 1-4 A and B). The transcript accumulation of the corresponding genes in roots were reduced to 30 to 40% of that of Col-0 in *heb1-1* and *heb2-1* (Figure 1-4 C) and were not detected in *heb1-2* and *heb2-2* in my experiment (Figure 1-4 D). Both T-DNA insertion mutants showed the similar short-root phenotype as observed in *heb1-1* and *heb2-1* under the excess B condition (Figure 1-4 E). To further confirm that At1g64960 corresponds to *HEB1* and At3g16730 corresponds to *HEB2*, complementation analyses were conducted. *pHEB1::HEB1::GFP* and *pHEB2::HEB2::GFP* were introduced into *heb1-1* and *heb2-1,* respectively, and several independently transformed lines were obtained. All the transgenic lines elongated roots

similar to the wild-type in the presence of 3 mM boric acid in the media (Figure 1-5 A and B). The expressions of *HEB1::GFP* and *HEB2:GFP* were confirmed by GFP fluorescence observation in these transgenic plants (Figure 1-5 C), establishing that the introduced gene expressed and rescued the phenotypes of both *heb1-1* and *heb2-1.* Taken together, these data established that *HEB1* and *HEB2* correspond to At1g64960 and At3g16730, respectively.

Based on the database analysis, HEB1/At1g64960 has been identified as CAP-G2 and AtHEB2/At3g16730 has been identified as AtCAP-H2 (Ono et al., 2003). AtHEB1/CAP-G2 and AtHEB2/CAP-H2 proteins as well as another protein AtCAP-D3 (At4g15890) are non-SMC subunits of chromosome-associated protein complex condensin II (Ono et al., 2003) (Figure 1-4 F). This complex has a role in chromosome condensation and segregation in concert with another type of condensin, condensin I, in human cells (Hirota et al., 2004; Ono et al., 2004). Condensin I shares catalytic subunits AtCAP-C and AtCAP-E with condensin II and contains a different set of non-SMC proteins AtCAP-H (At2g32590), AtCAP-G (At5g37630) and AtCAP-D2 (At3g57060) (Ono et al., 2003) (Figure 1-4 F). Although HEB1 and HEB2 are subunits of the condensin II complex, it is possible that these proteins have novel functions independently from the condensin II complex. In the present study, both *heb1* and *heb2* mutants, representing different subunits of the condensin II complex, showed similar phenotypes in my experiments as described in this study. Therefore I considered that the results obtained from the analyses of the *heb* mutants can be regarded as the results from the defects in function of condensin II complex.

1.4.3 Roots of the *heb* mutants showed severe defects in meristematic organization and morphology under the excess B condition

Excess B can affect root morphology (Liu et al., 2000). I investigated the root morphology of the *heb* mutants under the normal and the excess B conditions. The morphology of *heb1-1* and *heb2-1* roots was similar to that of Col-0 roots under the control condition (Figure 1-6 A-C). In contrast, under the excess B condition, twisted roots, ectopic lateral root formations, dense root hairs were observed in *heb1-1* and *heb2-1*, but not in Col-0 (Figure 1-6 D-F). The position of root hair emergence was closer to a root tip in the *heb* mutants than in Col-0 under the B excess condition, but this phenotype was not observed under the control condition (Figure 1-6 A-F). Longitudinal confocal sections revealed that in root tips of *heb1-1* and *heb2-1,* a meristematic zone was reduced in its length especially under the excess B condition (Figure 1-7 B). Propidium iodide (PI)-stained, “dead” cells were observed in the mutant root tips even at the control condition, whereas all observed cells were not stained with PI in Col-0 (Figure 1-6 G-I). Under the excess B condition,

some PI-stained “dead” cells were found in root tips of Col-0 (Figure 1-6 J) and in *heb1-1* and *heb2-1* mutants, the number of “dead” cells increased and the “dead” cells were observed in a larger area of root tips (Figure 1-6 K and L). The enlarged and abnormal-shaped cells were observed in root tips of *heb1-1* and *heb2-1*, and their root apical meristems (RAMs) appeared disorganized compared to that of Col-0 under the excess B condition, but not under the control condition (Figure 1-6 G-L). These data suggest that *HEB1* and *HEB2* genes are involved in the maintenance of cell viability under the control condition. It is also suggested that the genes are also involved in cell division/elongation under the excess B condition.

1.4.4 The *heb* mutants are sensitive to induction of DSBs

The involvement of condensin I complex in DNA repair has been reported in yeast (Aono et al., 2002; Chen et al., 2004) and human cells (Heale et al., 2006). Human condensin II was shown to function in homologous recombination repair after DSBs (Wood et al., 2008). To investigate whether *A. thaliana* condensin II has a role in DNA damage response, I examined the sensitivity of the *heb* mutants to induction of DSBs. The sensitivity of the *heb* mutants to radiomimetic reagents, zeocin and bleomycin, which are known to induce DSBs were evaluated by root elongation-assay. Plants were grown on the normal medium for 5d and subsequently transferred to media containing various concentrations of DSBs-inducible reagents. After 4d-incubation, the root elongation during the incubation was evaluated. In the presence of 5 and 7.5 μM zeocin, both *heb* mutants showed severer inhibition of the root elongation compared to Col-0 (Figure 1-8 A). Similarly, both *heb* mutants were more sensitive to bleomycin than Col-0 when treated with 1 and 2 μg/ml bleomycin (Figure 1-8 B). It should be also mentioned that there was no significant difference between the *heb1-1* and *heb2-1* mutants regarding their sensitivity to bleomycin and zeocin.

I also examined the effect of DSBs-inducible reagents on root morphology (Figure 1-8 C). In the presence of 2.5 μM zeocin, no visible effect on root morphology was observed in Col-0, whereas *heb1-1* showed slight alteration in root morphology such as ectopically generated root hairs. Abnormal root morphology was clearly observed in *heb1-1* when exposed to > 5 μM zeocin, whereas Col-0 showed clear defects of root morphology by 7.5 μM zeocin treatment. Bleomycin affected the root morphology in similar fashion to zeocin. *heb1-1* showed the defects in root morphology when treated with lower concentration of bleomycin compared to the case of Col-0. The fact that the *heb* mutants are more sensitive to DSBs-inducible reagents both in terms of root elongation and root morphology suggests that HEB1 and HEB2 are involved in DSBs repair and/or in tolerance to genotoxicity.

1.4.5 Excess B induces DSBs in root tip cells

Based on the results that the *heb* mutants are sensitive to both excess B and induction of DSBs, I hypothesized that excess B toxicity induces DSBs and that induced DSBs were alleviated with the support of condensin II. To examine this hypothesis, I first conducted real-time RT-PCR to quantify the expression of DSBs-inducible genes in the root tips exposed to excess B for 4d. The genes analyzed are as follows; breast cancer susceptibility1 (*BRCA1*; Lafarge and Montane, 2003), gamma response1 (*GR1*; Deveaux et al., 2000), *RAD51* (Doutriaux et al., 1998) and poly (ADP-ribose) polymerase1 (*PARP1*; Doucet-Chabeaud et al., 2001). Expressions of these genes were up-regulated by the excess B treatment in both Col-0 and the *heb* mutants (Figure 1-9 A). This supports the hypothesis that excess B causes DNA damage and *A. thaliana* condensin II functions in DNA damage response. The transcripts of all analyzed genes were 1.5- to 2-fold higher in the *heb* mutants than Col-0 both under the control and the excess B conditions (Figure 1-9 A), suggesting that the increased levels of DSBs in the *heb* mutants irrespective of the B conditions.

I next investigated the levels of DSBs in root tips of Col-0 and the *heb* mutants under both the control and the excess B conditions by the comet assay (Menke et al., 2001). In line with the results that the *heb* mutants showed higher expression of the DSBs-inducible genes, significantly higher accumulation of DSBs was observed in root tips of the *heb* mutants than in Col-0 irrespective of the B conditions (Figure 1-9 B). Four-day-treatment of excess B significantly elevated the levels of DSBs in both Col-0 and the *heb* mutants (Figure 1-9 B and C). These results directly demonstrate that excess B causes DSBs in root tip cells and that *A. thaliana* condensin II is involved in the alleviation of this DNA damage.

1.4.6 *atr* mutant but not *atm* mutant was sensitive to excess B

In eukaryotic cells, two related kinases, ataxia telangiectasia mutated (ATM) and ATM & Rad3-related (ATR) are well-known molecular players required for DNA damage responses in different pathways: ATM is required for sensing of DSBs, and ATR is required for detection of stalled replication forks (Cools and De Veylder 2009). To investigate possible involvement of these kinases in excess B-dependent DNA damage, I examined the growth response of ATM and ATR mutants, *atm-2* and *atr-2*, respectively, under the excess B condition. These mutants have been established to show hypersensitivity to various types of genotoxicities (Garcia et al., 2003; Culligan et al., 2004). Unexpectedly, when grown on medium with excess B for 10d, the root growth of *atm-2* was similar to that of Col-0, whereas the root growth of *atr-2* was more reduced than that of Col-0 (Figure 1-9 D). This result

suggests that ATR has crucial roles in DNA damage responses caused by excess B rather than ATM. It also supports the fact that DNA damage is a cause of B toxicity in root cells.

1.4.7 Simultaneous induction of DSBs and replication blocks mimicked the effect of excess B on root growth in the *heb* mutants

In *A. thaliana*, *atr* is known to be hypersensitive to replication blocks induced by aphidicolin, inhibitor of DNA polymerase α, and hydroxyl urea (HU) that reduce dNTP pools (Culligan et al., 2004). Therefore, the high sensitivity of *atr-2* to excess B gives rise to the possibilities that DNA replication pathway is impaired by the excess B treatment and that condensin II is also involved in the maintenance of replication process. To elucidate these possibilities, I evaluated the sensitivity of the *heb* mutants to aphidicolin and HU by root elongation-assay. When exposed to 8 and 10 μg/ml aphidicolin, the root elongation of the *heb* mutants was severely inhibited compared to that of Col-0 (Figure 1-10 A). On the other hand, the *heb* mutants did not show any sensitivity to another type of replication block reagent, HU (Figure 1-10 B). In terms of alteration of root morphology, the distinct responses of the *heb* mutants to two types of replication block reagents were evident (Figure 1-10 C). In the presence of 8 μg/ml aphidicolin, ectopic root hairs were appeared in the *heb* mutants, but not in Col-0. The difference in the defects of root morphology was cleared by the treatment of 12 μg/ml aphidicolin. Under the aphidicolin treatments, root elongation was inhibited by 30-70% (Figure 1-10 A). By contrast, alteration of root morphology was not observed both in Col-0 and the *heb* mutants even by the treatment of 3 mM HU (Figure 1-10 C), which resulted in 80% inhibition of root elongation (Figure 1-10 B). These results indicate that the *heb* mutants are sensitive to replication blocks induced by aphidicolin in terms of both root elongation and root morphology but not to that caused by HU.

Given that HEB1 and HEB2 are involved in responses to both DSBs and replication blocks, it is possible that both stresses are responsible for excess B hypersensitivity of the *heb* mutants. In root elongation assay, 3mM B treatment reduced the root elongation by about 20% of that under the control condition in Col-0 and by about 60% in the *heb* mutants (Figure 1-10 D). The extents of the inhibition of root elongation under 3 mM B are 3-fold higher in the *heb* mutants than that of Col-0. In contrast, DSBs-inducible (Figure 1-8 A and B) and replication block (Figure 1-10 A) reagents did not differentiate the mutant from the wild-type to such extents. In zeocin treatments, the difference in the inhibition of root elongation was 1.5-fold at the maximum. Similarly, aphidicolin treatments did not differentiate the mutant from the wild-type to an extent of the 3 mM B treatment (Figure 1-10 D). These observation suggest that either DSBs or replication blocks is not sufficient for excess B hypersensitivity of the *heb* mutants.

I then examined the combined effect of induction of DSBs and replication blocks by the root elongation assay. I chose the concentrations of zeocin and aphidicolin (1 μM and 4 μg/ml, respectively) to the level that cause 20% inhibition of root elongation in Col--0, similar extents to the 3 mM B treatments. Single treatment of zeocin and aphidicolin at these concentrations did not differentiate root elongation of the *heb* mutants from Col-0 to an extent of 3 mM B treatment (Figure 1-10 D). On the other hand, simultaneous treatment of these two reagents induced severe root growth reduction only in the *heb* mutants which was comparable to that observed under the excess B condition (3 mM) in the *heb* mutants (Figure 1-10 D). In regards to root morphology, single treatment of zeocin and aphidicolin did not severely alter root morphology in both Col-0 and the *heb* mutants, whereas the simultaneous treatment caused severe defects in root morphology only in the *heb* mutants (Figure 1-10 E). By contrast, root morphology of both Col-0 and the *heb* mutants were not severely altered by 3 mM B treatment (Figure 1-10 E). The severe defects in root morphology in the *heb* mutants were observed at 6 mM B treatment that reduces relative root elongation by about 20% Figure 1-10 D and E). Overall, it was strongly suggested that both induction of DSBs and impairment of replication process are involved in excess B toxicity. I also think that the findings supported the idea that HEB1 and HEB2 are required for the responses to both types of DNA damages. In addition, excess B (3 mM) inhibited root elongation without showing severely altered root morphology as caused by DNA damaging reagents in the *heb* mutants, implying that the functions of HEB1 and HEB2 are most likely to contribute to proper root elongation rather than structural maintenance of root tips.

1.4.8 B toxicity affects cell cycle progression in roots

Plants have checkpoint control systems to delay and/or arrest the cell cycle progression in response to a variety of DNA stresses (Cools and De Veylder 2009). The present study established that B toxicity causes DNA damage in *A. thaliana* root tips. In addition, a mutant of ATR that is known to regulate G2 checkpoint showed excess B sensitivity. It is possible that excess B treatment leads to defect in cell cycle progression in roots. The number of cells in meristematic zone both in Col-0 and the *heb* mutants were reduced by 4d excess B treatment (Figure 1-11 A). Extents of the reduction were higher in the *heb* mutants (about 50%) than in Col-0 (about 20%) (Figure 1-11 A), suggesting that cell division was impaired by excess B, especially in the *heb* mutants. To examine cell cycle progression in root tips exposed to excess B for 4d, cell ploidy was examined (Figure 1-11 B). In the mitotic cells, the counts of 2C and 4C correspond mostly to the number of cells in G1 and G2 phase, respectively (López-Juez et al., 2008). The value of 4C/2C was 0.36 in

Col-0, whereas it was 0.50 and 0.58 in *heb2-1* and *heb2-2*, respectively. Excess B treatment increased 4C/2C ratio in both Col-0 and the *heb* mutants (0.42 in Col-0, 0.73 in the *heb* mutants). These data suggest that transition from G2 phase to M phase is disturbed in the *heb* mutants and consequently excess B prolongs the duration of G2 phase, which might result in the reduction of cells in the meristematic zone

1.4.9 Effect of excess B and condensin II on expression of cell cycle-related genes

I then investigated expression of the cell cycle-related genes such as *CYCA*, *CYCB* and *CDKs* (cyclin dependent kinases) in the root tips by real time RT-PCR (Figure 1-11 B). Total RNA was extracted from the tip of the root tissues (1 cm in length) exposed to excess B for 4d and subjected to the analysis. *CYCA2;1* is known to be expressed at G2/M phase (Menges et al., 2005). The *heb* mutants showed more than 5.9-fold higher accumulation of *CYCA2;1* transcript than Col-0 and excess B treatment drastically increased *CYCA2;1* transcript accumulation in both Col-0 (8.4-fold) and the *heb* mutants (> 17-fold). However, in contrast to the case of *CYCA2;1*, the transcripts of other A2-type cyclin genes (*CYCA2;2*, *CYCA2;3* and *CYCA2;4*) did not show more than two fold differences between Col-0 and the *heb* mutants. Excess B treatment did not evidently induce these genes. As like *CYCA2;1*, *CYCA1;1* also expressed at G2/M phases (Menges et al., 2005). Excess B treatment increased the transcript of *CYCA1;1* in the *heb* mutants but decreased in Col-0. *CDKA1* activates both types of *Cyclins* A and B and regulates G1/S and G2/M progression (Hemerly et al., 1995). The transcript level of *CDKA1* was significantly induced by excess B in both Col-0 and the *heb* mutants. The *heb* mutants showed higher expression of *CDKA1* than Col-0 under both the control and the excess B conditions. I also examined the expressions of *CYCB1;1* and *CDKB2;1,* G2/M specific markers (Menges et al., 2005; Culligan et al., 2006). Compared to Col-0, transcript level of *CYCB1;1* was slightly higher in *heb2-1*, but was not changed in *heb1-1*. Excess B treatment increased the transcripts of *CYCB1;1* in the *heb* mutants but did not in Col-0. Expression of *CDKB2;1* was not different between Col-0 and the *heb* mutants and excess B did not affect the expression both in Col-0 and the *heb* mutants.

Taken together, excess B affects expression of cell cycle-related genes in a unique manner in that not all the genes involved in G2/M progression were coordinately regulated. Among the genes examined, *CYCA2;1* is shown to be regulated through condensin II.

1.4.10 Expression of condensins responds to B toxicity

The published microarray data using synchronized *A. thaliana* cultured cell suggests that the expression of condensin subunits *CAP-H2 (HEB2)*, *CAP-D3* and *CAP-H* are most

abundant at late S to early G2 phases (Appendix Figure 1-1). Human *CAP-H* mRNA is also transcribed during G2 phase (Cabello et al., 2001). In this study, I found that excess B treatment induces G2 delay and thus it is possible that the condensin genes are induced by the excess B treatment. Real-time RT-PCR analysis of non-SMC subunits of condensins revealed that the transcripts encoding all non-SMC subunits of condensin I and II were increased more than 2-fold by the excess B treatment (Figure 1-12 A).

To examine if the regulation is conferred by the promoter, *pHEB2::GUS* construct were made and introduced into Col-0. In roots, GUS activities were observed in primary root tips and lateral roots, and steles (Figure 1-12 D-F). Strong GUS activities were observed in early developing lateral roots and the region surrounding the quiescent center and stem cells in RAMs (Figure 1-12 F), suggesting that condensin II is expressed strongly at the mitotic active tissues such as root tips. GUS activities in root tips are induced by excess B treatment (Figure 1-12 G), suggesting that B-dependent *HEB2* expression is regulated through the promoter region of the gene.

1.4.11 Condensin II is required for alleviation of DNA damage caused by UV-C in shoots

Plants cannot avoid exposure of UV lights that damage many aspects of plant processes at the physiological and DNA levels. Among UV lights, UV-C is usually irrelevant to plants since it is blocked by the earth's stratosphere. However, UV-C produces pyrimidine dimmer as produced by UV-B, and this DNA photoproduct causes replication blocks in plants (Britt 1996). Because *HEB2* is not only expressed in roots, but also expressed in shoot tissues such as cotyledon and shoot apical dome (Figure 1-12 B and C; Fujimoto et al., 2005), it is possible that condensin II is involved in alleviating UV-inducible DNA damage in the aerial portions of plants. I examined the UV-C sensitivity of the *heb* mutants and DSBs accumulation. The reduction of shoot growth by the UV-C radiation was severer in the *heb1* mutants than in Col-0 (Figure 1-13 A). The comet assay revealed that the *heb1* mutants highly accumulated DSBs compared to Col-0 regardless of UV-C radiation (Figure 1-13 B). Accumulation of DSBs was more increased by UV-C radiation in the *heb1* mutants than in Col-0 (Figure 1-13 B). These results suggest that condensin II is also essential for UV-C tolerance by alleviating the DNA damage in the aerial parts of *A. thaliana*.

1.5 Discussion

In this study, I established that two genes *CAP-G2* and *CAP-H2*, components of condensin II, are essential for excess-B toxicity tolerance through forward genetics using *A. thaliana* mutants, *heb1-1* and *heb2-1,* hypersensitive to excess B. Through the analysis, I

established the function of *A. thaliana* condensin II in alleviation of DSBs and possibly in the maintenance of replication process, which are required for the tolerance to B toxicity in plants. The fact that condensin II is also conserved in animals suggests that the basis of B toxicity mechanism may be common among plants and animals.

1.5.1 *A. thaliana* has a mechanism to tolerate excess B concentration in cells

It is well known that the levels of excess B tolerance of plants and B contents in the tissue are negatively correlated: tolerant cultivars of barley accumulate less B than sensitive cultivars (Nable 1991). Intracellular B content is also negatively correlated with the degree of excess B tolerance in barley (Hayes and Reid 2004). These studies established that reduction of B concentration in cells is a critical step in excess B tolerance in plants. However, in the case of the *heb* mutants, reduction of B concentration in cells is not critical for tolerance to excess boron. Contents of B in the *heb* mutants were less than that of the wild-type while the sensitivity to excess B condition is much higher in the mutants (Figure 1-1 E). This finding establishes that *A. thaliana* have a system to tolerate excess B concentration in cells. This idea is supported by the fact that *A. thaliana* RBP4c' involved in RNA transcription or processing has an ability to improve the boric acid tolerance of yeast without reducing B concentrations in cells (Nozawa et al., 2006). The lower B contents in the *heb* mutants could be due to shorter root length and/or alteration of transport activities.

1.5.2 DNA damages are major causes of B toxicity in roots of *A. thaliana*

Excess B is known to cause defects in chromosomal structure in soybean and onion, and it is thought that the chromosomal defects by excess B treatment are due to DNA damage (Liu et al., 2000; Konuk et al., 2008). In this study with the commet assay, I established that in root tip cells, excess B causes DSBs (Figure 1-9 B). I also demonstrated that in the excess B treated roots, *BRCA1*, *GR1*, *RAD51* and *PARP1,* genes known to be associated with the level of DNA damage (Doutriaux et al., 1998; Doucet-Chabeaud et al., 2001; Doutriaux et al., 2000; Lafarge and Montane, 2003) are induced (Figure 1-9 A). Moreover, dead cells were found in the region around quiescent center in the wild-type under the excess B condition (Figure 1-6 J). It is known that stem cell niches are hypersensitive to DNA damage and cell death primarily occurs in this region after treatments of DNA damaging reagents in roots of *A. thaliana* (Fulcher and Sablowski 2009). The cell death observed under the excess B condition may be due to the accumulations of DNA damage caused by the excess B. These observations established that the excess B treatment induces DNA damage.

I also observed that the extent of DNA damage negatively correlated with the root elongation (Appendix Figure 1-2), suggesting that inhibition of root elongation is due to DNA

damage in roots of *A. thaliana* exposed to excess B. Furthermore, in the case of *heb1-1* and *heb2-1*, I also revealed that the combined effects of zeocin and aphidicolin, both are known to cause DNA damages directly or indirectly, mimicked the effect of excess B (Figure 1-10 D), supporting that B toxicity is caused through DNA damage. Moreover, the observations that the wild-type roots treated with high concentrations of DSBs-inducible reagents or aphidicolin were short and exhibited severe root morphological defects (Figure 1-8 C; Figure 1-10 C). The morphological defects are similar to those observed in the roots of *heb1-1* and *heb2-1* treated with excess B (Figure 1-6 E and F). *atr-2*, a mutant with altered sensitivity to DNA damage (Culligan et al., 2004), was sensitive to excess B. These findings confirm the view that DNA damage is the major cause of B toxicity in roots.

How excess B treatment induces DNA damage? Oxidative stress is one of the causes of DNA damage (Roldań-Arjona and Ariza 2009), and it occurs in aerial parts of plants exposed to excess B (Gunes et al., 2006; Molassiotis et al., 2006; Cervilla et al., 2007). However, in the case of *heb1-1* and *heb2-1*, they were not sensitive to oxidative stress-inducible reagents (Figure 1-2 A and B), suggesting that oxidative stress is unlikely to be a major part of B toxicity in roots. Therefore, oxidative stress is not likely to be a cause of excess B-dependent DNA damage. Understanding of the mechanism of how B induces DNA damage is a key subject of future investigation of B toxicity.

1.5.3 B toxicity-induced DNA damage has a special character

I also found that *atm-2,* a mutant sensitive to DNA damage, was not sensitive to excess B in contrast to the case of *heb2-2* and *atr-2* (Figure 1-9 D). Cell death after DNA damage in the stem cell niche requires both ATM and ATR (Fulcher and Sablowski 2009). This implies that both ATM and ATR were required for excess B tolerance. However, I found that only ATR was crucial for excess B tolerance but not ATM. This can be interpreted as follows. It is known that ATM is primarily activated by DSBs and regulates transcription of genes including *BRCA1*, *GR1*, *RAD51* and *PARP1* (Garcia et al., 2003; Culligan et al., 2006). In contrast, ATR is not involved in the induction of these genes (Culligan et al., 2006). ATR, but not ATM, is required for sensing of ssDNA caused through replication blocks (Sancar et al., 2004). It is possible that excess B primarily causes replication blocks and DSBs observed under the excess B condition may be a consequence of the replication blocks, as it is proposed previously (Kozak et al., 2009; Schuermann et al., 2009). In support of this hypothesis, I found that the *heb* mutants were also sensitive to UV-C, inducer of replication blocks (Britt 1996), and accumulated more DSBs than the wild-type did (Figure 1-13 A and B). It is also known that sensing of replication blocks by ATR induces G2 delay through checkpoint system (Culligan et al., 2004). Therefore, if my hypothesis is correct, it

is possible that in both the wild-type and *atm-2*, ATR-mediated G2 delay still occurs in response to replicational stress derived from B toxicity and this G2 delay is likely to be required for damaged DNA repair. This could be a reason for the similar root growth in these plants under the excess B condition. On contrary, in the case of *atr-2*, ATR-mediated G2 delay is defective, which might result in the progression of cell cycle with damaged DNA and subsequent root growth inhibition under the excess B condition.

Aluminum is also known to be a genotoxic factor in plant cells (Rounds and Lersen 2008). However, in contrast to B toxicity-tolerance, aluminum toxicity-tolerance in *A. thaliana* does not require ATR function, since *atr* mutants are tolerant to aluminum toxicity compared to the wild-type (Rounds and Lersen 2008). This implies that although genotoxicities are common feature of both B and Al toxicity, the process of how toxicity develops is partially different. In other words, plants may have particular systems to attenuate genotoxicities induced by each abiotic stress.

1.5.4 Excess B affects cell cycle progression

I found that the excess B treatment increased the ratio of G2 cells and decreased the number of mitotic cells in root tips of the wild-type (Figure 1-12 A and B). These phenomena were more evident in the *heb* mutants exposed to excess B (Figure 1-12 A and B). Reduced numbers of mitotic cells by the excess B treatment might reflect the severe delay in G2 progression, resulting in the reduced rate of cell division. Furthermore, involvement of ATR in excess B tolerance indicates that G2 checkpoint and subsequent G2 delay is required for dealing with DNA damage caused by excess B treatment to prevent the proceeding of M phase with damaged DNA. These findings indicate that the treatment of excess B delays the cell cycle progression during G2 phase. To further support the cell cycle retardation by excess B, I examined expression of *Cyclins*. It is known that in the case of G2 delay induced by aphidicolin and ionizing irradiation, *A. thaliana* strongly induces *CYCB1;1* expression in the wild-type (Culligan et al., 2004, 2006). Thus, *CYCB1;1* is considered to be a marker for DNA-damaged cell as well as defects in G2/M progressions (Culligan et al., 2006). However, in the case of B toxicity, among G2/M specific cell cycle-related genes examined, only *CYCA2;1* was strongly induced whereas *CYCB1;1* was not (Figure 1-12 C). Different expression patterns of *Cyclins* in response to G2 delay may suggest the pattern is dependent on the type of stress that has an adverse impact on the cell cycle progression. Molecular characterization of *CYCA2;1* under the excess B condition may help understanding of B toxicity in cell cycle progression.

1.5.5 *A. thaliana* condensin II has a role in reducing DNA damage

In this study, I demonstrated that *HEB1* and *HEB2* encode different non-SMC subunits of condensin II, CAP-G2 and CAP-H2, respectively (Figure 1-4 A and B). Through characterization of the *heb* mutants, I found that condensin II is required for the tolerance to additional DSBs (Figure 1-8 A-C) and replication blocks (Figure 1-10 A and C) in regards to root elongation, indicating that condensin II functions in maintaining genomic stability through reducing DNA damage in roots. This is in agreement with the highly accumulated DSBs and well-expressed DNA repair genes such as *BRCA1* in root tips of the *heb* mutants in the absence of additional genotoxic stresses (Figure 1-9 A and B). I also found that condensin II is required for the tolerance to DNA damage induced by UV-C in the aerial parts (Figure 1-13 A and B). Analysis of *pHEB2*/*CAP-H2*::*GUS* revealed that condensin II is expressed in root and shoot including RAMs and the shoot apical domes (Figure 1-12 C and F) and responsive to excess B toxicity in RAMs (Figure 1-12 G) in which DNA damage appeared to be accumulated. Therefore, I propose that *A. thaliana* condensin II contributes to genomic stability through reducing DNA damage especially in the mitotically active site.

The mechanism of *A. thaliana* condensin II function in reducing DNA damages is unknown, but studies from animal and yeast condensin provide two hypotheses. One is that condensin II may physically protect the genome from the attack of genotoxic substrates. It has been established that yeast condensin compacts the genomes during interphase in response to nutrient starvation for genome stabilization (Tsang et al., 2007a, 2007b). Another one is that condensin II is involved in the repair of DSBs and damaged replication forks. Since among systems for damaged DNA repair in eukaryotic cells, recombinational repair plays important roles in both types of DNA damage, it is thus plausible that condensin II mediates homologous recombination. Indeed, human condensin II has been reported to function in homologous recombination repair after DSBs generation (Wood et al., 2008). In addition, Ide et al (2010) proposed that yeast condensin is crucial for making foothold for facilitating recombinational repair of DSBs and damaged replication forks by cohesion of sister chromatide in the ribosomal DNA array. Taken together, it is tempting to speculate that *A. thaliana* condensin II plays role in preventing and/or repairing DNA damages.

Plants have another type of condensin, condensin I (Ono et al., 2003; Fujimoto et al., 2005). Both condensins are localized on chromosomes during mitosis and function in proper chromosomal segregation as animal condensins do (Fujimoto et al., 2005). On contrary, interphase condensins might have distinct roles due to the different localizations during interphase: condensin I in the cytosol and condensin II in the nucleus (Fujimoto et al., 2005). However, I cannot rule out the possibility that the *A. thaliana* condensin I also

contributes to the maintenance of genomic stability during interphase. In animal cells, subportion of condensin I is remained in the nuclear (Schmiesing et al., 2000) and is involved in repair of ssDNA but not DSBs during interphase (Heale et al., 2006). In the case of B toxicity, non-SMC subunits genes of condensin I were upregulated as well as the genes of condensin II (Figure 1-12 A), suggesting that *A. thaliana* condensin I has roles in reducing DNA damage induced by the excess B treatment, similar to the case of condensin II. I could not examine this hypothesis because the *A. thaliana* condensin I non-SMC mutants were not obtained. Those mutants are likely to be embryonic lethal.

1.5.6 Requirement of *A. thaliana* condensin II in progression of G2 phase

Cell polidy analysis showed that the ratio of G2 phase cells in root tips were higher in the *heb* mutants than in the wild-type (Figure 1-11 B), indicating the prolonged G2 phase in the mutants. This established that condensin II is required for proper cell cycle progression during G2 pahse. The G2 delay in the mutants may be due to the defect in chromosomal maintenance through condensin II during G2 phase. If this is the case, the similar growth and developmental responses to HU among the wild-type and the *heb* mutants are reasonable (Figure 1-10 B and C). Culligan et al (2004) proposed that aphidicolin induces delay at G2 phase, whereas HU primarily induces delay at G1 rather than G2 phase in *A. thaliana*. The difference in sensitivity of the *heb* mutants to two distinct types of replication block reagents (Figure 1-10 A-C) suggests the importance of condensin II for the cell cycle progression during G2 phase but not during G1 phase for managing DNA damage.

A. thaliana mutants, *teb-1* and *nrp1*/*nrp2*, are known to have elevated DNA damage and to be defective in G2/M progression (Inagaki et al., 2006; Zhu et al., 2006). These mutants show short-root phenotype and ectopically accumulate the transcripts of *CYCB1;1* in root cells. However, among G2/M specific cell cycle-related genes examined, only *CYCA2;1* , but not *CYCB1;1,* was highly upregulated in the *heb* mutants than in the wild-type (Figure 1-11 C). These differences in the expression pattern of *Cyclins* in G2 progression may suggest that DNA damage responses including the regulation of cell cycle in the *heb* mutant is different from those in mutants like *teb-1* and *nrp1*/*nrp2*. I should note that the expression of *CYCA2;1* was also drastically induced by the excess B treatment in the *heb* mutants (Figure 1-11 C). The loss of *CYCA2;1* expression is known to result in increased cell polidy in *A. thaliana* (Yoshizumi et al., 2006). It is possible that condensin II may negatively control cell polidy level, especially under the DNA damaging condition such as excess B.

In the case of excess B tolerance in *A. thaliana*, both condensin II and ATR were essential (Figure 1-1 A; Figure 1-9 D), suggesting the possibility that condensin II acts with

ATR coordinately. Interestingly, human CAP-D2 and CAP-H2 were identified as candidates for ATM/ATR substrate by a proteomic analysis of phosphorylated proteins in response to DNA damage (Matsuoka et al., 2007). Sequence analysis revealed that *A. thaliana* HEB1/CAP-G2 and HEB2/CAP-H2 also have some SQ motifs, the phosphorylation site specifically recognized by ATM/ATR (data not shown). It is therefore possible that ATR/ATM interacts with condensin II and the condensin II mediates G2 checkpoint control in *A. thaliana*. Detailed analysis of the genetic interaction between mutants of condensin II, ATM and ATR genes may provide us new insights into the mechanisms of the regulation of condensin II and G2 checkpoint system.

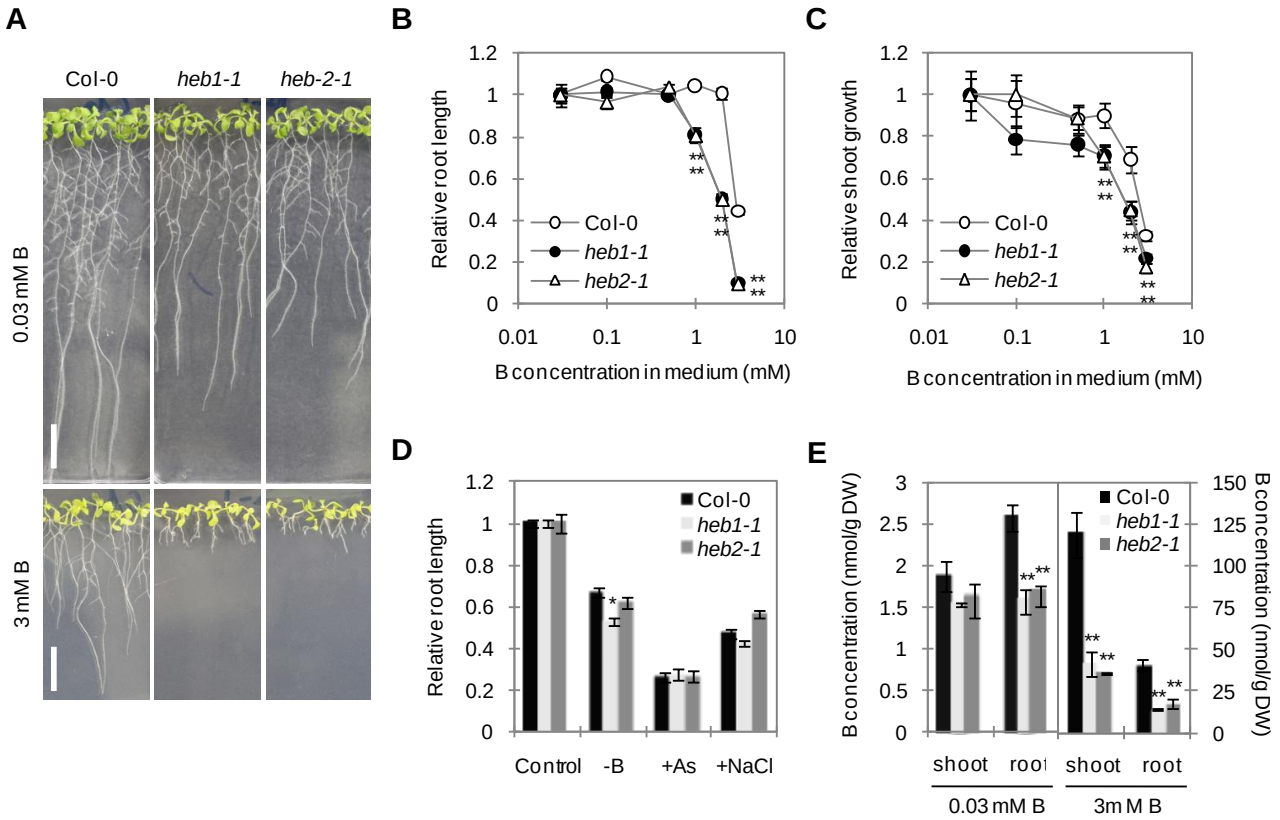

Figure 1-1 Hypersensitivity and specificity of *heb1-1* and *heb2-1* to excess B.
(A) Short-root phenotype of *heb1-1* and *heb2-1* under excess B condition. Col-0, *heb1-1* and *heb2-1* were grown under 0.03 mM (upper) and 3 mM B conditions (lower) for 14d. Bars, 1 cm. Dose-dependent (0.03, 0.1, 0.5, 1, 2 and 3 mM) effects of B on root (B) and shoot growth (C) of Col-0, *heb1-1* and *heb2-1*. The primary root length and shoot flesh weight of 14d-seedlins were measured. Data was expressed as a ratio relative to the value in 0.03mM B condition. Mean ± standard error is shown (n > 16). (D) Sensitivity of Col-0, *heb1-1* and *heb2-1* to mineral stresses; low B (0.03 μM B), arsenite (7.5 μM As) and salinity (75 mM NaCl). The primary root length of 14-d-seedlings was measured. Data was expressed as a ratio relative to the value in control condition. Mean ± standard error is shown (n > 12). (E) Determination of the B contents. Col-0, *heb1-1* and *heb2-1* were grown as described in (A). Mean of three replicates ± standard error is shown. DW, dry weight. Asterisks represent significant difference between Col-0 and each *heb* mutant (*, $P < 0.05$ and **, $P < 0.01$ by Student's *t*-test).

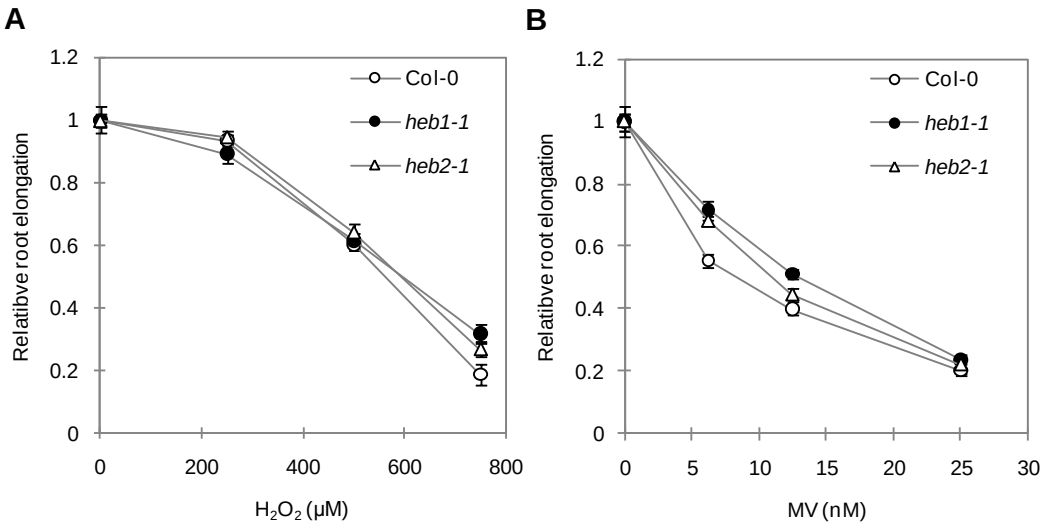

Figure 1-2 Sensitivity of Col-0, *heb1-1* and *heb2-1* to oxidative stress.
Effects of oxidative damage-inducing reagents, hydrogen peroxide (H_2O_2) (A) and methyl viologen (MV) (B) on root elongation during 4d (see detail in Materials and Methods). Data was expressed as a ratio relative to the value in control condition. Mean ± standard error is shown (n > 8).

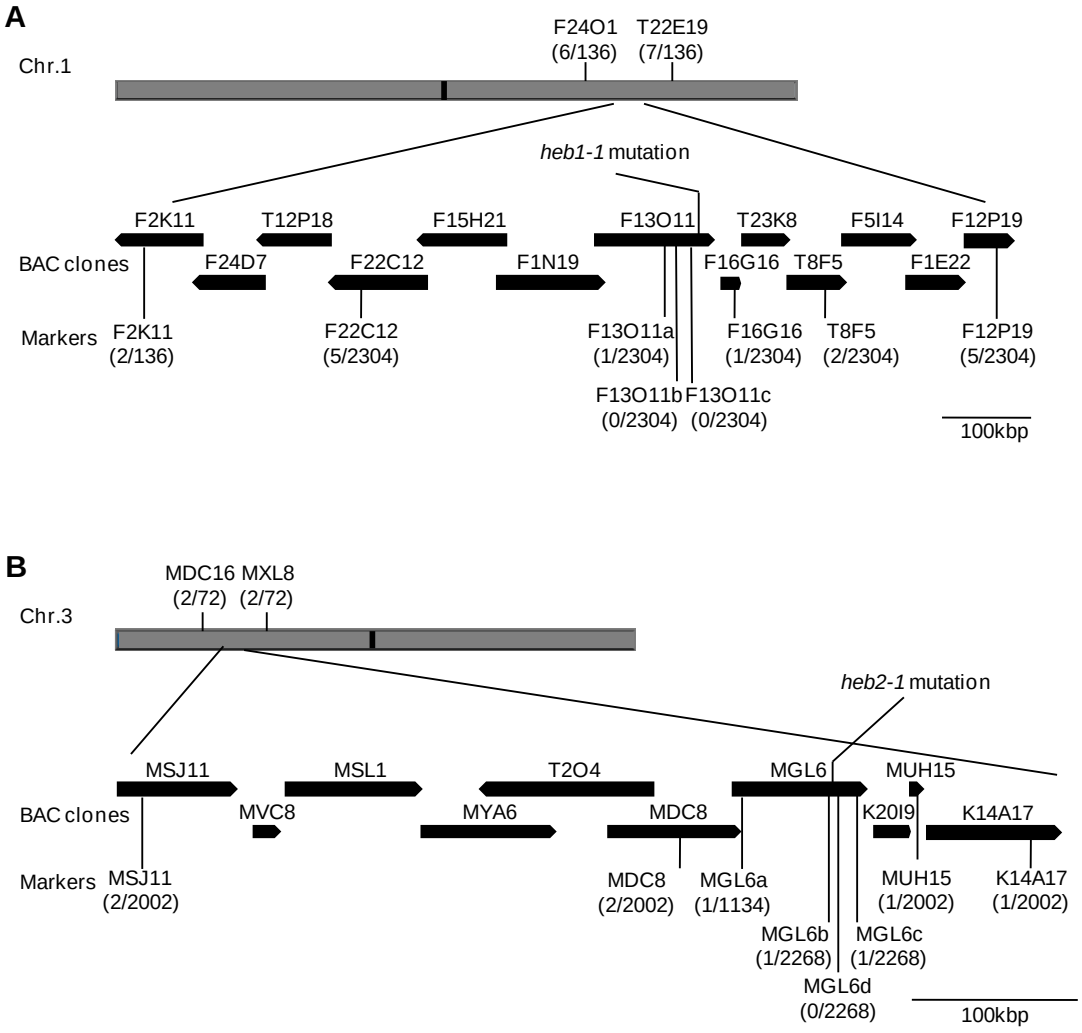

Figure 1-3 Mapping of *heb1* and *heb2* mutations.
Map position of *heb1-1* (A) and *heb2-1* (B) mutation. Marker used and the number of chromosomes at each marker position over the number of total chromosomes analyzed are shown.

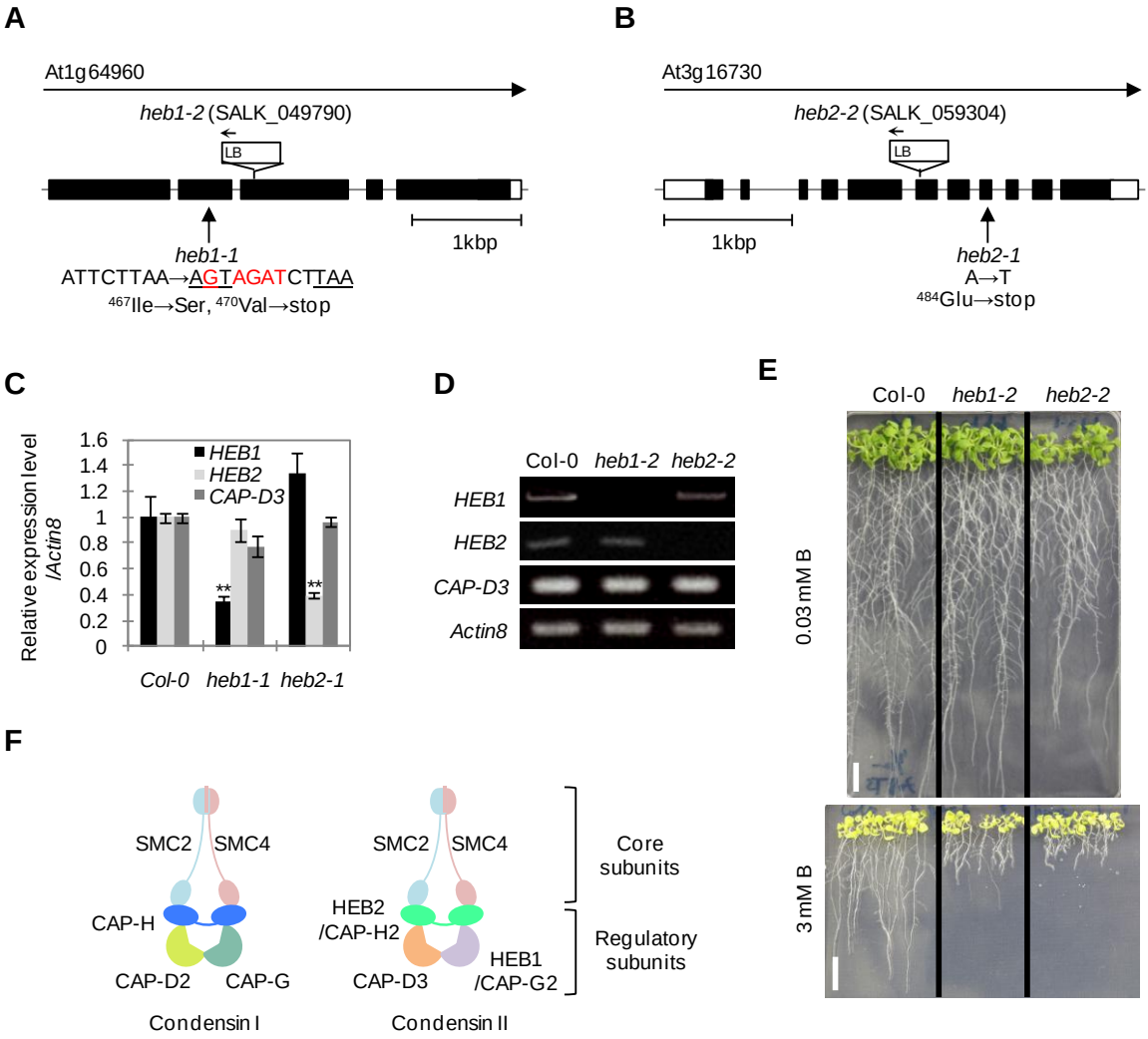

Figure 1-4 Molecular characterization of *HEB1* and *HEB2*.
Genomic structure of *HEB1* (A) and *HEB2* (B) genes. Black and white rectangles indicate the coding regions and untranslated regions (UTRs), respectively. The mutation sites for *heb* mutants and insertion site for SALK lines are shown. (C) Subunit organization of two types of condensin complexes. (D) Real time PCR analysis of condenisn II genes expressions in *heb1-1* and *heb2-1*. RNA was extracted from whole roots of 14-d-seedlings grown under 0.03 mM B condition. At least 10 plants were used per replicate. Condensin II genes expressions were normalized with *Actin8* expression. Data was expressed as a ratio relative to the value in Col-0. Mean of three replicates ± standard error is shown. Asterisks represent significant difference between Col-0 and each *heb* mutant (**, $P < 0.01$ by Student's *t*-test). (E) Semiquantitative RT-PCR for the expression of condenisn II genes in Col-0, *heb1-2* and *heb2-2*. RNA extraction was conducted as described in (D). *Actin8* was used as a reference. (F) Excess B-dependent short-root phenotype of alleles for *heb1* and *heb2* mutants. Col-0 and *heb* mutants were grown under 0.03 mM (upper) and 3 mM B conditions (lower) for 10d. Bars, 1 cm.

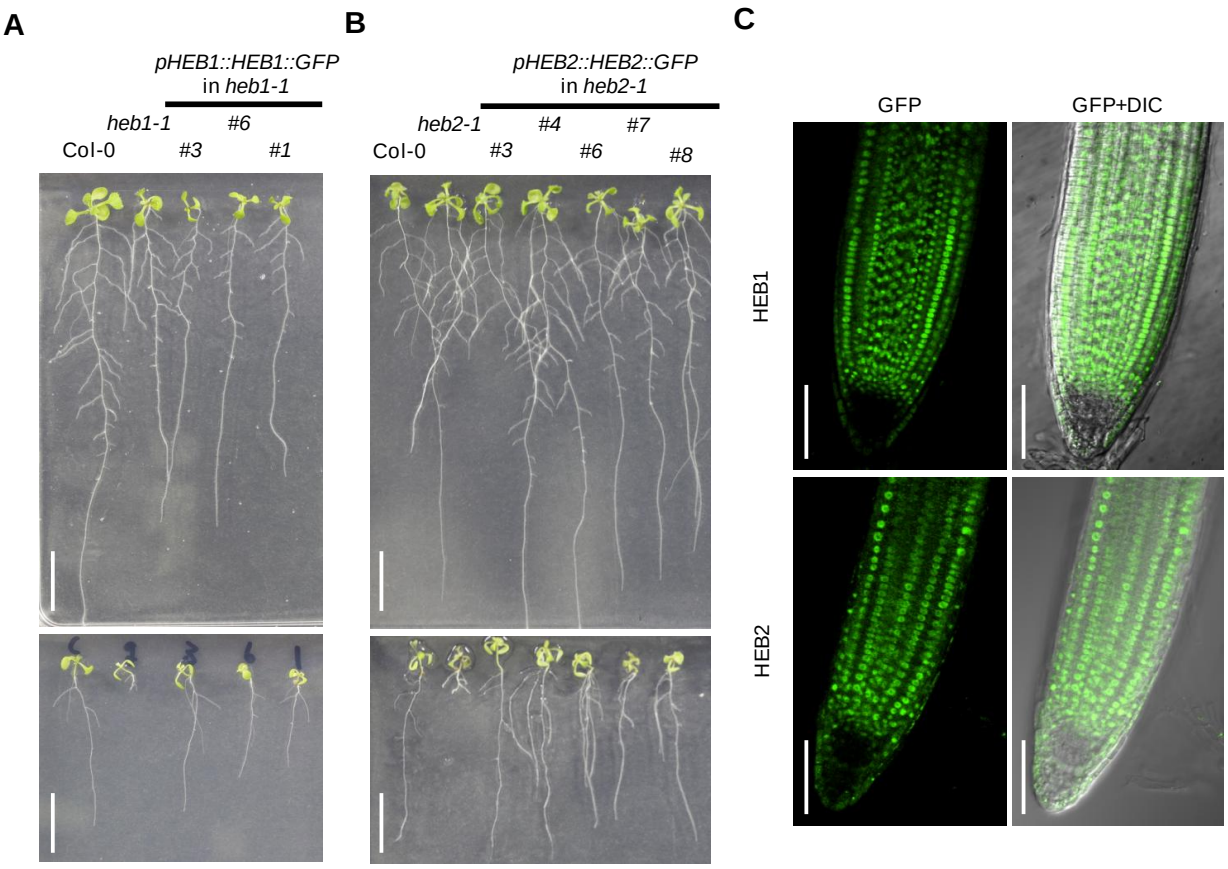

Figure 1-5 Complementation analysis of *heb1-1* and *heb2-1*.
Phenotype of *pHEB1::HEB1::GFP* introduced transgenic *heb1-1* plants (A). Phenotype of *pHEB2::HEB2::GFP* introduced transgenic *heb2-1* plants (B). At least three independent transgenic lines were analyzed. Plants were grown on 0.03 mM B (left) and 3 mM B (right) condition for 10d. Bars, 1 cm. (C) Expression of *HEB1:GFP* (upper) and *HEB2:GFP* (lower) in transgenic plants root described in (A) and (B), respectively. GFP fluorescence (left) and differential interference contrast (DIC) images (right) are shown. GFP was observed in 7d-old-seedlings using confocal microscopy. Bars, 50 μm.

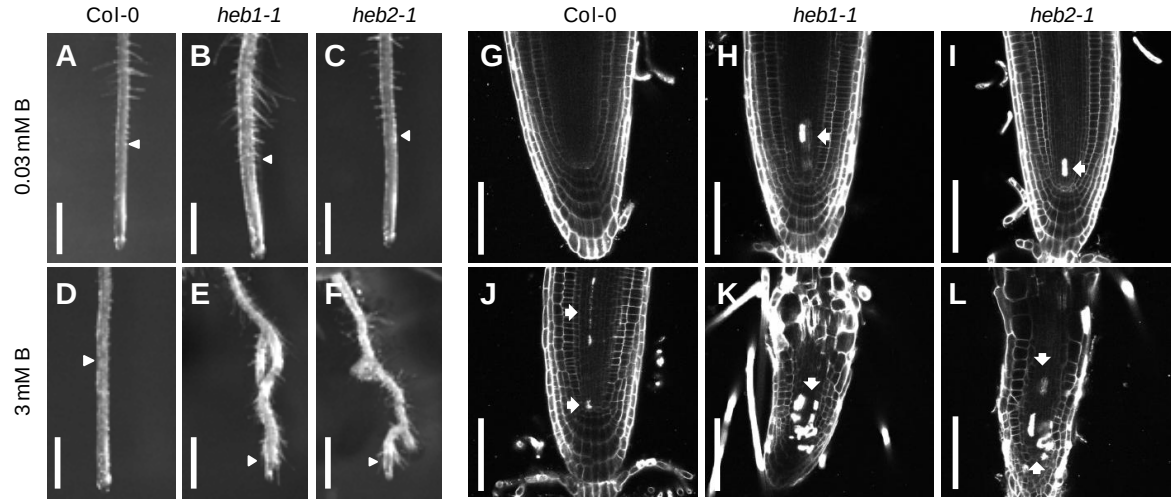

Figure 1-6 Effects of excess B on root morphology of condensin II mutants.
Primary roots of Col-0 [(A) and (D)], *heb1-1* [(B) and (E)] and *heb2-1* [(C) and (F)] grown under 0.03 mM B [(A) to (C)] and 3 mM B [(D) to (F)] conditions for 14d. Arrowheads indicate the first position of root hair. Bars, 1 mm. Longitudinal sections of root tips of Col-0 [(G) and (J)] *heb1-1* [(H) and (K)] and *heb2-1* [(I) and (L)] grown under 0.03 mM B [(G) to (I)] and 3 mM B [(J) to (L)] conditions for 14d. Propidium iodide was used for the visualization of cell walls. Entirely-stained cells are dead cells (arrows). Bars, 50 μm.

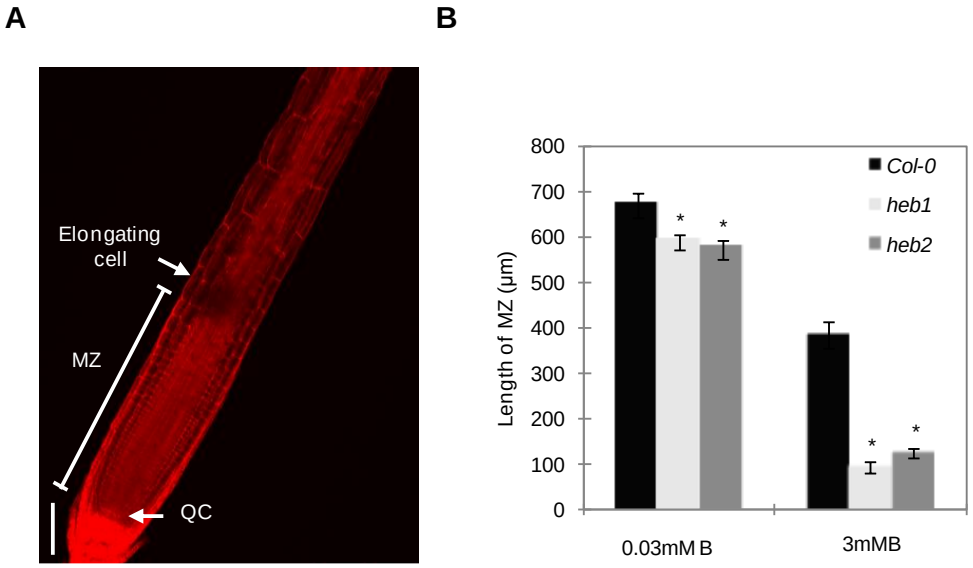

Figure 1-7 Effects of excess B on length of meristematic zone.
(A) Definition of the merstematic zone (MZ) in this study: from the quicent center (QC) to the first fully elongated cell. Cell walls were visualized using propidium iodide. Bar, 100 μm. (B) Measurement of the length of MZ using ImageJ software. Col-0, *heb1-1* and heb*2-1* were grown under 0.03 mM and 3 mM B conditions for 14d. Means ± standard error are shown (n > 10). Asterisks represent significant difference ($P < 0.01$ by Student's *t*-test) between Col-0 and each *heb* mutant.

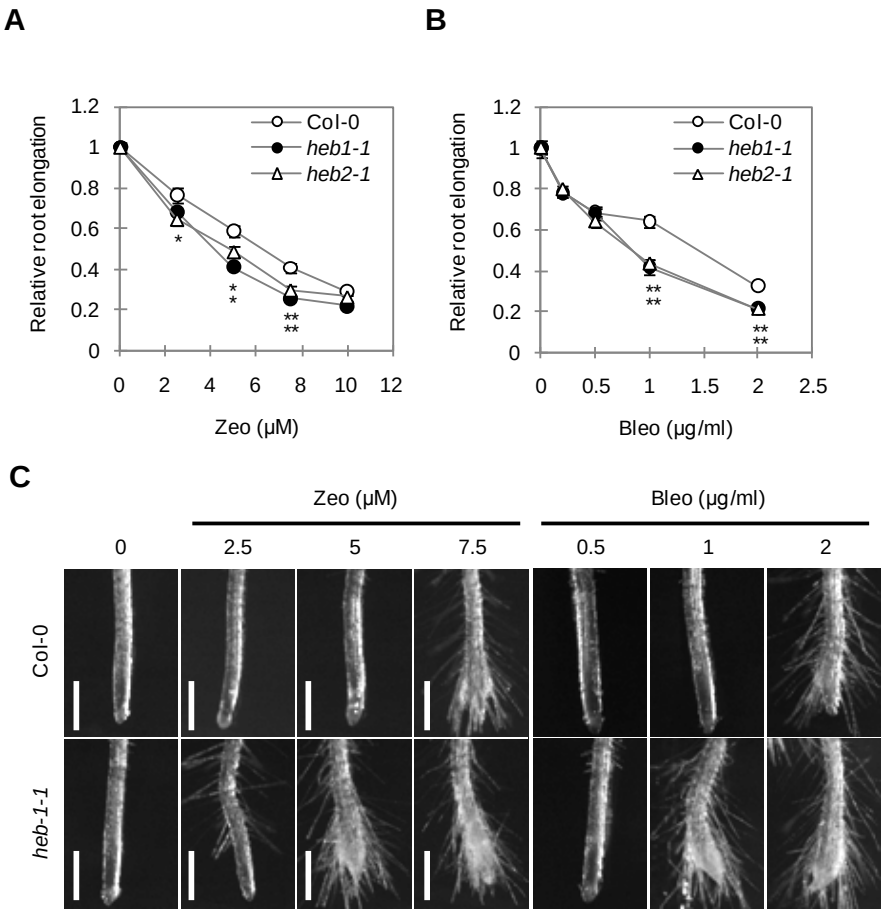

Figure 1-8 Sensitivity of the *heb* mutants to induction of DSBs in root growth.
Effects of DSBs-inducing reagents, zeocin (Zeo) (A) and bleomycin (Bleo) (B) on root elongation during 4d (see detail in Materials and Methods). Data was expressed as a ratio relative to the value in control condition. Mean ± standard error is shown (n > 13). Asterisks represent significant difference between Col-0 and each *heb* mutant (*, $P < 0.05$ and **, $P < 0.01$ by Student's *t*-test). (C) Root morphology of Col-0 and *heb1-1* mutant plants grown on media containing different concentrations of Zeo and Bleo as described above. Note that *heb2-1* also showed similar morphological defects as observed in *heb1-1*. Bars, 500 μm.

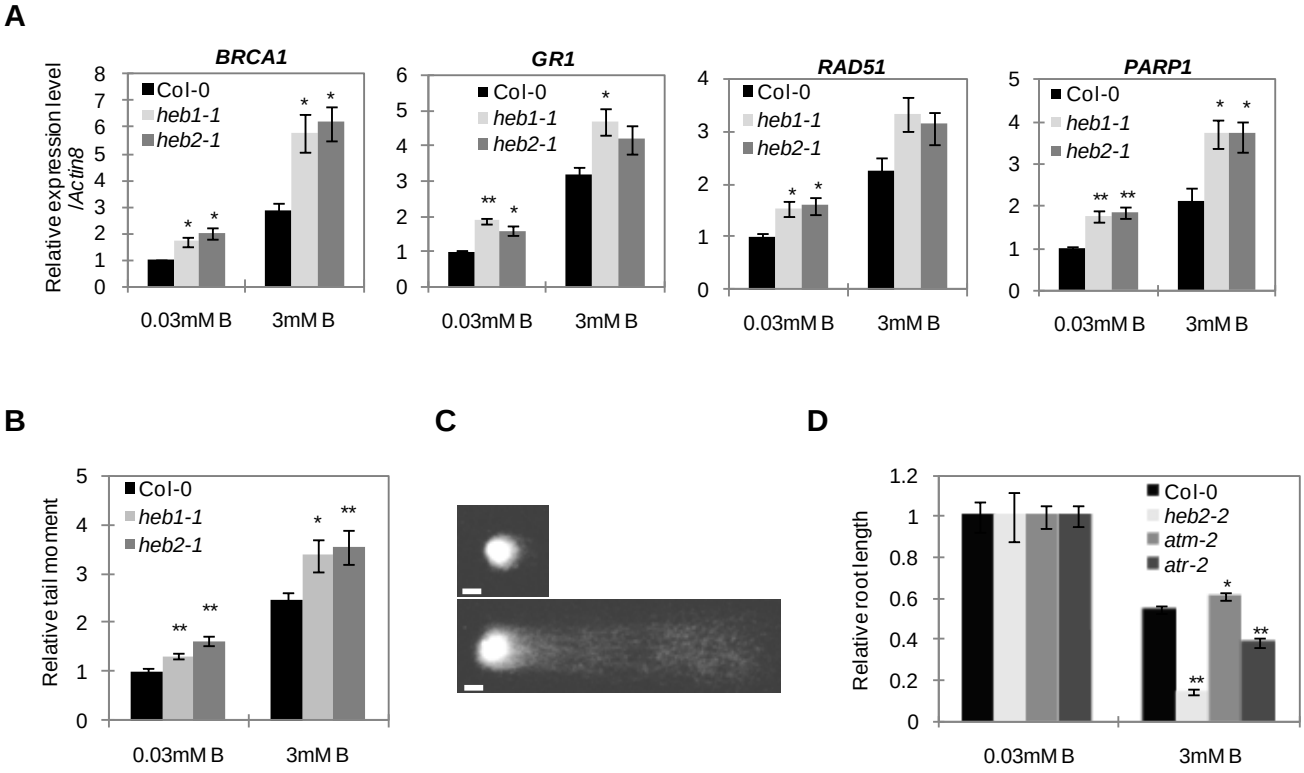

Figure 1-9 Elevated DSBs in the *heb* mutants and induction of DSBs by excess B in roots.
(A) Real time PCR analysis of DNA damage-inducible genes expressions in root tip in response to B toxicity. 5d-seedlings of Col-0 and *heb1-1* and *heb2-1* were transferred to 0.03 mM and 3 mM B conditions. After the additional 4d incubation, RNA was extracted from 1 cm-long-root tips. At least 50 plants were used per replicate. DNA damage-inducible genes expressions were normalized with *Actin8* expression. Data was expressed as a ratio relative to the value in Col-0 grown under 0.03 mM B condition. Mean of three replicates ± standard error is shown. (B) Statistical analysis of a comet assay comparing relative DNA damage in root tip in response to B toxicity. Plants were grown as described in (A). Nuclei were extracted from root tips. The extent of DNA double strand breaks in the nucleus is represented as tail moment. Data was expressed as a ratio relative to the value in Col-0 grown under 0.03 mM B condition. Mean of at least 125 comets ± standard error is shown. This experiment was repeated three times. (C) Examples of comets exhibiting almost intact nuclei (upper, short tail) and severely damaged nuclei by boron toxicity (lower, long tail) in Col-0. Bars, 10 μm. (D) Sensitivity of DNA damage sensitive and tolerant mutants to B toxicity. Col-0, *heb2-2*, *atm-2* and *atr-2* were grown under 0.03 mM B and 3 mM B conditions for 10d. The primary root length was measured. Data was expressed as a ratio relative to the value in control (0.03 mM B) condition. Mean ± standard error is shown (n > 12). Asterisks represent significant difference between Col-0 and each *heb* mutant (*, $P < 0.05$ and **, $P < 0.01$ by Student's *t*-test).

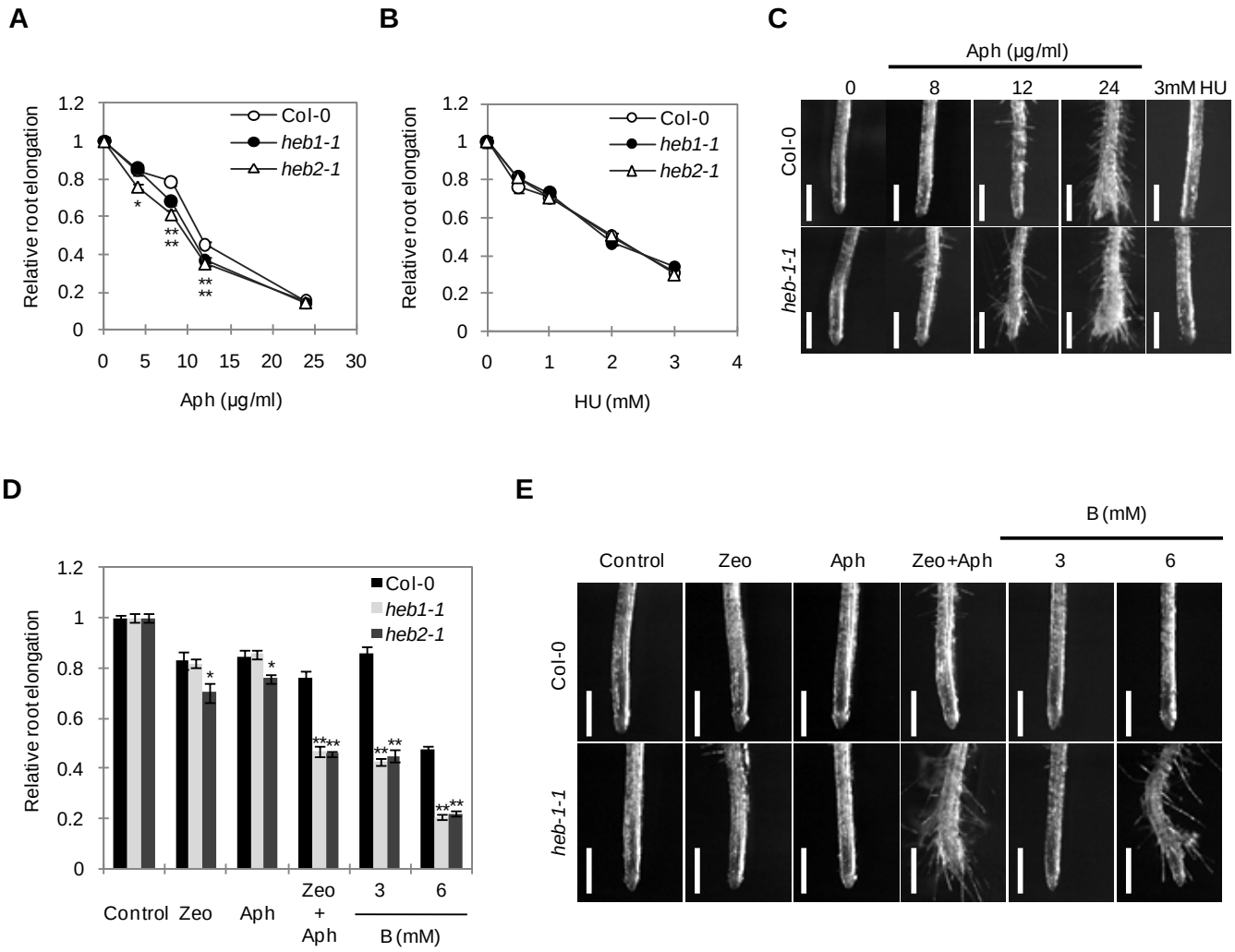

Figure 1-10 Comparison of sensitivity of the *heb* mutants to combined DNA stress with that to excess B in root growth.

Effects of replication block reagents, aphidicolin (Aph) (A) and hydroxy urea (HU) (B) on root elongation (see detail in Materials and Methods). Data was expressed as a ratio relative to the value in control condition. Mean ± standard error is shown (n > 13). (C) Root morphology of Col-0 and *heb1-1* mutant plants grown on media containing different concentrations of Aph and 3mM HU. Note that *heb2-1* also showed similar morphological defects as observed in *heb1-1*. Bars, 500 μm. (D) Comparison of the effect of Zeo and Aph with the effect of excess B on root elongation. After 5d-incubation at normal MGRL medium (control condition), plants were transferred to media containing 1 μM Zeo, 4 μg/ml Aph, 1 μM Zeo and 4 μg/ml Aph, 3mM B and 6 mM B. The length of newly elongated roots was measured. Data was expressed as a ratio relative to the value in control condition. Mean ± standard error is shown (n > 13). (E) Root morphology of Col-0 and h*eb1-1* mutant plants grown as described in (D). Note that *heb2-1* also showed similar morphological defects as observed in *heb1-1*. Bars, 500 μm. Asterisks represent significant difference between Col-0 and each *heb* mutant (*, $P < 0.05$ and **, $P > 0.01$ by Student's *t*-test).

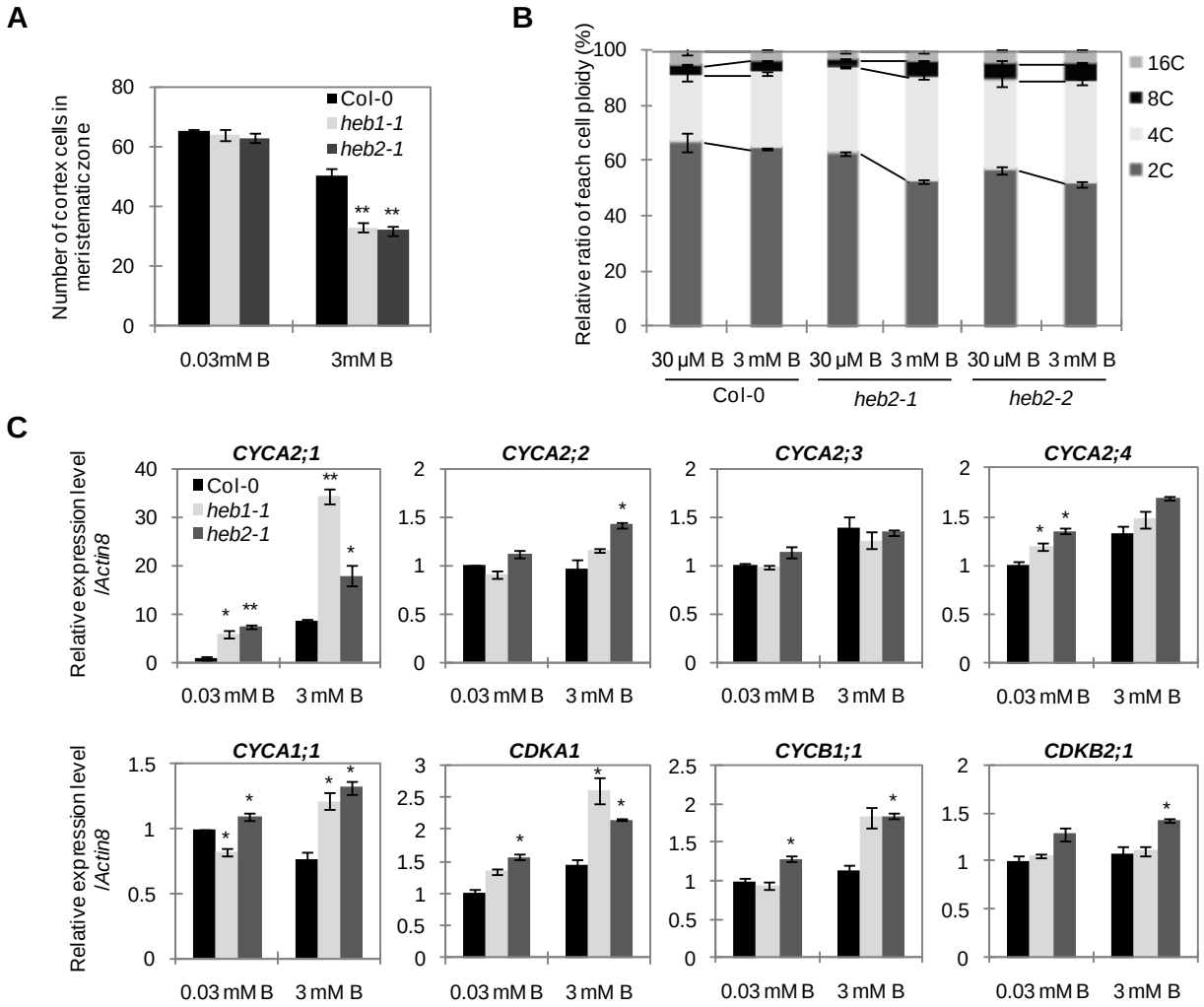

Figure 1-11 Effects of excess B on mitotic activities in the roots of condensin II mutants.
(A) Effect of excess B on the number of cortex cells in meristematic zone in root. 5d-old-seedlings of Col-0 and *heb1-1* and *heb2-1* were transferred to 0.03 mM and 3 mM B conditions and then were incubated for 4d. The roots were stained with PI and the number of cortex cells in meristematic zone was counted under the image of confocal microscopy. Mean of five replicates ± standard error is shown. (B) Statistical analysis of cell ploidy in root tip in response to B toxicity. Plants were grown as described in (A). Approximately 5000 nuclei were analyzed in Col-0, *heb2-1* and *heb2-2*. Mean of three replicates ± standard error is shown. Note that with regard to 2C and 4C ratio in *heb2-1* and *heb2-2,* there is a significant difference ($P < 0.05$ by Student's *t*-test) between 0.03 mM B and 3 mM B conditions. (C) Real time PCR analysis of cell cycle-related genes expressions in root tips in response to B toxicity. Plants were grown as described in (A). RNA was extracted from 1 cm-long-root tips. At least 50 plants were used per replicate. Data was expressed as a ratio relative to the value in Col-0 grown under 0.03 mM B condition. Mean of three replicates ± standard error is shown. Asterisks represent significant difference between Col-0 and each *heb* mutant (*, $P < 0.05$ and **, $P < 0.01$ by Student's *t*-test).

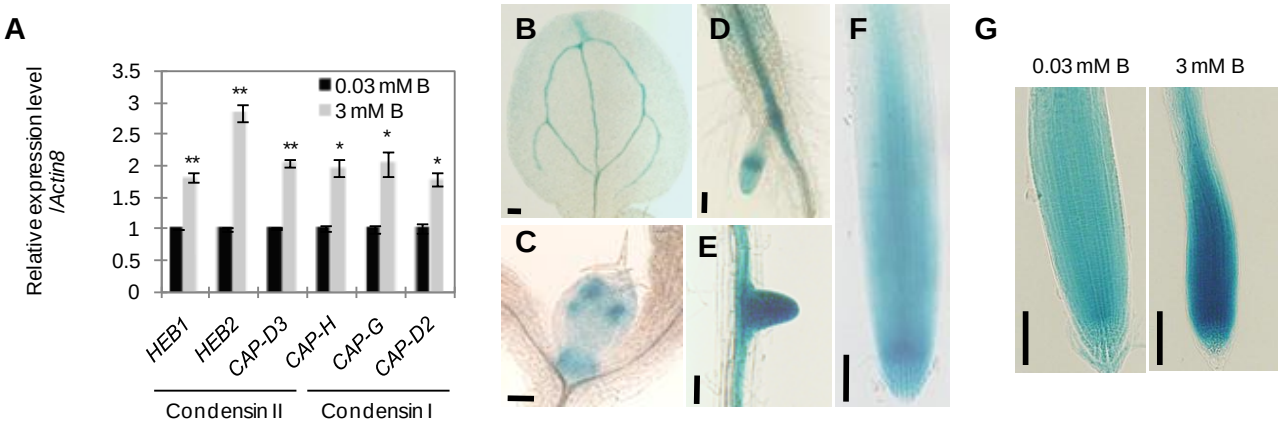

Figure 1-12 Responsiveness of condensin genes to excess B.
(A) Real time PCR analysis of condensin I and condensin II genes expression in response to B toxicity. Col-0, *heb1-1* and *heb2-1* were grown under 0.03 mM and 3 mM B conditions for 14d. RNA was extracted from whole roots. At least 10 plants were used per replicate. Data was expressed as a ratio relative to the value in 0.03 mM B condition. Mean of three replicates ± standard error is shown. Asterisks represent significant difference between 0.03 mM B and 3 mM B conditions (*, $P < 0.05$ and **, $P < 0.01$ by Student's *t*-test). (B) To (F) *HEB2* expression pattern in *A. thaliana*. *pHEB2::GUS* expression was detected in cotyledon (A), shoot apical dome (B), root-hypocotyl junction (C), lateral root meristem (D) and primary root apical meristem (E) of transgenic Col-0 grown on 0.03 mM B condition for 5d.. GUS expression was observed in three independent transformants. Bars, 100 µm. (G) *pHEB2::GUS* activities in response to excess B. Transgenic Col-0 plants carrying *pHEB2::GUS* were grown under 0.03 mM B (left) and 3 mM B (right) conditions for 14d. GUS expressions were observed in three independent transformants and their expression pattern in response to excess B were same. Bars, 100 µm.

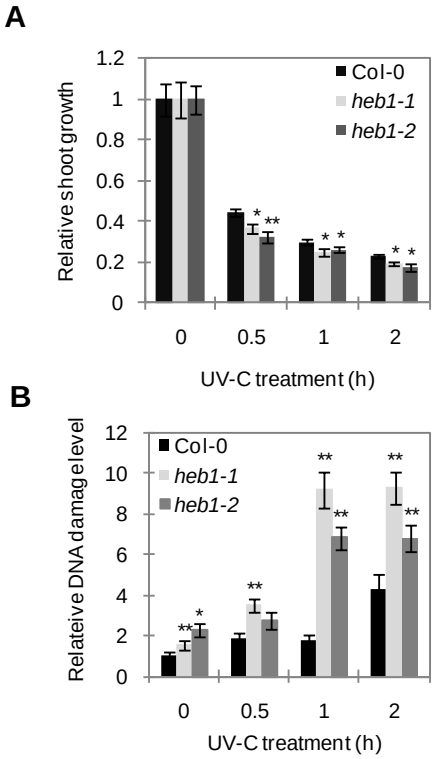

Figure 1-13 DNA damage by UV-C in the shoots of condensin II mutants.
(A) Sensitivity of Col-0 and *heb1* mutants to UV-C irradiation. The shoot flesh weight was expressed as a ratio relative to the value in control condition. Mean ± standard error is shown (n > 12). (B) DSBs accumulation in cotyledon by UV-C irradiation. DSBs levels were determined by comet assay and represented as tail moment. Data was expressed as a ratio relative to the value in Col-0 grown under 0.03 mM B condition. Mean of at least 80 comets ± standard error is shown. This experiment was repeated twice. Asterisks represent significant difference between Col-0 and each *heb* mutant (*, $P < 0.05$ and **, $P < 0.01$ by Student's *t*-test).

Chapter 2 Involvement of 26S proteasome in excess B tolerance in *Arabidopsis thaliana*-Identification of possible targets involved in excess B tolerance-

2.1 Abstract

Three of seven *A. thaliana* mutants, *heb3*, *heb6* and *heb7* were identified as *rpn8a-2*, *rpt5a-5* and *rpt5a-6*, respectively. These are the mutants of genes encoding subunits of 19S regulatory particle (RP), a subparticle of 26S proteasome (26SP). Among T-DNA inserted RP mutants I examined, *rpn2a* and *rpt2a* mutants also showed hypersensitivity to excess B. But *rpn2b*, *rpn8b*, *rpt2b* and *rpt5b* mutants were not sensitive to excess B. In *A. thaliana*, most of the RP subunits were encoded by two genes. This suggests that diverse population of 26SP is assembled in plants, which may expand the target specificity and functions of ubiquitin (Ub)-dependent proteolysis. Taken together, it is suggested that 26SP containing specific combination of RP subunits is functional in B toxicity-tolerance.

The root growth of *rp5a* mutants was sensitive to L-canavanin treatment which is known to cause accumulation of abnormal proteins. Moreover, immunoblot analysis revealed that in roots, *rpt5a-6* accumulated more poly-ubiquitinated proteins under excess B condition than the wild-type. These suggest the reduced activity of Ub-dependent proteolysis in the *rpt5a* mutants. Next I tried to indentify he target proteins involved in B toxicity-tolerance. Proteome analysis of poly-ubiquitinated proteins indicated that at least 27 proteins were more than two-fold accumulated by excess B treatment both in the wild-type and *rpt5a-6* mutants. Extents of accumulation of these proteins were higher in the *rpt5a-6* mutants. Accumulation of undegraded poly-ubiquitinated proteins might inhibit cellular metabolisms. Taken together, it is possible that all or some of 27 candidate proteins may be excess B-dependent targets of 26SP and that RPT5a contributes to the processing of those proteins. Two revertants of *rpt5a-6* which showed similar root growth as the wild-type under excess B condition were isolated. The revertants are expected to be defective in the excess B-dependent targets of 26SP. These two approaches opened up the possibility to determine the existance and the type of proteins degraded through 26SP in response to excess B.

2.2 Introduction

In this chapter 2, I characterized three of seven *heb* mutants, *heb3*, *heb6* and *heb7*, and established that *HEB3* encodes RP non-ATPase 8a (RPN8a) and both *heb6* and *heb7* encode RP triple-A-ATPase 5a (RPT5a). Both proteins are subunits of 26S proteasome (26SP). Among other RP subunits, I also established that RPN2a and RPT2a are required

for B toxicity-tolerance.

26SP is an ATP-dependent protease complex catalyzing protein degradation in the nucleus and cytoplasm. Proteins targeted by this proteolytic device are mostly modified by ubiquitin (Ub) (Smalle and Vierstra 2004; Vierstra 2009). 26SP is composed of functionally different two subcomplexes, 20S proteasome (20SP) and 19S regulatory particle (RP). 20SP contains three types of proteolytic subunits mediating ATP- and Ub-independent peptidase activities. On the other hand, RP has roles in recognition and unfolding of poly-ubiquitinated proteins. Unfolded proteins are guided into 20SP chamber for degradation. The RP is further separated into two subparticles, the lid and the base. The lid contains eight RPN subunits (RPN3, 5-9, and 11-13) and is thought to form a platform for recognition and processing of target proteins. The base contains six RPT subunits (RPT1-6), and three additional RPN subunits (RPN1, RPN2 and RPN10). The base is thought to function in recognition, promotion of unfolding and translocation of target proteins (Smalle and Vierstra 2004).

Protein ubiquitination is mediated by the sequential action of Ub-activating enzyme E1, Ub-conjugating enzyme E2, and Ub ligase E3. The E3 ligase largely determines substrate specificity. E3 ligases can be classified into several classes and are encoded by more than 1,300 genes in the *A. thaliana* genome (Smalle and Vierstra 2004). This implies that the existence of specific targets in response to various cellular processes.

There are several reports on distinct and common functions of individual RP subunits in *A. thaliana*. RPN12a and RPN10 are involved in response to cytokinin and abscisic acid, respectively (Smalle et al., 2002, 2003). RPT2a is required for the maintenance of root apical meristems (Ueda et al., 2004). RPT2a, RPN10 and RPN12a (Kurepa et al., 2008, 2009) and RPN1a (Wang et al., 2009) are shown to be involved in optimal growth and stress responses. In *A. thaliana*, most of the RP subunits were encoded by two genes, suggesting that various combination of 26SP subunits are present in *A. thaliana* and this may contribute to functional diversity of 26SP (Yang et al., 2004; Book et al., 2010). It has also been demonstrated that the two paralogous genes of *A. thaliana* RP subunits have both similar and unique roles. RPN1a and RPN1b are functionally equivalent in embryogenesis (Brukhin et al., 2005). RPT5a and RPT5b play a similar role in gametophyte development (Gallois et al., 2009). RPN5a and RPN5b are essential for gametogenesis, whereas overexpression of these genes in the wild-type showed different abnormal phenotypes, indicating both common and unique roles of these proteins in development (Book et al., 2009). Mutation in *RPT2a* causes increased ploidy levels, whereas these phenotypes were not observed in the *RPT2b* mutant (Kurepa et al., 2009; Sonoda et al., 2009). These functional differences are believed to arise from the specific

association of individual RP subunits and its paralogue with poly-ubiquitinated proteins.

In animal cells, glucose starvation decreased Ub-dependent 26SP proteolysis for several substrates through glycosylation of proteasome subunits, particularly RPT2 (Yang et al., 2002). This indicates the existence of a subunit-dependent target specific to certain nutritional stress. However, to my knowledge, there is no information about proteins degraded by 26SP in response to excess B and about the involvement of RP subunits in targets selection in plants.

Considering the fact that at least four RP subunits are required for B toxicity-tolerance, it is possible that these subunits are involved in recognition of proteins processed by Ub-dependent proteolysis in response to excess B. In this chapter 2, I focused on this possibility and attempted to isolate possible excess B-dependent targets of 26SP.

2.3 Materials and methods

2.3.1 Plant materials and growth conditions

The *heb3*, *heb6-1* and *heb6-2* mutants of *A. thaliana* (ecotype Col-0) were isolated as described previously (Sakamoto et al., 2009). The mutants were backcrossed to Col-0 for three times and were then used for the subsequent studies. The T-DNA insertion mutants used in this chapter were listed in Table 2-1. The T-DNA homozygous mutants were confirmed by PCR using primer sets listed in Table I. Regarding to *rpt1b*, *rpt2a-1*, *rpt3*, *rpt4a*, *rpt4b*, *rpt6a* and *rpt6b*, the T-DNA homozygous mutants were established by Ms. Sako of Hokkaido University.

In all experiments, described seeds were sown on the media containing MGRL solution (Fujiwara et al., 1992), 1% (w/v) sucrose and 1.5% (w/v) Gellan gum. Boric acid was used for the adjustment of B concentrations in the medium. After 3d incubation at 4°C, the plates were placed vertically in the growth chamber (16-h light/8-h dark cycle, 22°C) until analysis.

2.3.2 Positional mapping of the *HEB* genes

heb3, *heb6* and *heb7* mutants (M3 generation) (Col-0 background) were crossed with Ler wild-type plants. DNA was extracted from shoots of 2925 (for *heb3*), 25 (for *heb6-1*) and 2243 (for *heb6-2*) F2 plants and were analyzed using simple sequence length polymorphism and cleaved-amplified polymorphic sequence markers (Table II), which were generated based on Cereon Arabidopsis Polymorphism Collection (http://www.Arabidopsis.org/Cereon). F3 progeny of F2 recombinants were grown on excess B condition and short-root phenotype was used to map the *heb* mutations.

2.3.3 Observation of root morphology

Root morphologies of 14d-old-seedlings were observed and imaged using stereomicroscope SZH10 (Olympus, Japan) equipped with the digital camera (Olympus) after the treatments of excess B. To observe the root tip structures, 14d-old-seedlings roots were stained with propidium iodide (10 μg/ml) for 5 to 10 min. Then images were captured using confocal microscope FV-1000 (Olympus) 619 nm emission and 559 nm excitation.

2.3.4 Sensitivity to L-canavanin

Plants were pre-incubated vertically on MGRL media for 5d. To test the sensitivity of plants to L-canavanin (CAN, Sigma-Aldrich, USA) which is known to cause accumulation of misfolded proteins, 5d-old-seedlings were transferred to the media containing different concentrations of CAN, and root tip position of each plant was recorded that is to recognize the new root growth. After an additional 4d-incubation, the length of newly elongated primary roots were measured using ImageJ software.

2.3.5 Accumulation of poly-ubiquitinated proteins

For the evaluation of accumulation profile of poly-ubiquitinated proteins in roots, proteins were extracted using phosphate-buffered saline with “protease inhibitor cocktail complete” (Roche, Switzerland) and 1 mM phenylmethylsulfonyl fluoride (Wako, Japan). The extract was centrifuged at 8,000 g for 15 min at 4°C. After the determination of protein concentrations of the supernatants with Pierce® 660nm protein assay reagent (Thermo Scientific, USA), equal amounts of extracted proteins were separated by SDS-PAGE and transferred onto polyvinylidene fluoride membranes. Poly-ubiquitinated proteins were detected with anti-poly-Ub chain antibody (FK1, Nippon Biotest Labo, Japan) and visualized with enhanced chemiluminescence (GE Healthcare, UK).

2.3.6 Proteome analysis of poly-ubiquitinated proteins

Plants were pre-incubated vertically on MGRL media for 7d. Then plants were transferred to 0.03 and 3 mM B containing MGRL media. After an additional 4d-incubation, plant roots were harvested and stored at -80°C.

For purification of poly-ubiquitinated proteins, I used CycLex® Poly-Ubiquitinated Protein Enrichment & Detection Kit (MBL International, USA). Total soluble proteins were extracted in the provided extraction buffer with “protease inhibitor cocktail complete” (Roche). The extract was centrifuged at 8,000 g for 15 min at 4°C. Protein

concentrations of the supernatants were determined using *Dc* protein assay kit (Bio-Rad, USA). Twenty five mg of extracted proteins (2 mg/ml) were incubated with 650 µl of GST-hHR23B-UBA domain fused resin (provided) for 4h at 4°C. The proteins that bound to resin were collected following the manufacture's protocol and were extracted in 200 µl of 2 x SDS sample buffer without bromophenol blue.

One hundred µg of purified poly-ubiquitinated proteins were precipitated with the trichloroacetic acid method. Then precipitates were dissolved in dissolution buffer provided in isobaric tag for relative and absolute quantification (iTRAQ) kit (Applied Biosystems, USA). Labeling of samples with iTRAQ^{TM} reagents were performed following the manufacture's protocol. The iTRAQ^{TM}-labeled samples were mixed and fractionated using cation exchange chromatography (ICAT® Cation Exchange Buffer Pack, Applied Biosystems). Identification and quantification of samples were conducted by Dr. Fukao using LC-MS/MS (LTQ-Orbitrap XL, Thermo Scientific) and MASCOT database.

2.3.7 Screening for revartants of *rpt5a-6* under the excess B condition

rpt5a-6 (ecotype Col-0) was used as a parental line. About 20,000 seeds were incubated with 0.2% ethyl methansulfonate (EMS) for 16h. All seeds were sowen on rockwool and then M2 seeds were harvested.

About twenty thousand M2 seedlings were grown on MGRL solid media containing 3 mM B for 10d. Then plants showing more root elongation than that of *rpt5a-6* were selected and transferred to 0.03 mM B condition. After a few days incubation, plants were transferred to rockwool to harvest M3 seeds. The phenotype of selected mutants was confirmed using M3 seeds.

2.4 Results

2.4.1 *HEB3*, *HEB6* and *HEB7* encode subunits of 26S proteasome

heb3, *heb6* and *heb7* mutants show moderately reduced root growths under the normal B condition and extremely short-roots under the excess B condition (Figure 2-1 A and B). Using this short-root phenotype as an index, phenotyping of F2 generation of the *heb* mutants crossed with Ler were conducted. Genotyping using Simple Sequence Length Polymorphysm were also done to genetically map the *heb* loci.

As a result, the locations of *heb3* and *heb6-2* loci were limited to about 100 and 24 kb regions containing At5g05780 and At3g05530, respectively (Figure 2-1 C and D). DNA sequences of At5g05780 in *heb3* and DNA sequence of the 24 kb region in *heb6-2* were determined. In *heb3* a mutation was found in At5g05780. In *heb6-2* a mutation was found in At3g05530, but not in the other ORFs (Figure 2-1 E and F). *heb3* possessed a

base substitution in the start codon of At5g05780 which resulted in a generation of aberrant ORF. *Heb6-2* possessed a nonsense mutation at the predicted fifth exon of At3g05530 at amino acid residue 194. Regarding to *heb6-1*, genetic mapping revealed that *heb6-1* locus is located to the region containing *heb6-2* locus, indicating the possibility that *heb6-1* and *heb6-2* are alleles. Sequence analysis determined that *heb6-1* also possessed a nonsense mutation in At3g05530 at a different site (amino acid residue 101) from *heb6-2* (Figure 2-1 D).

At5g05780 and At3g05530 are known as *regulatory particle non-ATPase 8a* (*RPN8a*) (Huang et al., 2006) and *regulatory particle triple-A-ATPase 5a* (*RPT5a*) (Gallois et al., 2009), respectively. Both RPN8a and RPT5a are subunits of 19S regulatory particle (RP), a subcomplex of 26S proteasome (26SP). Based on these information and known alleles of these genes, I renamed *heb3*, *heb6-1* and *heb6-2* as *rpn8a-2*, *rpt5a-5*, *rpt5a-6*, respectively.

From the collection of T-DNA mutant of SALK institute (Alonso et al., 2003), I identified new T-DNA inserted mutant alleles, *rpn8a-3* (SALK_151595) and *rpt5a-4* (SALK_046321) (Figure 2-1 C and D). *rpn8a-3* carried a T-DNA insertion in the 3' untranslated region (UTR) of *RPN8a* and *rpt5a-4* carried a T-DNA insertion in the fifth intron of *RPT5a.* Both T-DNA insertion mutants showed similar short-root phenotypes as observed in isolated *rpn8a* and *rpt5a* mutants under the excess B condition (Figure 2-1 E and F). These results established that HEB3 and HEB6/HEB7 are At5g05780 and At3g05530, respectively.

2.4.2 RPN8a and RPT5a mutants show short-root phenotype under moderate levels of excess B and are not hypersensitive to other mineral stresses.

I examined the growth property of *rpn8a* and *rpt5a* mutants under various levels of B conditions (Figure 2-2 A). *rpt5a-6* showed 20 to 40% reduction in root lengths under the non-toxic levels of B (0.1 and 0.5 mM B). Reduction in root length of *rpt5a-5* was also observed at 0.5 mM B condition (40%). On the other hand, *rpn8a-2* and Col-0 grew normally up to 0.5 mM B and 1 mM B treatment, respectively. Under the toxic levels of B (more than 1 mM B), the root growths of all mutants were highly reduced compared to that of Col-0. Taken together, these results established that *rpn8a* and *rpt5a* mutants are hypersensitive to excess B in both terms of B concentration required for growth inhibition and the extents of growth inhibition.

To examine whether the short-root phenotypes of *rpn8a* and *rpt5a* mutants are specific to B toxicity, sensitivity of the mutants to low B (-B), arsenite (As), salinity (NaCl) and cadmium (Cd) stresses were investigated (Figure 2-2 B). *rpn8a-2* showed sensitivity to Cd

stress. *rpt5a-5* was sensitive to –B and NaCl stresses, whereas *rpt5a-6* was sensitive only to -B stress. However, the extents of reduction in root lengths of the mutants under -B, NaCl and Cd stress conditions were less than those observed under the excess B conditions (Figure 2-2 A). Interestingly, all mutants tested were tolerant to As stress compared to Col-0 (Figure 2-2 B). These results suggested that the short-root phenotypes of *rpn8a* and *rpt5a* mutants are specific to B toxicity among mineral stresses. Moreover, considering the generation of reactive oxygen species (ROS) under –B, NaCl, As (described in chapter 1.4.1) and Cd stress (Romero-Puertas et al., 2002) conditions, it is suggested that ROS generation is not a cause of hypersensitivity to excess B in roots of *rpn8a* and *rpt5a* mutants.

2.4.3 Root morphology of *rpn8a* and *rpt5a* mutants were severely altered by excess B treatment

Excess B can affect root morphology (Liu et al., 2000) and *heb1* and *heb2* were shown to be more susceptible to excess B in root morphology (described in chapter 1.4.3). I investigated the root morphology of *rpn8a* and *rpt5a* mutants under the normal and the excess B conditions (Figure 2-3 A-P).

The root morphology of the mutants was visibly similar to that of the wild-type under the normal condition (Figure 2-3 A-D), whereas longitudinal confocal sections cleared the difference in the morphology of root tips between Col-0 and both *rpn8a* and *rpt5a* mutants under the normal condition (Figure 2-3 I-L). Width of root tips was narrow in the mutants compared to that of the wild-type. Furthermore, alignment of cells around the quiescent center was abnormal and cells entirely stained with propidium iodide (dead) cells were observed in large area of roots in the mutants. Excess B treatment severely affected the root morphology of the mutants (Figure 2-3 E-H). Twisted roots, ectopic lateral roots formation, dense root hairs and markedly pointed root tips were observed in the mutants, but not in Col-0. The position of root hair emergence was very close to the tip of the root in the mutants under the excess B condition, but not in Col-0. In confocal images (Figure 2-3 M-P), root apical meristem of the mutants appeared to be disorganized. In addition, enlargement of cells was occurred in the mutants at closer position to root tips than in Col-0. Dead cells were appeared in Col-0 by excess B treatment, whereas area of dead cells were reduced in the mutants treated with excess B compared to those in the mutants treated with normal level of B (Figure 2-3 L-P). These data suggest that RPN8a and RPT5a are involved in the maintenance of cell viability and organization of cells in root tips under the normal condition. It was also suggested that defects in cell maintenance in root tips lead to hypersensitivity of root growth to the excess B condition.

2.4.4 Four 19S regulatory particle subunits are identified to be essential for excess B tolerance

RP is composed of twelve RPN subunits and six RPT subunits, and most of the RPN and RPT subunits are encoded by two genes in the *A. thaliana* genome (Table 2-1). It was reported that distinct subunits and paralogues have common functions such as gametogenesis and organ size regulation. It is possible that in addition to RPN8a and RPT5a several subunits and their paralogues are essential for excess B tolerance in *A. thaliana*. To find novel requirements of RP subunits to excess B tolerance and to examine whether function of the subunits in B toxicity is common among the paralogues, I examined sensitivity of other RPN and RPT mutants to excess B.

Among the RP subunit mutants I tested (Table 2-1), RPN2a and RPT2a mutants were also hypersensitive to excess B (Figure 2-4 A). Two types of T-DNA insertion mutants of RPT2a and RPN2a both showed similar short-root phenotypes under the excess B condition (Figure 2-4 B and D). It was thus established that in addition to RPN8a and RPT5a, lwsRPN2a and RPT2a are also essential for B toxicity-tolerance in roots.

Interestingly, the mutants of RPN2b, RPN8b, RPT2b and RPT5b (*rpn2b*, *rpn8b*, *rpt2b-1* and *rpt5b-3*) were not sensitive to the excess B (Figure 2-4 A). These proteins are paralogues of subunits that required for excess B tolerance, indicating the possibility that RPN2b, RPN8b, RPT2b and RPT5b are not essential for excess B tolerance in the presence of each paralogue. However, the functional redundancy in excess B tolerance among each paralogue remains a possibility.

2.4.5 *rpt5a* mutants are reduced in ubiquitin-dependent proteolytic activity in roots

RP subcomplex is known to function in recognition and unfolding of poly-Ub tagged substrates of 26SP. It is possible that mutation in RP subunits affects total Ub-dependent 26SP pathway. Indeed, the T-DNA insertion mutants of RPT2a, RPN10 and RPN12a are shown to reduce Ub-dependent proteolytic activity (Kurepa et al., 2008). To elucidate total Ub-dependent proteolytic activity in *rpt5a* mutants, I first examined the sensitivity of the *rpt5a* mutants to amino acid analog L-canavanin (CAN) (Figure 2-5 A). CAN is incorporated into proteins in place of arginine, leading to generation of misfolded proteins which are considered to be processed by Ub-dependent 26SP pathway (Kurepa et al., 2008). Thus, mutants with decreased Ub-dependent proteolytic activity are expected to be more susceptible to effects of misfolded proteins than the wild-type plants, and as a consequence the mutant should have a reduced tolerance to CAN treatment. As expected, the root elongation of both *rpt5a-5* and *rpt5a-6* were more reduced under 0.5 and 1 μM CAN

condition than that of Col-0 (Figure 2-5 A), suggesting the reduced Ub-dependent proteolytic activity in *rpt5a* mutants.

If Ub-dependent proteolytic pathway has crucial roles in excess B tolerance in plants, it is possible that the *rpt5a* mutants are defective in the processing of poly-Ub tagged proteins and consequently accumulates more poly-ubiquitinated proteins under the excess B conditions. To investigate this possibility, I compared accumulation profiles of poly-ubiquitinated proteins in Col-0 and the *rpt5a* mutants (Figure 2-5 B). Western blot analysis revealed that levels of accumulation of poly-ubiquitinated proteins in Col-0 roots were similar between the normal and the excess B conditions. In contrast, in the *rpt5a* mutants, poly-ubiquitinated proteins were more accumulated in the excess B condition than in the normal condition, suggesting that RPT5a is required for Ub-dependent proteolysis in response to excess B in roots. Compared to Col-0, accumulation levels of poly-ubiquitinated proteins were higher in *rpt5a-6*, but similar in *rpt5a-5* under the excess B condition, implying that in addition to accumulation levels of undegraded proteins, population of them in the *rpt5a* mutants are different from those in Col-0 under the excess B condition.

2.4.6 Screening of subunits specific substrates of 26SP in response to excess B

Based on the results that the *rpt5a* mutants are reduced in Ub-dependent proteolytic activity in the excess B condition, I hypothesized that the *rpt5a* defective in targeting of proteins degraded through Ub-dependent proteolityc pathway in response to excess B. To search the candidates of that kind of proteins, I performed proteome analysis of poly-ubiqutinated proteins in roots.

Poly-ubiqutinated proteins were purified and enriched from roots of more than 3,000 seedlings of Col-0 and *rpt5a-6* grown under the normal and the excess B conditions using resin containing Ub binding domain that selectively recognizes the Ub moiety but not free Ub (see chapter 2.3.6). Approximately 25 mg of total soluble proteins were applied to the affinity purification of poly-ubiqutinated proteins. Purified proteins were extracted in 200 µl of the sample buffer. The profiles of purified proteins were similar among lines and treatments (Figure 2-6 A). Enrichment of poly-ubiquitinated proteins by the purification were confirmed by western blot analysis (Figure 2-6 B). We should note that the abundant proteins with less than 50 kDa observed in the SDS-PAGE were not detected in western blot analysis of poly-ubiquitinated proteins indicating that non-ubiquitinated proteins were also purified in my system (Figure 2-6 A and B). For the proteome analysis of the purified proteins I adopted iTRAQ LC-MS/MS method. iTRAQ reagents can label all peptides in different samples enabling identification and quantification of proteins from different sources

in one single experiment. After trypsin digestion of the purified proteins, all peptides were labeled by iTRAQ reagents. Then, mass and intensity of each peptides included were analyzed by LC-MS/MS. Database analysis revealed that LC-MS/MS identified 57 proteins and 30 of them were relatively quantified (Table 2-2). Among 30 proteins relatively quantified, 29 proteins were more than two-fold accumulated by the excess B treatment both in Col-0 and *rpt5a-6* mutants. This result suggests that the degradation of those proteins is required for B toxicity-tolerance. Extents of accumulation of these 29 proteins by excess B treatment were higher in *rpt5a-6* than in Col-0, and among them, 22 proteins were highly accumulated in *rpt5a-6* than in Col-0 irrespective of B conditions, suggesting that RPT5a is involved in the processing of those proteins.

The potential poly-ubiquitination of identified proteins was predicted by analyzing the potential ubiquitination-targeting signal motifs, D-box, KEN-box and PEST motif. D-box and KEN-box are short sequence elements seen in the substrates of the anaphase-promoting complex/cyclosome (APC/C), a multisubunit RING-type E3 ligase (King et al., 1996; Pfleger and Kirschner, 2000). PEST motif that is rich in proline (P), glutamic acid (E), serine (S), and threonine (T) were found in a number of short-lived proteins controlled by proteolysis, mostly through Ub-dependent. Seventeen of the identified proteins contained at least one motif among listed above, implying that they are the potential substrates of Ub-dependent proteolysis by 26SP.

Overall, proteome analysis of poly-ubiquitinated proteins indicated a list of potential substrates of 26SP in response to excess B, and that RPT5a might be required for the processing of proteins that negatively affect the growth under the excess B condition..

2.4.7 Screening and isolation of revartants of *rpt5a-6* under the excess B condition

As another investigation to elucidate molecular mechanisms of RPT5a involvement in excess B tolerance, I conducted screening of revartants of *rpt5a-6* which do not show hypersensitivity to excess B.

Among about two thousand EMS mutagenized M2 seedlings *rpt5a-6*, I selected plants showing better root growth than the parental line, *rpt5a-6.* As a result, I obtained two candidates. I confirmed the phenotypes of two candidates in the M3 generation (Figure 2-7).

2.5 Discussion

In this chapter 2, I established that the function of RP, one of the subcomplexes of 26SP, is essential for excess B tolerance in *A. thaliana*. Among RP subunits, at least four subunits, RPN2a, RPN8a, RPT2a and RPT5a are required for the root growth of *A. thaliana* under the

excess B condition, but not RPN2b, RPN8b, RPT5b and RPT2b. Moreover, I detected about 30 candidate proteins that are considered to be selectively degraded by 26SP containing RPT5a under the excess B conditions. Based on these findings, I proposed that specific degradation of proteins through processing by subsets of RP is crucial for excess B tolerance.

In *A. thaliana*, both common and unique functions among distinct subunits of RP have been reported (Smalle et al., 2002, 2003; Ueda et al., 2004; Kurepa et al., 2008, 2009; Wang et al., 2009). These functional similarities and differences are thought to be provided by targeting of specific or common substrates of 26SP by individual RP subunits. In addition, in plants most of RP subunits have two gene copies in the genome, leading to the hypothesis that plants might assemble multiple 26SP forms with different composition of subunits and such multiple forms contribute to unique properties and/or substrate specificities (Yang et al., 2004; Book et al., 2010). Unique function among each paralogue has been reported in *A. thaliana* and supports this hypothesis (Book et al., 2009; Kurepa et al., 2009; Sonoda et al., 2009). In my study, among RP subunits, RPN2a, RPN8a, RPT2a and RPT5a showed similar phenotype under the excess B condition, indicating that these subunits have common function in response to B toxicity, but not the others I analyzed. In addition, the mutants of paralogues of RPN2a, RPN8a, RPT2a and RPT5a did not show excess B hypersensitivity. Moreover, the mutants of RPN8a and RPT5a were not sensitive to B deficiency, arsentie toxicity, salinity stress and cadmium toxicity. Overall, these data indicate the distinct functional roles for B toxicity-tolerance among paralogues and the possibility that 26SP containing RPT2a, RPN8a, RPT2a and RPT5a is formed to express unique functions required for excess B tolerance.

Mutations in RP subunits often results in the impairment of total Ub-dependent proteolytic activity of 26SP (Kurepa et al., 2008, Sonoda et al., 2009) and extents of the impairment is thought to relate to the strength of mutant phenotype (Kurepa et al., 2009). The *rpt5a* mutants were hypersensitive to the accumulation of misfolded proteins induced by application of CAN, indicating reduced total 26SP activity in the mutants. At the same time, it is possible that hypersensitivity to excess B may be due to accumulation of misfolded proteins and that excess B may causes accumulation of misfolded proteins.

It is often, but not always, observed that reductions in total 26SP activity lead to the accumulation of poly-ubiquitinated proteins in the cell (Kurepa et al., 2008; Book et al., 2009). Recent reports indicated that the degree of accumulation of poly-ubiquitinated proteins reflects the strength of the defect in total 26SP activity (Smalle et al., 2002, Kurepa et al., 2008). The *rpt5a* mutants showed similar or lower levels of total poly-ubiquitinated proteins compared to that of the wild-type under the normal B condition, suggesting that the

levels of the accumulation of poly-ubiquitinated proteins may not reflect the strength of the defect in total 26SP activity in the *rpt5a* mutants. On the other hand, the *rpt5a* mutants increased poly-ubiqutinated proteins by the excess B treatment, whereas the wild-type not. It is possible that the poly-ubiquitinated proteins induced by excess B are present and RPT5a is involved in the degradation of those kinds of proteins. Taken together, I proposed that the activity of 26SP containing RPT5a rather than the total activity of 26SP is required for excess B tolerance.

To my knowledge, there is no report focusing on the population of poly-ubiquitinated proteins in mutants of individual subunit gene and the effect of environmental stresses on it. Determination of the population of poly-ubiquitinated proteins in mutants of a particular RP subunit would help to understand the subunit-specific recognition of substrates. Proteome analysis using affinity-purified poly-ubiqutinated proteins suggested that 28 proteins were processed by specific subsets of 26SP containing RPT5a in response to excess B. Among these, three proteins belong to the heat shock protein 70 family and nine belong to the glutathione S transferase (GST) family. Ubiquitinated heat shock protein 70 (HSP70) are known to function in recruitment of misfolded proteins to 26SP (Qian et al., 2006). After the recruitment HSP70 are known to be degraded by 26SP together with the substrates. My finding that HSP70 are accumulated in *rpt5a-6* under the excess B condition suggests that misfolded proteins are also accumulated, further supporting the possibility that excess B causes protein misfolding. GSTs are well known to function in many cellular process and response to stresses (Dixon et al., 2002). Although it is not known, one possible role of GSTs in excess B tolerance is processing of substrates for 26SP through forming a complex of ubiquitinated GST and the substrates, similar to the case of HSP70.

It was shown that root tips are highly susceptible to the effects of excess B (Reid et al., 2004, chapter 1). I found that *rpn8a* and *rpt5a* mutants were defective in root morphogenesis even under the normal condition, and excess B enhanced the severity of the defect. In addition, *rpt2a-2*, which is previously established to show short-root and be defective in root meristem organization (Ueda et al., 2004), were hypersensitive to excess B. These suggests that the function of these RP subunits in the maintenance of root meristems are crucial for excess B tolerance, and that proteins negatively affect root meristem organization are among substrates of 26SP. Interestingly, At1g26360 encoding hydrolase, alpha/beta fold family protein and At4g16340 encoding SPIKE1 were included among the 28 proteins identified. The former protein has about 50% amino acid homology to SPIRAL1 which is associated to cell expansion and cell wall deposition processes through stabilizing microtubules (Nakajima et al., 2004; Sedbrook et al., 2004). The latter, SPIKE1, is known

to be involved in cell shape formation and tissue organization through regulation of microtubule cytoskeleton (Qiu et al., 2002). Increase of Ub modified SPIKE1 by excess B was highest (147-fold) among the 28 proteins in the wild-type. Taken together, these data implies that misregulation of these proteins under excess B through RPT5a may be attributed to severe morphological defects in *rpt5a-6* mutants.

As another approach for further analysis of molecular function of RPT5a in excess B tolerance, I performed screening of revartants of *rpt5a-6*. As a result, I obtained at least two revertants which showed better growth under the excess B condition compared to *rpt5a-6* mutant. Among various possible explanations for the phenotype of revertants, one may be that the revertants have mutations in genes encoding proteins that possibly be involved in inhibition of root elongation under the excess B condition. Identification of the responsible genes of the revertatns will provide us better understanding of RPT5a action in B toxicity-tolerance.

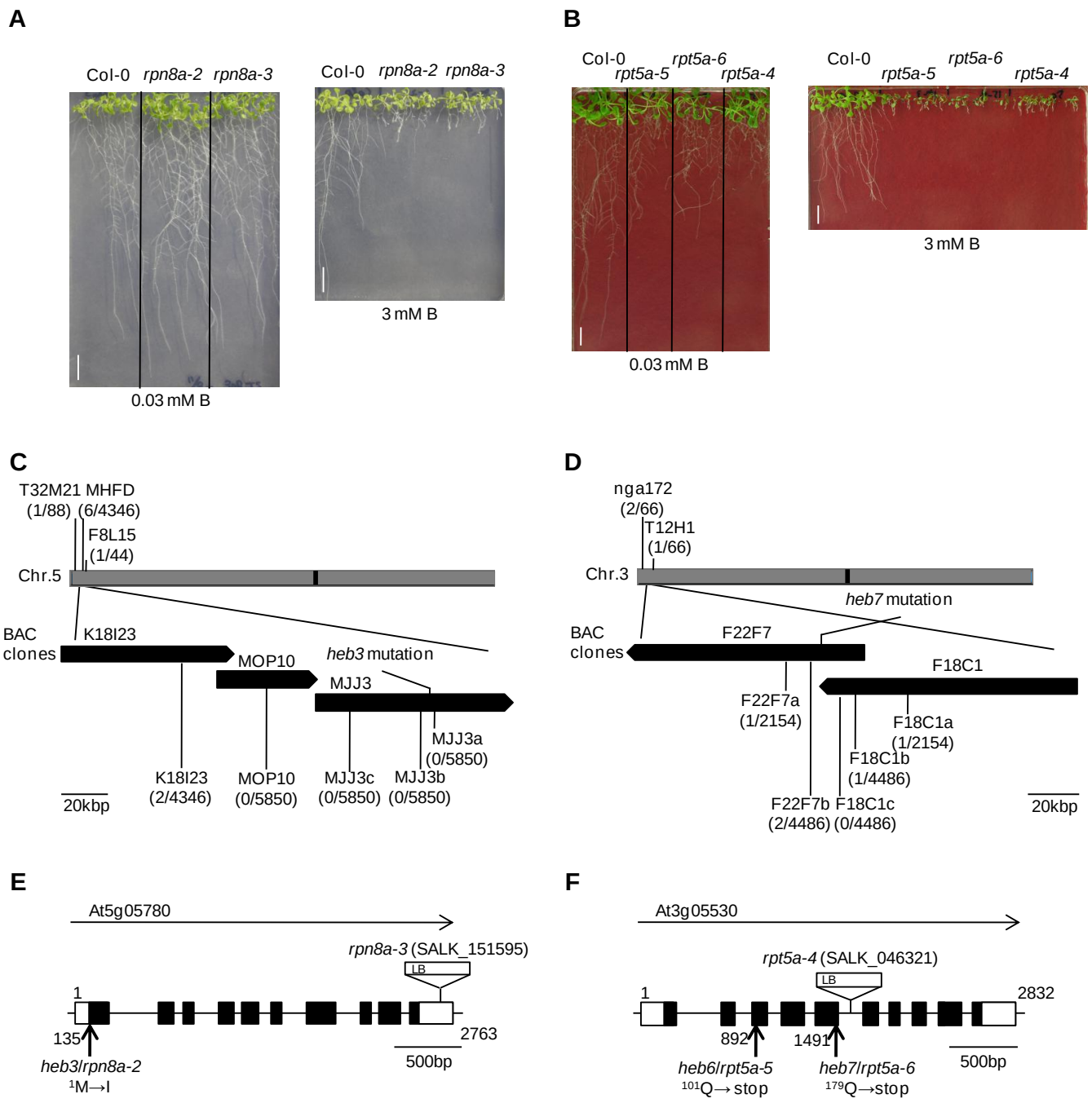

Figure 2-1 Characterization of *HEB3*, *HEB6* and *HEB7* genes.
(A) and (B) Excess B-dependent short-root phenotype of alleles for *rpn8a* and *rpt5a* mutants. Col-0 and the *heb* mutants were grown under 0.03 mM (upper) and 3 mM B conditions (lower) for 14d. Bars, 1 cm. Map position of *HEB3* (C) and *HEB7* (D) loci. Marker used and the number of chromosomes at each marker position over the number of total chromosomes analyzed are shown. Genomic structure of *HEB3* (E) and *HEB7* (F) genes. Black and white rectangles indicate the coding regions and untranslated regions (UTRs), respectively. The mutation site for *heb* mutants and insertion site for SALK lines are shown. Genetic analysis revealed that *HEB6* and *HEB7* are same gene.

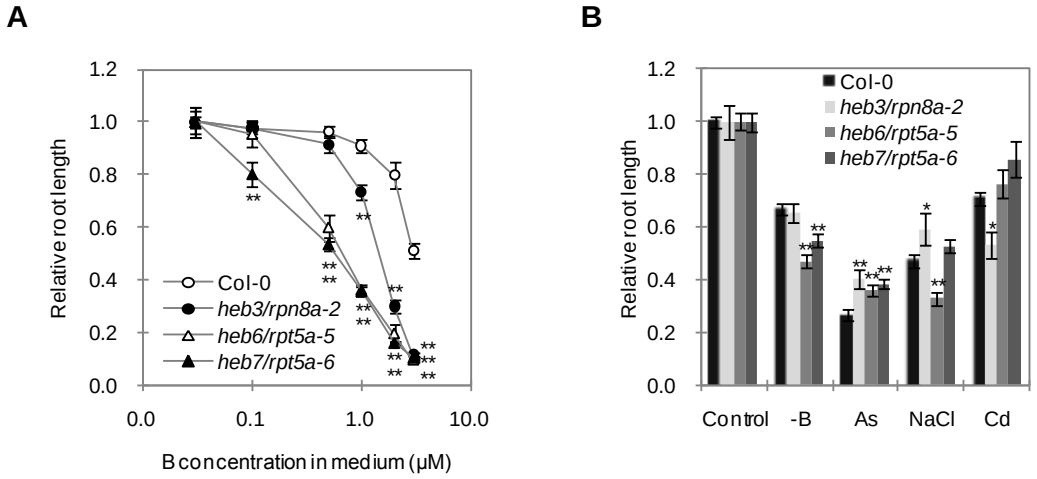

Figure 2-2 Hypersensitivity and specificity of *rpn8a* and *rpt5a* mutants to excess B.
(A) Dose-dependent (0.03, 0.1, 0.5, 1, 2 and 3 mM) effects of B on root growth of Col-0, *rpn8a-2*, *rpt5a-5* and *rpt5a-6*. The primary root length of 14d-seedlings were measured. Data was expressed as a ratio relative to the value in 0.03mM B condition. Means ± standard error are shown (n > 19). (B) Sensitivity of Col-0, *rpn8a-2*, *rpt5a-5* and *rpt5a-6* to mineral stresses; low B (0.03 μM B), arsenite (7.5 μM As) salinity (75 mM NaCl) and cadmium (100 μM Cd). The primary root length of 14d-seedlings was measured. Data was expressed as a ratio relative to the value in control condition. Means ± standard error are shown (n > 12). Asterisks represent significant difference between Col-0 and each *heb* mutant (*, $P < 0.05$ and **, $P < 0.01$ by Student's *t*-test).

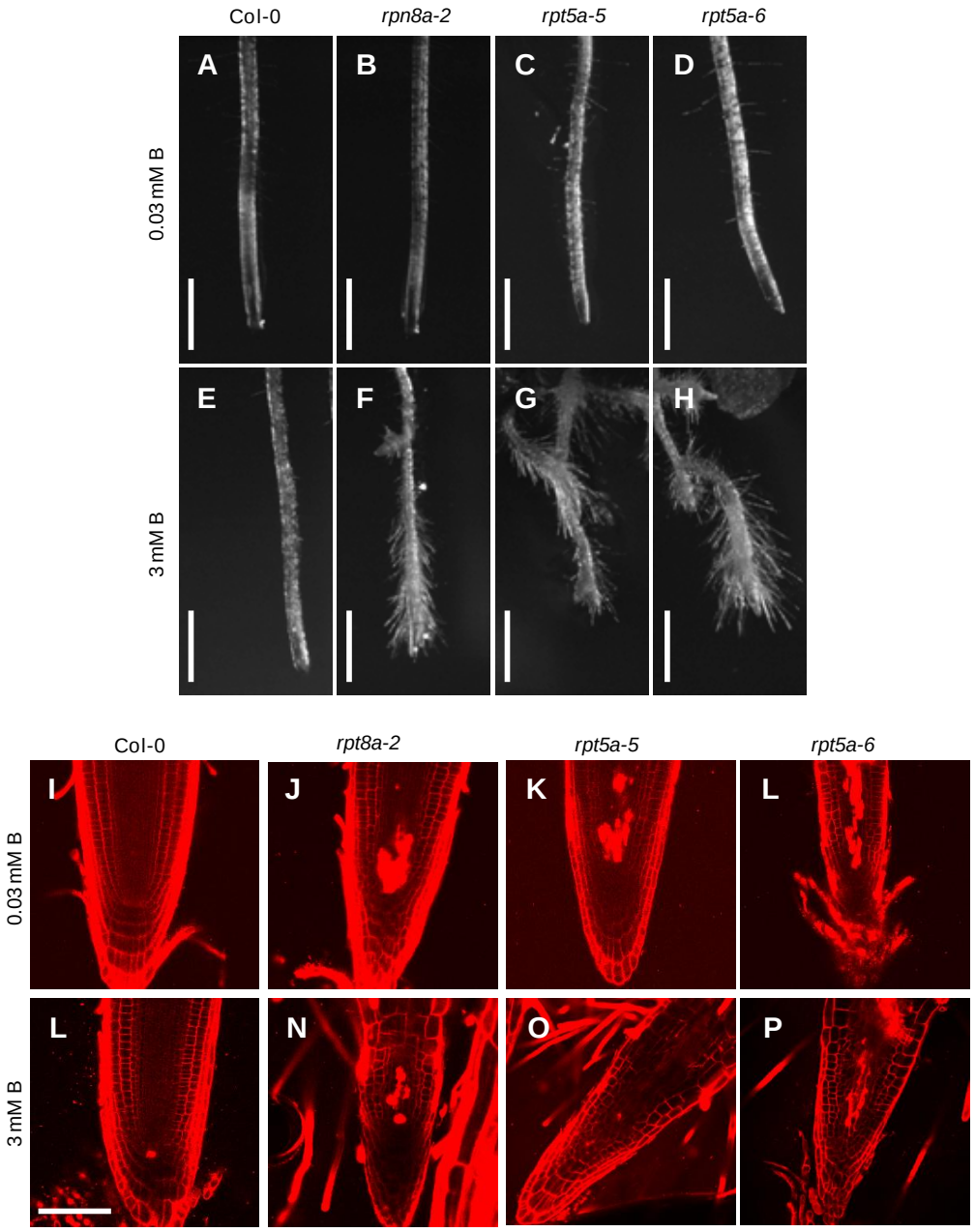

Figure 2-3 Effect of excess B on root morphology of *rpn8a* and *rpt5a* mutants.
(A) to (H) Primary roots of Col-0 [(A) and (E)], *rpn8a-2* [(B) and (F)], *rpt5a-5* [(C) and (G)] and *rpt5a-6* [(D) and (H)] grown under 0.03 mM B [(A) to (D)] and 3 mM B [(E) to (H)] conditions for 14d. Bars=1mm. (I) to (P) Longitudinal sections of root tips of Col-0 [(I) and (L)])], *rpn8a-2* [(J) and (N)], *rpt5a-5* [(K) and (O)] and *rpt5a-6* [(L) and (P)] grown under 0.03 mM B [(I) to (L)] and 3 mM B [(L) to (P)] conditions for 14d. Propidium iodide was used for the visualization of cell walls. Entirely-stained cells are dead cells. Bars, 50µm.

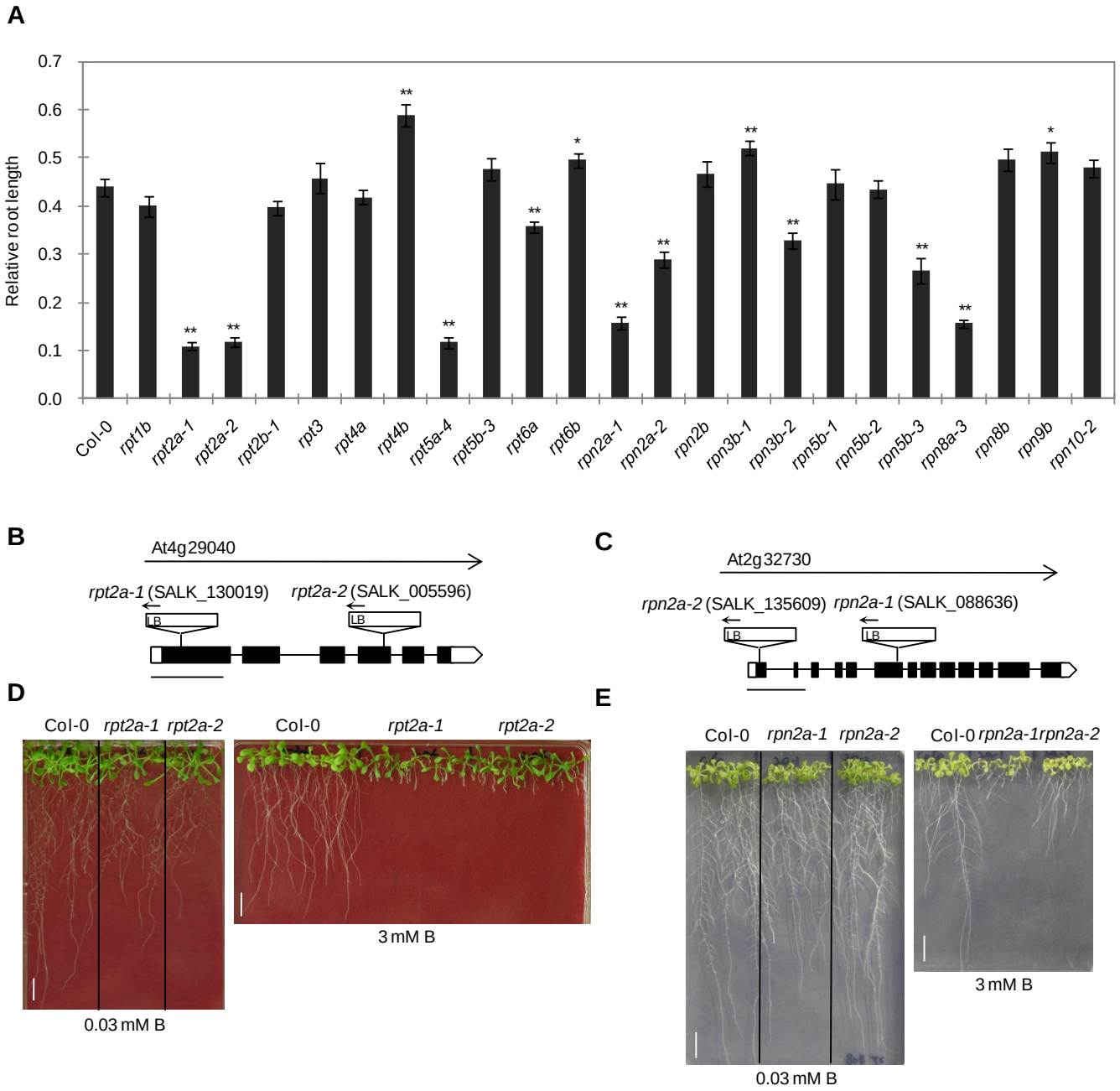

Figure 2-4 Elucidation of the involvements of other subunits of 19S regulatory particle in excess B-tolerance.

(A) Effects of excess B (3 mM) on the root growth of various mutants of 19S regulatory particle subunits. The primary root length of 14d-seedlins were measured. Data was expressed as a ratio relative to the value in 0.03 mM B condition. Means ± standard error are shown (n > 8). Asterisks represent significant difference between Col-0 and each mutant (**, $P < 0.01$ by Student's *t*-test). (B) and (C) Genomic structure of *RPT2a* and *RPTN2a* and location of T-DNA insertions. Open and closed boxes indicate UTR and coding sequences, respectively. Bars, 500 bp. (D) and (E) Excess B-dependent short-root phenotype of alleles for *rpt2a* (D) and *rpn2a* (E) mutants. Col-0 and the mutants were grown under 0.03 mM (left) and 3 mM B conditions (right) for 10d. Bars, 1cm.

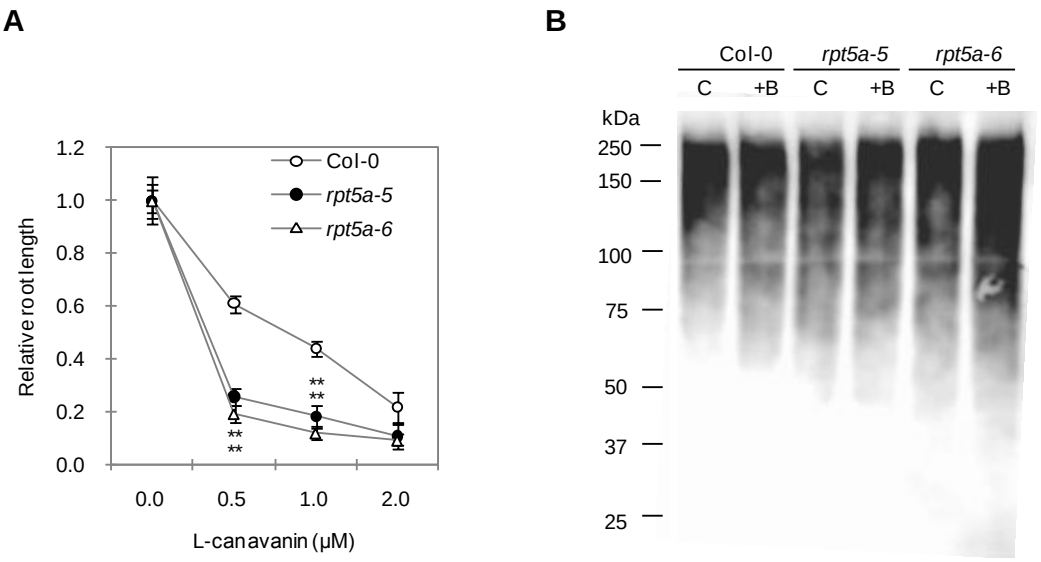

Figure 2-5 Elucidation of activity of poly-ubiquitin dependent proteolysis in *rpt5a* mutants.
(A) Effects of amino acid analogue L-canavanin (CAN) on root growth. After 5d-incubation at normal MGRL medium, plants were transferred to media containing various concentrations of CAN. The length of newly elongated roots during additional 4d-inucubation were measured. Data was expressed as a ratio relative to the value in control condition. Means ± standard error is shown (n > 6). Asterisks represent significant difference between Col-0 and each *rpt5a* mutant (**, $P < 0.01$ by Student's *t*-test). (B) Effect of excess B (3 mM) on accumulation profile of poly-ubiquitinated proteins. Equal amounts of total protein extracts were separated on SDS-PAGE, transferred to a membrane and probed with FK1. Molecular weights (kDa) of the protein standards are shown on the left side of the photograph.

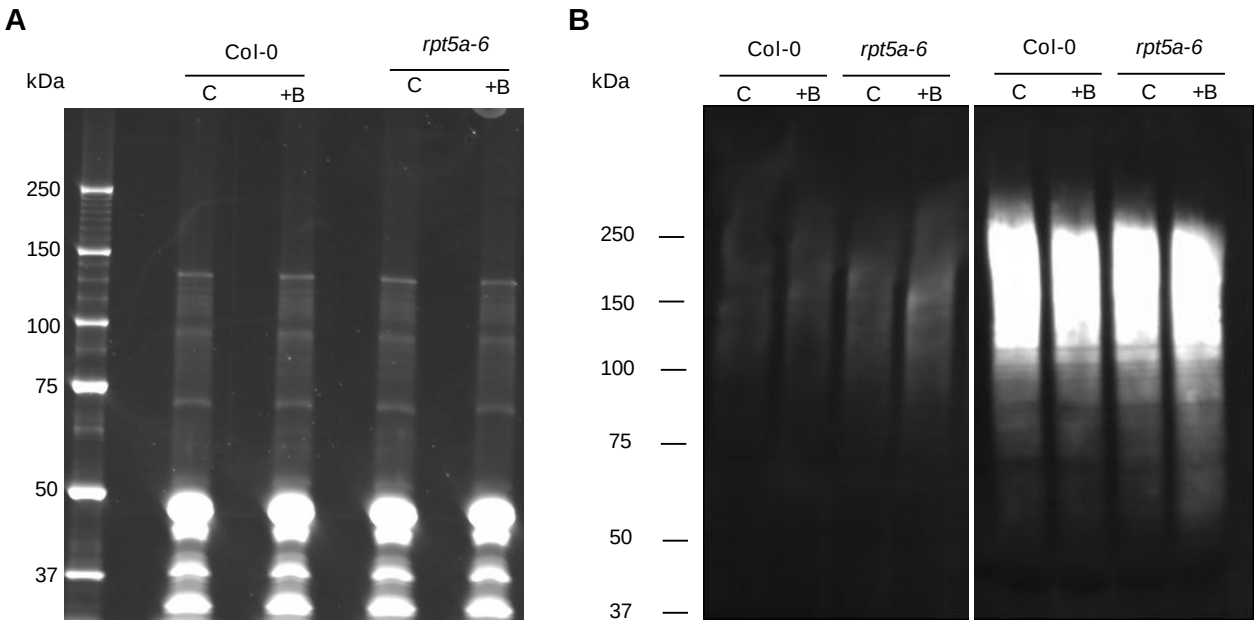

Figure 2-6 Purification and enrichment of poly-ubiquitinated proteins.
(A) Immunopurified proteins (15 µg) with GST-hHR23B-UBA domain fused resin from seedlings of Col-0 and *rpt5a-6* were subjected to SDS-PAGE and stained with Flamingo™. (B) Detection of poly-Ub from 20 µg of crude extracts (left) and 6 µg of immunopurified proteins with FK1 (right).

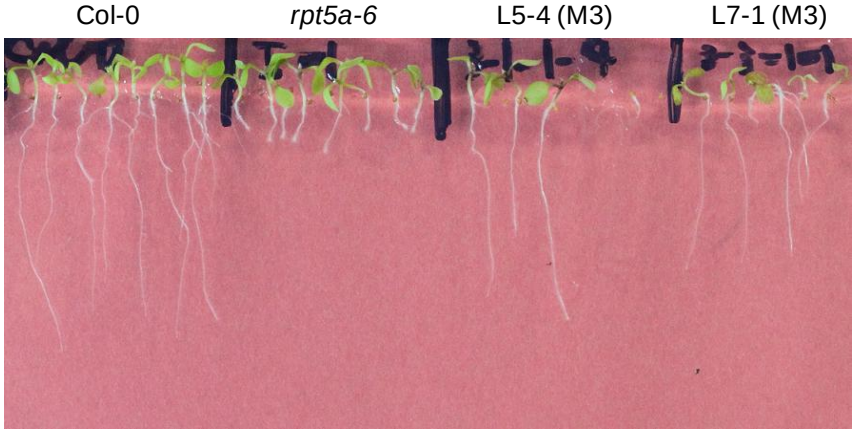

Figure 2-7 Candidates of revertant of *rpt5a-6* showing moderate root growth under the excess B condition.
The phenotypes of isolated two revertants of *rtp5a-6* grown on medium containing 3 mM B for 10d.

Table 2-1 List of 19S prteasome subunits and mutatns used in the present thesis

Subunit		AGI code	Mutant name
RPTs	*RPT1a*	At1g53750	
	RPT1b	At1g53780	SALK_106176 (*rpt1b*)
	RPT2a	At4g29040	SALK_130019 (*rpt2a-1*)
			SALK_005596 (*rpt2a-2*)
	RPT2b	At2g20140	SALK_043450 (*rpt2b-1*)
	RPT3	At5g58290	SALK019265 (*rpt3)*
	RPT4a	At5g43010	SALK_052732 (*rpt4a*)
	RPT4b	At1g45000	SALK_101982 (*rpt4b*)
	RPT5a	At3g05530	SALK_046321 (*rpn5a-4*)
			heb6/*rpt5a-5*
			heb7/*rpt5a-6*
	RPT5b	At1g09100	SAIL_293_H08 (*rpt5b-3*)
	RPT6a	At5g19990	SAIL_443_F04 (*rpt6a*)
	RPT6b	At5g20000	GABI_483G04 (*rpt6b*)
RPNs	*RPN1a*	At2g20580	
	RPN1b	At4g28470	
	RPN2a	At1g08140	SALK_088636 (*rpn2a-1*)
			SALK_135609 (*rpn2a-2*)
	RPN2b	At2g32730	SALK_024347 (*rpn2b*)
	RPN3a	At1g20200	
	RPN3b	At1g75990	SALK_117415 (*rpn3b-1*)
			SALK_088176 (*rpn3b-2*)
	RPN5a	At5g09900	
	RPN5b	At5g64760	SALK_134671 (*rpn5b-1*)
			SALK_133892 (*rpn5b-2*)
			SALK_127791 (*rpn5b-3*)
	RPN6	At1g29150	
	RPN7	At4g24820	
	RPN8a	At5g05780	*heb3*/*rpn8a-2*
			SALK_151595 (*rpn8a-3)*
	RPN8b	At3g11270	SALK_009871 (*rpn8b*)
	RPN9a	At5g45620	SALK_043310 (*rpn9b*)
	RPN9b	At4g19006	
	RPN10	At4g38630	SALK_009616 (*rpn10-2*)
	RPN11	At5g23540	
	RPN12a	At1g64520	
	RPN12b	At5g42040	SALK_057729 (*rpn12b*)

Table 2-2 List of poly-ubiquitinated proteins identified and relatively quantified

No.	Motifs			Score	AGI code	Description	Relative accumulation			
							Col-0		*rpt5a-6*	
	PEST	KEN-Box	D-Box				control	+B	control	+B
1	+	-	+	232	At2g30870	ATGSTF10 (EARLY DEHYDRATION-INDUCED 13); glutathione transferase	1.00	6.49	1.76	99.5
2	+	-	-	220	At2g30860	ATGSTF9 (Arabidopsis thaliana Glutathione S-transferase (class phi) 9); glutathione transferase	1.00	6.32	2.91	78.7
3	+	-	-	192	At5g02500	HSC70-1 (heat shock cognate 70 kDa protein 1); ATP binding	1.00	7.91	4.00	22.0
4	+	-	+	149	At3g09260	PYK10 (phosphate starvation-response 3.1); hydrolase, hydrolyzing O-glycosyl compounds	1.00	1.12	1.21	1.96
5	++	-	-	142	At1g31340	RUB1 (Related to ubiquitin 1)	1.00	11.6	7.05	27.9
6	+	-	-	139	At3g09440	Heat shock cognate 70 kDa protein 3 (HSC70-3) (HSP70-3)	1.00	7.92	4.00	21.9
7	+	-	+	124	At1g17190	AtGSTU26 (Arabidopsis thaliana Glutathione S-transferase (class tau) 26); glutathione transferase	1.00	7.13	1.13	14.7
8	+	-	-	116	At1g78380	AtGSTU19 (Glutathione transferase 8); glutathione transferase	1.00	6.63	0.68	33.7
9	+	-	-	100	At2g17360	40S ribosomal protein S4 (RPS4A)	1.00	1.94	1.11	3.74
10	+	-	-	86	At1g16030	HSP70B (heat shock protein 70B); ATP binding	1.00	4.31	2.07	11.01
11	+	-	+	85	At5g61120	Zinc ion binding	1.00	15.5	8.35	35.4
12	+	-	-	80	At1g78370	AtGSTU20 (Arabidopsis thaliana Glutathione S-transferase (class tau) 20); glutathione transferase	1.00	3.48	0.43	23.1
13	+	-	++	64	At1g02650	DNAJ heat shock N-terminal domain-containing protein	1.00	5.91	3.53	12.38
14	+	-	-	63	At1g17180	AtGSTU25 (Arabidopsis thaliana Glutathione S-transferase (class tau) 25); glutathione transferase	1.00	9.93	3.36	81.9
15	+	-	-	56	At1g78320	AtGSTU23 (Arabidopsis thaliana Glutathione S-transferase (class tau) 23); glutathione transferase	1.00	9.75	1.11	46.5
16	+	-	-	52	At1g17170	AtGSTU24 (Arabidopsis thaliana Glutathione S-transferase (class tau) 24); glutathione transferase	1.00	15.0	3.64	70.3
17	+	-	+	37	At1g26360	hydrolase, alpha/beta fold family protein	1.00	7.38	3.91	17.1
18	-	-	++	34	At4g02520	ATGSTF2 (Arabidopsis thaliana Glutathione S-transferase (class phi) 2); glutathione transferase	1.00	21.3	3.59	46.0
19	+	+	-	32	At2g12550	Ubiquitin-associated (UBA)/TS-N domain-containing protein	1.00	12.4	8.55	27.1
20	+	-	++	32	At2g26560	PLP2 (Phospholipase A 2A); nutrient reservoir	1.00	25.2	8.26	15.2
21	+	-	+	30	At4g10680	Transcription factor IIB (TFIIB) family protein	1.00	26.8	1.19	58.6
22	+	-	-	29	At3g04640	Glycine-rich protein	1.00	1.74	0.92	6.77
23	++	+	++	29	At5g58440	Phox (PX) domain-containing protein	1.00	3.91	2.32	6.63
24	+	-	-	27	At4g19710	AK-HSDH/AK-HSDH II	1.00	4.21	2.33	6.09
25	+	-	+	26	At1g52370	Ribosomal protein L22 family protein	1.00	6.63	5.08	8.46
26	+++	-	+	26	At4g16340	SPK1 (SPIKE1); GTP binding / GTPase binding / binding / guanyl-nucleotide exchange factor	1.00	147	62.7	367
27	+++	-	+	26	At4g21330	DYT1 (DYSFUNCTIONAL TAPETUM 1); DNA binding / transcription factor	1.00	4.77	2.23	7.57
28	++	-	-	24	At1g77810	Galactosyltransferase family protein	1.00	4.20	2.36	6.92
29	+	-	++	22	At5g17230	PSY (Phytoene synthase); geranylgeranyl-diphosphate geranylgeranyltransferase	1.00	4.43	2.89	8.18
30	-	-	-	22	At5g63660	LCR74/PDF2.5 (Low-molecular-weight cysteine-rich 74)	1.00	5.25	2.97	10.5

For PEST motif; +, at least one poor PEST motif, ++, one potential PEST motif, +++, more than two potential PEST motifs. For KEN-Box and D-Box; +, one potential region, ++, more than two potential regions.

Chapter 3 *Arabidopsis thaliana* 26S proteasome subunits RPT2a and RPT5a are crucial for Zinc deficiency-tolerance

3.1 Abstract

RPTs (Regulatory Particle triple-A-ATPase) are components of 26S proteasome. I found novel roles of RPT2a and RPT5a in Zn deficiency-tolerance. *Arabidopsis thaliana* mutants carrying T-DNA in *RPT2a* and *RPT5a* were more sensitive to Zn deficiency than the wild-type. In the *rpt* mutants, shoot Zn contents were similar to that of the wild-type. Transcripts of Zn deficiency-inducible genes were highly accumulated in the *rpt* mutants, suggesting the possibility that the *rpt* mutants are suffering from various Zn deficiency symptoms although Zn levels are not reduced. Lipid peroxidation levels, known to be increased under Zn deficiency, were higher in the *rpt* mutants than in the wild-type. Poly-ubiquitinated proteins were accumulated upon exposure to Zn deficiency, especially in the *rpt* mutants. Overall, the present thesis established that RPT2a and RPT5a are involved in Zn deficiency response, possibly through alleviation of oxidative stresses and/or processing of poly-ubiquitinated proteins.

3.2 Introduction

26S proteasome (26SP) is composed of 20S proteasome (20SP) and 19S regulatory particle (RP). RP is a complex of thirteen RP non-ATPase (RPN) subunits and six RP triple-A-ATPase (RPT) subunits. 26SP regulates various cellular processes by catalyzing poly-ubiquitin (Ub) dependent proteolysis as described in chapter 2.

As well as poly-ubiquitinated proteins, oxidized proteins are known to be substrates for 20SP without Ub-dependent targeting pathway (Shringapure et al., 2003). It is shown that under carbon starvation, activity of 20SP is elevated together with accumulation of oxidatively damaged proteins (Basset et al., 2002). Several kinds of other nutrient starvations are known to induce oxidative stress (Cakmak and Marschner 1993; Kosiba et al., 2009; Yu and Rengel 1999). Under these conditions, it is likely that protein oxidation is accelerated. Recently, Kurepa et al (2008) reported that the mutation in *RPT2a*, *RPN10* and *RPN12a* caused repression of total Ub-dependent proteolytic activity but increase in Ub-independent 20SP activity. This suggests that the importance of RP subunits in maintaining of Ub-independent 20SP activity in response to nutrient starvations.

In chapter 2, through characterization of the *heb* mutants, I first established that 26SP with specific subsets of RP subunits is required for excess boron (B) tolerance in *A. thaliana*. Moreover, the potential proteins processed through specific subunit in response to excess B were listed. It is conceivable that 26SP with same of different subsets of RP

subunits is involved in various nutritional responses in a way as in the case of B toxicity-tolerance.

To find novel functions of RP subunits in nutritional responses, I first searched profiles of nutrient and trace elements in the shoots of *A. thaliana* RPT mutants on Purdue ionomics information managing system (http://www.ionomicshub.org/home/PiiMS). In this database, the mutants of RPT2a and RPT5a showed higher accumulations of zinc (Zn) and lower accumulations of B compared to the wild-type, whereas those accumulations in the mutants of RPT2b and RPT5b were similar with the wild-type. This suggests that among 26SP subunits, at least RPT2a and RPT5a are involved in Zn homeostasis in shoots.

In this chapter 3, I focused on functions of RPT2a and RPT5a in Zn deficiency-tolerance in *A. thaliana*. Zn deficiency is known to induce oxidative stress (Cakmak and Marschner 1993; Cakmak et al., 1993; Pinton et al., 1994; Wang et al., 2005), suggesting the possibility that RPT2a and RPT5a are involved in the response to oxidative stress. Here, the possible roles of RPT2a and RPT5a in Zn deficiency-tolerance through both Ub-independent and Ub-dependent proteolysis are characterized.

3.3 Materials and Methods

3.3.1 Plant materials and growth conditions

All the *A. thaliana* (ecotype Col-0) mutants used in the present thesis were obtained from the ABRC and they carry T-DNA in corresponding genes. The mutants used in the thesis are *rpt2a-2* (SALK_005596), *rpt2b-1* (SALK_043450), *rpt5a-4* (SALK_046321) (Alonso et al., 2003) and *rpt5b-3* (SAIL_293_H08) (Sessions et al., 2002). Lines carrying T-DNA in homozygote were established and presence of T-DNA was determined by PCR listed in Table I.

In all experiments, seeds were sown on solid medium containing MGRL solution (Fujiwara et al., 1992), 1% (w/v) sucrose (BioUltra, Sigma-Aldrich, USA) and 1% (w/v) agar (Agar Purified, Nakarai Tesuque, Japan). For the adjustment of Zn concentration in the medium, $ZnSO_4$ was used. In the case of Zn-deficient condition, $ZnSO_4$ was not supplemented to the medium. After 3d incubation at 4°C, the plates were placed vertically in the growth chamber (16-h light/8-h dark cycle, 22°C) for 14d.

3.3.2 Measurement of metal contents in plant tissues

Whole shoots (20-50 mg F.W.) were harvested and dried at 60°C for 2d and then weighed. The samples were digested with concentrated nitric acid (13 M, Wako, Japan) at 130°C. The residue was resolved in the 0.1 M nitric acid solution containing 2 $\mu g l^{-1}$ indium (In). Manganese (^{55}Mn), iron (^{57}Fe), copper (^{63}Cu) and ^{66}Zn contents were measured by

inductively coupled plasma-mass spectrometry (SPQ-9700, Seiko Instrument Inc., Chiba, Japan) using In as an internal standard.

3.3.3 Gene expression analyses

Total RNA was extracted using RNeasy plant mini kit (Qiagen, USA). RNase-free DNase set (Qiagen) was used to remove the contaminated DNA. Total RNA (500 ng) was used for the cDNA synthesis using RrimeScript RT reagent kit (Takara, Japan) and was subjected to gene expression analyses. *Actin8* mRNA was used as loading reference for semi-quantitative RT-PCR. Transcript levels of *RPT2a*, *RPT2b*, *RPT5a*, *RPT5b* and *Actin8* were determined by PCR with optimum cycles for each gene by corresponding primer sets listed in Table I.

Quantitative real time RT-PCR was performed with SYBER premix ex*Taq*® II (Takara) on a Thermal Cycler Dice® Real Time System (Takara). The Ct values were calculated by second derivative maximum method and the calculation of relative transcript levels were based on a standard curve generated with serial dilutions of cDNA solution. The primer sets for *ZIP4*, *ZIP9*, *CSD1*, *CSD2*, *CCS* were listed in Table I. *Actin8* were used for the normalization.

3.3.4 Evaluation of levels of oxidative effects in plant tissue

Lipid peroxidation levels in shoots were determined as the contents of 2-thiobarbituric acid reactive substances (TBA-rs) as described previously (Uraguchi et al., 2009). Typically, 50 mg shoots in fresh weight was subjected to the analysis. Oxidized protein levels were evaluated using carbonyl assay as described previously (Romero-Puertas et al., 2002).

3.3.5 Analysis of proteasome activity

20SP extraction and its activity assay were conducted as described previously (Kurepa et al., 2008). Concentrations of extracted proteins were determined using quick start protein assay (BioRad, USA) and equal amounts of protein were subjected to the analysis of 20SP activity. Chymotrypsin-like (CT-L) peptidase activity was determined using fluorogenic peptide and fluorescence was measured using a fluorometer (Infinite® M1000, Tecan Trading AG, Switzerland).

For the evaluation of accumulation profile of poly-ubiquitinated proteins, proteins were extracted using phosphate-buffered saline with protease inhibitor cocktail complete (Roche, Switzerland) and 1 mM phenylmethylsulfonyl fluoride (Wako, Japan). The extract was centrifuged at 8000 g for 15 min at 4°C. After the determination of protein concentrations of the supernatants with Pierce® 660nm protein assay reagent (Thermo

Scientific, USA), equal amounts of extracted proteins were separated by SDS-PAGE and transferred onto polyvinylidene fluoride membranes. Poly-ubiquitinated proteins were detected with anti-poly-Ub chain antibody (FK1, Nippon Biotest Labo, Japan) and visualized with enhanced chemiluminescence (GE Healthcare, UK).

3.4 Results

3.4.1 Sensitivity of 26S proteasome mutants, *rpt2a-2* and *rpt5a-4*, to Zn deficiency

For each T-DNA insertion lines, *rpt2a-2* and *rpt5a-4*, I established homozygotes for the T-DNA insertion and used for subsequent studies (Figure 3-1 A). In the shoots of these mutants, the transcripts of corresponding genes were below the detection limit in my semi-quantitative RT-PCR (Figure 3-1 B). Both *rpt2a-2* and *rpt5a-4* mutants showed similar shoot growth as Col-0 under the control condition (1 μM Zn), whereas under the Zn-deficient condition (without Zn supplement), the shoot growth of these mutants were severely inhibited and were approximately 50% of that of Col-0 (Figure 3-1 C and D). Leaves turned purple in both *rpt2a-2* and *rpt5a-4* only under Zn-deficient condition, whereas leaves of wild-type plants stayed green under Zn-deficient condition (Figure 3-1 C).

I also examined possible roles of paralogues of *RPT2a* and *RPT5a* in Zn response. Both *PRT2b* and *RPT5b* are paralogous genes having more than 90% of similarity at the amino acid sequence level to *RPT2a* and *RPT5a* (data not shown). A T-DNA inserted mutant of *RPT2b* and *RPT5b*, *rpt2b-1* and *rpt5b-3*, were established. In the shoots of these mutants, the transcripts of corresponding genes were not detected (Appendix Figure 3-1 A and B). In contrast to the case of *RPT2a* and *RPT5a*, there is no significant difference in the shoot growth between Col-0 and T-DNA inserted mutants, *rpt2b-1* and *rpt5b-3,* both under the control and Zn-deficient conditions (Figure 3-1 C and D). No obvious difference was observed in leaf colors, either. These results suggest that both RPT2a and RPT5a are required for Zn deficiency-tolerance but their paralogues are not.

3.4.2 Response of *RPT2a* and *RPT5a* genes to Zn deficiency

To investigate whether expression of *RPT2a* and *RPT5a* genes responds to Zn deficiency, transcript accumulation of these genes were analyzed by semi-quantitative RT-PCR. My semi-quantitative RT-PCR revealed that accumulations of both *RPT2a* and *RPT5a* transcripts were higher under the Zn-deficient condition than the control conditions (Figure 3-1 B). On the other hand, the transcript accumulations of both *RPT2b* and *RPT5b* were similar among distinct Zn conditions (Figure 3-1 B). Interestingly, *RPT2a* expression in *rpt5a-4* and *RPT5a* expression in *rpt2a-2* were drastically induced under the Zn-deficient condition compared to those in Col-0, but not *RPT2b* and *RPT5b* (Figure 3-1 B). These

results suggest that expression of *RPT2a* and *RPT5a* genes is induced by Zn deficiency and that transcripts accumulation of *RPT2a* and *RPT5a* influence to each other.

3.4.3 Measurement of metal concentrations in *rpt2a-2* and *rpt5a-4* under the Zn-deficient condition

To investigate whether the Zn deficiency-sensitive phenotypes of *rpt2a-2* and *rpt5a-4* are associated with reduced accumulation of Zn, contents of several metals in shoots of Col-0 and the *rpt* mutants were determined (Figure 3-2). When the plants were grown under the control condition, there was no significant difference in Zn contents between Col-0 and the *rpt* mutants (Figure 3-2 A). Shoot Zn contents were also similar among Col-0 and the *rpt* mutants under the Zn-deficient condition (Figure 3-2 A). No significant difference in Fe contents between Col-0 and the *rpt* mutants were detected irrespective of Zn conditions (Figure 3-2 B). Cu contents in the *rpt* mutants were approximately 75% of that in Col-0 under the control condition but were not different from Col-0 under the Zn-deficient condition (Figure 3-2 C). On the other hand, Mn contents under the Zn-deficient condition were lower in the *rpt* mutants than in Col-0 (Figure 3-2 D). It was also found that Zn deficiency enhanced Mn accumulation in Col-0 and *rpt2a-2* but not in *rpt5a-4* (Figure 3-2 D). Mn contents in the *rpt* mutants were approximately 60% of that in Col-0 under the control condition (Figure 3-2 D). Taken together, these results suggest that RPT2a and RPT5a are involved in the regulation of Mn accumulation but not in Zn accumulation in shoots in response to Zn deficiency.

3.4.4 Expression patterns of Zn deficiency-responsive genes in *rpt2a-2* and *rpt5a-4* under the Zn-deficient condition

To investigate whether the transcriptional response to Zn deficiency in the Zn deficiency-sensitive *rpt* mutants is altered, I next analyzed the expression patterns of Zn transporters and super oxide dismutase (SOD)-related genes in *rpt2a-2* and *rpt5a-4* under the Zn-deficient condition. Accumulation of transcripts of *ZIP4* and *ZIP9*, Zn transporter genes, are elevated in response to Zn deficiency (Wintz et al., 2003). The accumulations of both *ZIP4* and *ZIP9* transcripts were higher in the *rpt* mutants than in Col-0 under the Zn-deficient condition. The differences of both *ZIP4* and *ZIP9* transcripts accumulations between Col-0 and the *rpt* mutants were less evident under the control condition (Figure 3-3 A). The expressions of *CSD1*, *CSD2* and *CCS* genes are known to be reduced in response to Zn deficiency (Wintz et al., 2003). These genes encode proteins for SOD synthesis and assembly. The expression of *CCS*, *CSD1* and *CSD2* genes was lower in the Zn-deficient condition than that in the control condition both in Col-0 and the *rpt* mutants

(Figure 3-3 B). There was no clear difference in expression of *CCS*, *CSD1* and *CSD2* between Col-0 and the *rpt* mutants. These studies established that a part of expression of Zn-responsive genes is affected in the *rpt* mutants.

3.4.5 Evaluation of oxidative stress in *rpt2a-2* and *rpt5a-4a* under the Zn-deficient condition

It has been suggested that oxidative damage to critical cell components caused by reactive oxygen species (ROS) is the basis of plant growth inhibition under Zn-deficient condition (Cakmak 2000). I speculated that the Zn deficiency-sensitive *rpt* mutants may suffer strongly from oxidative stress under the Zn-deficient condition. To investigate this possibility, I determined lipid peroxidation levels and accumulation of oxidized proteins in Zn-deficient shoots (Figure 3-4 A). Lipid peroxidation levels were evaluated by measuring TBA-rs contents. Under the control condition, TBA-rs levels were similar between Col-0 and *rpt2a-2*, whereas in *rpt5a-4,* TBA-rs level was reduced by 25% compared to Col-0 (Figure 3-4 A). Zn deficiency increased accumulation of TBA-rs both in Col-0 and the *rpt* mutants and TBA-rs increments under the Zn deficient condition were higher in the *rpt* mutants (Figure 3-4 A). These results suggest that lipid peroxidation caused by ROS occurs more in the *rpt* mutants under the Zn-deficient condition than in the wild-type plants.

ROS generation and lipid peroxidation cause oxidized protein generation Romero-Puertas et al., 2002). I next evaluated the accumulation of oxidized proteins by measuring carbonyl groups. Considering the elevated lipid peroxidation levels under the Zn deficient condition, it is expected that Zn deficiency also enhances the generation of oxidized proteins especially in the Zn deficiency-sensitive *rpt* mutants. However, unexpectedly, the carbonyl groups contents in Col-0 were reduced by Zn deficiency (Figure 3-4 B). In the *rpt* mutants, no significant reduction in carbonyl groups contents by the Zn deficiency treatment was observed. The carbonyl groups contents were not different between Col-0 and the *rpt* mutants irrespective of Zn conditions, either (Figure 3-4 B). This suggests that the shoot growth phenotype of the *rpt* mutants under the Zn-deficient condition is not caused through increase in oxidized protein accumulation.

3.4.6 Evaluation of 26S proteasome activities in *rpt2a-2* and *rpt5a-4* under the Zn-deficient condition

As another characterization of the mutant phenotype, I determined activity of 20SP. It is known that oxidative stress increases 20SP activities (Basset et al., 2002). To investigate whether the Zn condition affects 20SP activity, I determined CT-L peptidase activity. As expected, CT-L activities in shoots were higher under the Zn-deficient condition than those

under the control condition both in Col-0 and the *rpt* mutants (Figure 3-5 A). The *rpt* mutants exhibited higher CT-L activities than Col-0 irrespective of Zn conditions (Figure 3-5 A). These results suggest that Ub-independent 20SP activity responds to Zn deficiency-stress and that mutations in *RPT2a* and *RPT5a* promote this response. Ub-independent proteolysis by 20SP is known to be one of the degradation pathways of oxidized proteins (Shringapure et al., 2003; Kurepa et al., 2008) and this may explain the fact that accumulation of oxidized proteins was not increased as a result of Zn deficiency (Figure 3-2 B).

To further investigate the effects of Zn deficiency on the Ub-dependent proteolysis through 26SP, I compared profiles of Ub conjugated proteins among Col-0, *rpt2a-2* and *rpt5a-4*. Western analysis indicated that poly-ubiquitinated proteins were highly accumulated by Zn deficiency treatment in the shoots of both Col-0 and the *rpt* mutants, and more poly-ubiquitinated proteins were accumulated in the *rpt* mutants compared with Col-0 under the Zn-deficient condition (Figure 3-5 B). This suggests that Ub-dependent 26SP activity is inhibited under the Zn-deficient condition, especially in the *rpt* mutants.

3.5 Discussion

In this chapter 3, I found that 26SP subunits, RPT2a and RPT5a are involved in Zn deficiency-tolerance in *A. thaliana* (Figure 3-1 B and C). To my knowledge, this is the first report on the function of specific subunits of RP in Zn homeostasis in plants.

In *A. thaliana*, both similar and unique functions among RPT paralogues have been reported (Gallois et al., 2009; Kurepa et al., 2009; Sonoda et al., 2009). I found that the T-DNA insertion mutants of *RPT2b* and *RPT5b* were not Zn deficiency-sensitive (Figure 3-1 D). These results suggest that as to Zn deficiency-tolerance, RPT2a and RPT5a act differently from each corresponding paralogues RPT2b and RPT5b, respectively. Based on the hypothesis that plants assemble multiple 26SP forms with different composition of subunits (Small et al., 2004), it is possible that 26SPs containing RPT2a and/or RPT5a function in Zn deficiency-tolerance.

It is easy to speculate that Zn deficiency-sensitive *rpt* mutants are defective in Zn transport or its regulation which result in lower Zn accumulation in shoots and subsequent suppression of shoot growth. My results demonstrated that Zn contents both under the control and the Z-deficient conditions were not different between the wild-type plants and the *rpt* mutants (Figure 3-2 A). This suggests that change in Zn accumulation is not a cause of the phenotype and that RPT2a and RPT5a are not likely to be involved in Zn transport to shoots. I should note that the misregulation of cellular Zn distribution in the *rpt* mutants remains to be a possibility.

The Zn deficiency-responsible Zn transporter genes *ZIP4* and *ZIP9* (Wintz et al., 2003) were highly expressed in the *rpt* mutants compared to the wild-type, especially under the Zn-deficient condition (Figure 3-3 A). It is possible that higher expression of *ZIP4* and *ZIP9* genes might respond to Zn concentrations in a certain compartment in the cell and that both RPT2a and RPT5a are involved in regulation of Zn concentrations in the compartment, but not the overall concentration of Zn. On the other hand, the *rpt* mutants showed reduced Cu and Mn contents in the control condition (Figure 3-2 C and D), suggesting that RPT2a and RPT5a are associated to the regulation of Cu and Mn transport to shoots. Considering the Mn increment by Zn deficiency in the wild-type, Mn regulation might affect the tolerance to Zn deficiency in plants.

It has been considered that the breakdown of defense systems against oxidative stress is the early effects of Zn deficiency (Sharma et al., 2004). I found that Zn-deficiency reduced expression of Cu/Zn-SOD genes (Figure 3-3 B) and elevated lipid peroxidation levels in shoots both in the wild-type plants and the *rpt* mutants (Figure 3-4 A). It is important to note that the increments of lipid peroxidation by Zn deficiency treatment were much higher in *rpt2a-2* and *rpt5a-4* than that in wild-type (Figure 3-4 A). ROS causes lipid peroxidation and SODs can eliminate ROS. It is possible that RPT2a and RPT5a function in anti-oxidative stress by suppressing ROS production under the Zn-deficient condition.

ROS also causes protein oxidation. Accumulation of oxidized proteins was not increased by Zn deficiency both in the wild-type plants and the *rpt* mutants (Figure 3-4 B). Oxidized proteins are known to be a substrate for Ub-independent 20SP proteolysis (Basset et al., 2002; Shringarpure et al., 2003, Kurepa et al., 2008). In the present thesis, 20SP activity was elevated under the Zn-deficient condition both in the wild-type plants and in the *rpt* mutants and the increase in the activity was more evident in the *rpt* mutant (Figure 3-5 A). It is possible that highly activated 20SP reduces contents of oxidized proteins to normal levels under the Zn-deficient condition. If this is the case, this indicates that the high 20SP activity in the *rpt* mutants may reflect high ROS production in these mutants under the Zn-deficient condition.

It has been demonstrated that Ub-independent 20SP activity increases when Ub-dependent 26SP activity is inhibited (Kurepa et al., 2008). The profiles of poly-Ub conjugated proteins in the total soluble extracts indicated that Ub-dependent 26SP activity is inhibited by Zn deficiency, especially in the *rpt* mutants (Figure 3-5 B). It has been known that up-regulation of 26SP subunit genes reflects the decrease in Ub-dependent 26SP activity in plants (Kurepa et al., 2008). Zn deficiency induced expression of both *RPT2a* and *RPT5a* genes, and the extents of induction of these genes were much higher in *rpt2a-2* and *rpt5a-4* (Figure 3-1 B), supporting my hypothesis.

The fact that Ub-dependent 26SP activity is inhibited by Zn deficiency indicates the possible existence of specific unknown substrates degraded through Ub-dependent proteolytic pathway in response to Zn deficiency. In animal cells, RPT2 is known to be glycosylated in response to glucose starvation resulting in the decrease in Ub-dependent 26SP activities to several substrates (Yang et al., 2002). It is therefore tempting to speculate that the unknown substrates specifically processed through RPT2a and RPT5a associated to Zn deficiency-tolerance.

The present study gives rise to the possibility of multiple functions of 26SP in a variety of stress tolerance. In my results, transcripts of *RPT2a* and *RPT5a* were Zn-deficiency responsive, but their paralogues *RPT2b* and *RPT5b* were not (Figure 3-1 B). Thus, it is possible that the induction of a certain subunit gene by a certain stress indicates its involvement in the stress tolerance. The published transcriptome data using *A. thaliana* (Kilian et al., 2007) showed that transcripts of six *RPTs* were both similarly and distinctively induced by various types of stresses such as cold, osmotic, salinity, genotoxic and heat shock stresses. It is suggested that including RPT2a and RPT5a, the respective subunits of RP have common and unique function in a variety of stresses in addition to Zn-deficiency.

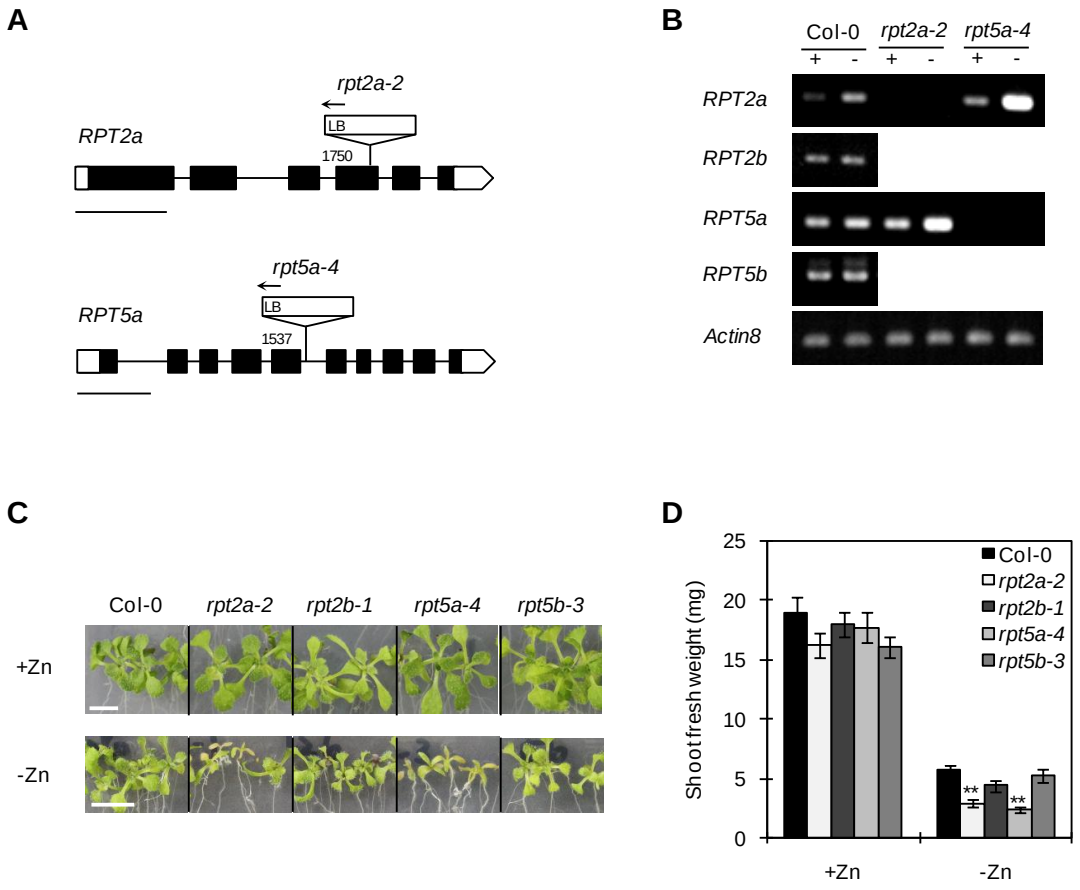

Figure 3-1 Characterization of *rpt2a-2* and *rpt5a-4* mutants and their sensitivity to Zn deficiency.
(A) Genomic structure of *RPT2a* and *RPT5a* and location of T-DNA insertions. Open and closed boxes indicate untranslated regions and coding sequences, respectively. Position of T-DNA insertion in the *rpt* mutants were represented by the relative nucleotide positions of left border (LB) from the first base of the coding sequence. Bars, 500 bp. (B) Accumulation of *RPT2a* and *RPT5a* transcript under Zn deficiency. RNA was extracted from shoots of 14d-old-seedlings grown on medium with or without Zn supply. Transcripts were detected by semi-quantitative RT-PCR. *RPT2a* (22 cycles), *RPT2b* (23 cycles), *RPT5a* (22 cycles), *RPT5b* (30 cycles) and *Actin8* (28 cycles) were PCR amplified from cDNA. Gels were stained with ethidium bromide. (C) Photographs of Col-0 and the *rpt* mutants grown on medium with or without Zn for 14d. Bars,5 mm. (D) Effect of Zn deficiency on shoot fresh weights of Col-0 and the *rpt* mutants. Fresh weights of plants grown as described in C were measured. Values are shown by mean ± standard error of mean. n ≥ 15. Asterisks represent significant difference ($P < 0.01$) between Col-0 and each *rpt* mutants by Student's *t*-test.

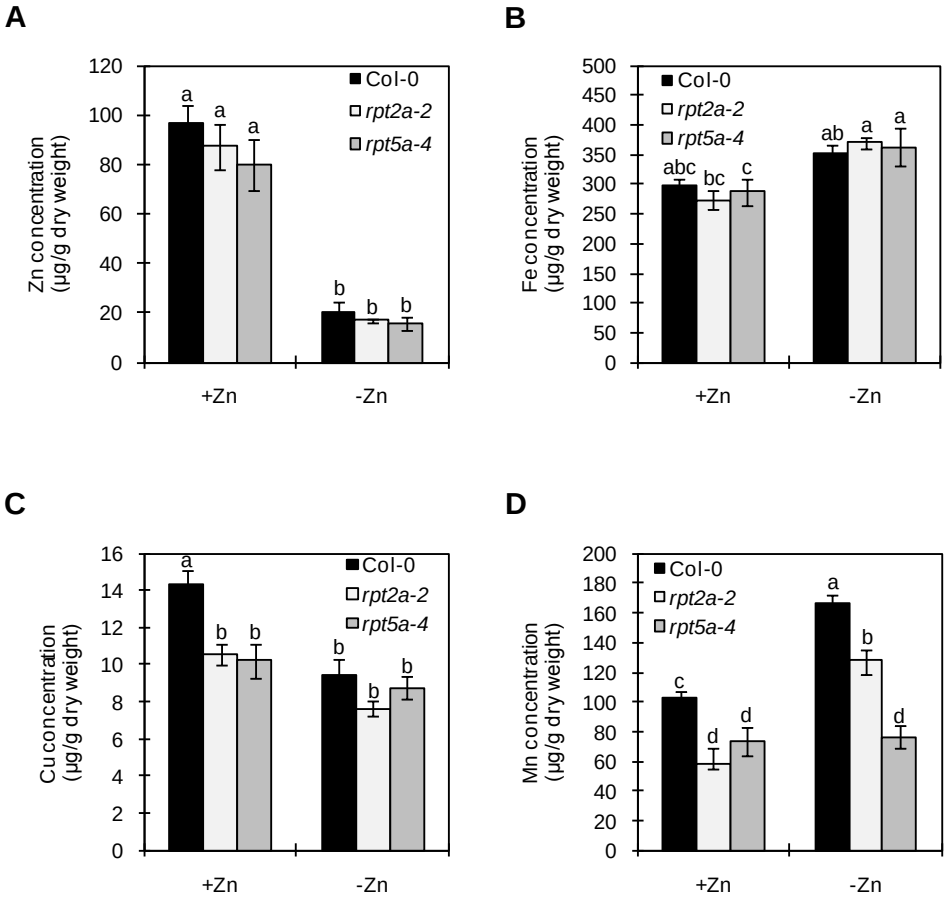

Figure 3-2 Metal concentrations in *rpt2a-2* and *rpt5a-4* under the Zn-deficient condition.

Zn (A), Fe (B), Cu (C) and Mn(D) concentrations in the shoots of Col-0, *rpt2a-2* and *rpt5a-4.* Plants were grown on medium with or without Zn were determined by ICP-MS. Values are shown by mean ± standard error of mean. n ≥ 5. Means sharing same letter within columns for each species are not significantly different at 5% level of probability according to Turkey's multiple range test.

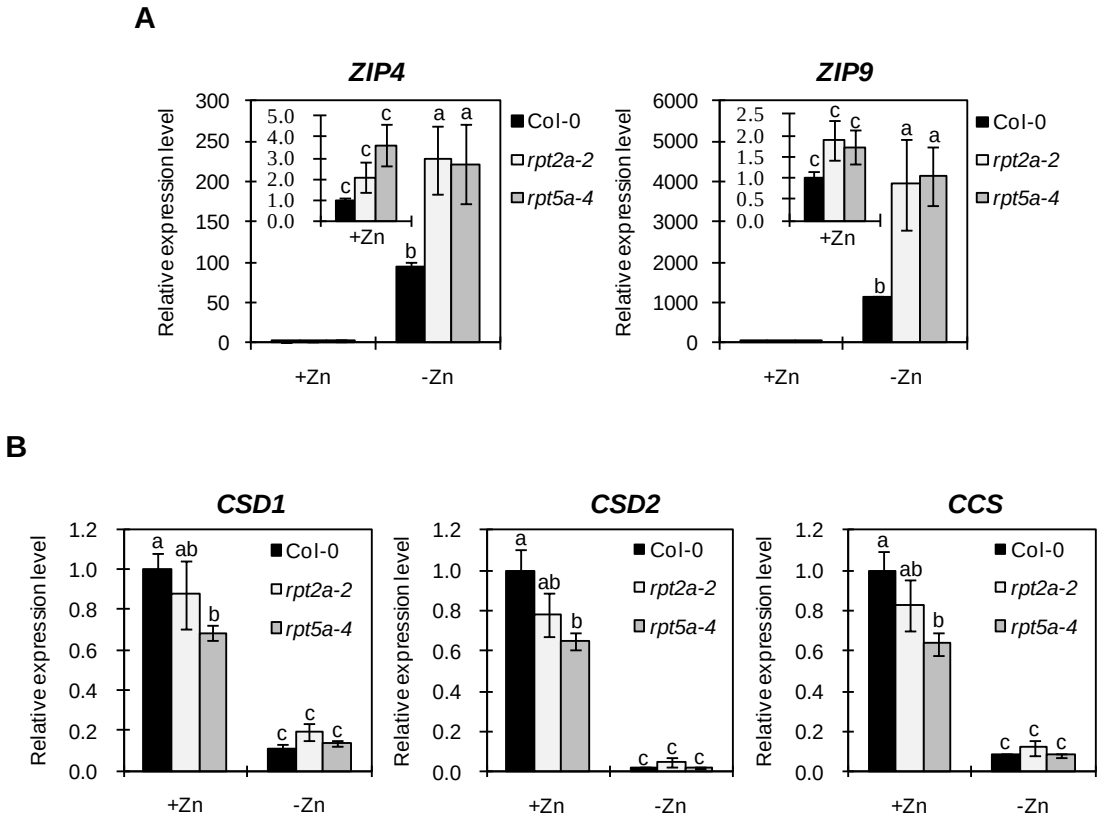

Figure 3-3 Response of Zn transporters and SOD-related genes in *rpt2a-2* and *rpt5a-4* under the Zn-deficient condition.

cDNA were synthesized using the shoots of 14d-old-seedlings of Col-0, *rpt2a-2* and *rpt5a-4* grown on medium with or without Zn. Quantitative real time RT-PCR were performed. Transcriptional responses of Zn transporter, *ZIP4* and *ZIP9* (A), Cu/Zn-SOD (*CSD1* and *CSD2*), copper chaperon (*CCS*) (B) in the shoots of Col-0, *rpt2a-2* and *rpt5a-4*. Genes expressions were normalized with *Actin8* expression. Values are shown by mean ± standard error of mean. n = 3. Means sharing the same letter within columns for each species are not significantly different at 5% level of probability according to Turkey's multiple range test.

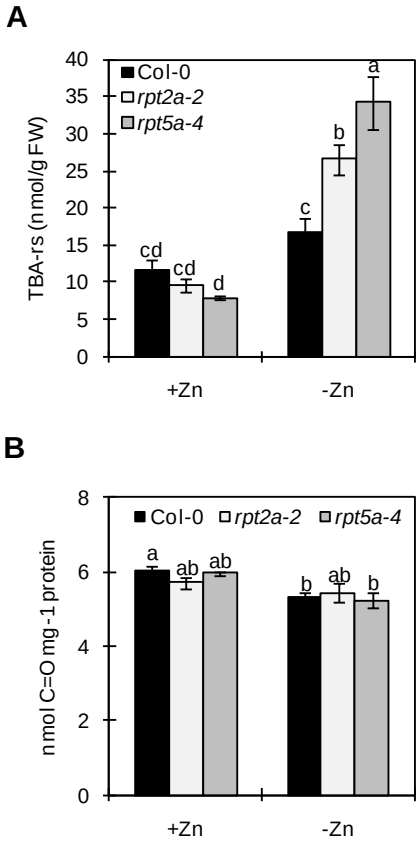

Figure 3-4 Oxidative stress levels in *rpt2a-2* and *rpt5a-4* under the Zn-deficient condition..

The oxidative stress levels in the shoots of 14d-old-seedlings of Col-0, *rpt2a-2* and *rpt5a-4* grown on medium with or without Zn were evaluated. (A) Effects of Zn deficiency on lipid peroxidation levels in the shoots of Col-0, *rpt2a-2* and *rpt5a-4*. TBA-rs concentration as an index of the levels of lipid peroxidation was determined. (B) Effects of Zn deficiency on the accumulation of oxidized proteins in the shoots of Col-0, *rpt2a-2* and *rpt5a-4*. The production of carbonyl groups in the molecule was used as an index of oxidative damage to proteins. Values are shown by mean ± standard error of mean. n > 3. Means sharing the same letter within columns for each species are not significantly different at 5% level of probability according to Turkey's multiple range test.

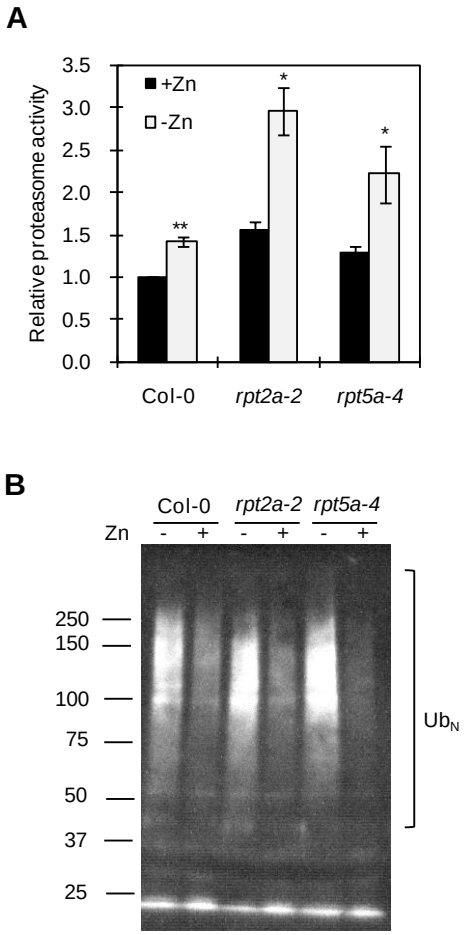

Figure 3-5 20S proteasome activities and protein ubiqutination in r*pt2a-2* and *rpt5a-4* under the Zn-deficient condition.

Total protein fraction were purified from the shoots of 14d-old-seedlings of Col-0, *rpt2a-2* and *rpt5a-4* grown on medium with or without Zn. (A) Effect of Zn deficiency on 20S proteasome activity. Values are normalized to the Col-0 level under Zn sufficient condition and shown by mean ± standard error of mean. n = 3. Means sharing same letter within columns for each species are not significantly different at 5% level of probability according to Turkey's multiple range test. (B) Effect of Zn deficiency on accumulation profile of poly-ubiquitinated proteins. Equal amounts of total protein extracts were separated on SDS–PAGE, transferred to a membrane and probed with anti-poly-Ub antibody. Ub_N, poly-ubiquitinated proteins. Molecular weights (kDa) of the protein standards are shown on the left side of the photograph.

CONCLUSION

In the present thesis, through identification of the responsible genes of four *heb* mutants, I first established that two protein complexes, condensin II and 26S proteasome (26SP), have essential functions in B toxicity-tolerance in plants.

Through characterization of condensin II in B toxicity-tolerance, novel function of this complex in DNA damage response was established. Moreover, it was also established that excess B causes DNA double strand breaks. Taken together, I established an aspect of molecular mechanisms of B toxicity-tolerance: Condensin II is required for mitigating the DNA damage derived from B toxicity as well as other genotoxins such as UV-C (Chapter 1).

Characterization of several subunits of 19S proteasome (RP) and proteome analysis in excess B strongly suggested two possibilities: (1) plants can assemble specific 26SP array in response to B toxicity, and (2) substrates of 26SP that are specifically processed through respective RP subunits are present. Based on these, I proposed that generation of abnormal proteins and/or alteration of protein metabolism is an aspect of B toxicity (Chapter 2). I also found that subunits specific function in Zn deficiency-tolerance (Chapter 3). In conclusion, these findings suggested that 26SP regulates a variety of nutritional responses through the specific subsets of RP subunits.

Most interestingly, condensin II is conserved among animals and 26SP is highly conserved among living organisms. Considering the fact that excess B is toxic to living organisms, the basis of B toxicity mechanism may be common. Therefore, my thesis is expected to be use of investigation of molecular mechanisms of B toxicity in other organisms.

REFERENCES

Alonso, J.M., et al. (2003). Genome-wide insertional mutagenesis of *Arabidopsis thaliana*. *Science* **301:** 653–657.

Aono, N., Sutani, T., Tomonaga, T., Mochida, S. and Yanagida, M. (2002). Cnd2 has dual roles in mitotic condensation and interphase. *Nature* **417:** 197–202.

Basset, G., Raymond, P., Malek, L. and Brouquisse, R. (2002). Changes in the expression and enzymic properties of the 20S proteasome in sugar-starved maize roots. Evidence for an in vivo oxidation of the proteasome. *Plant Physiol.* **128:** 1149–1162.

Birnbaum, K., Jung, J.W., Wang, J.Y., Lambert, G.M., Hirst, J.A., Galbraith, D.W. and Benfey, P.N. (2005). Cell type-specific expression profiling in plants via cell sorting of protoplasts from fluorescent reporter lines. *Nat. Methods* **2:** 615–619.

Blevins, D.G. and Lukaszewski, K.M. (1998). Boron in plant structure and function. *Annu. Rev. Plant Physiol. Plant Mol. Boil.* **49:** 481–500.

Book, A.J., Smalle J., Lee K.H., Yang P., Walker J.M., Casper S., Holmes J.H., Russo L.A., Buzzinotti Z.W., Jenik P.D. and Vierstra R.D. (2009) The RPN5 subunit of the 26S proteasome is essential for gametogenesis, sporophyte development, and complex assembly in Arabidopsis. *Plant Cell* **21:** 460–478.

Book, A.J., Gladman, N.P., Lee, S,S., Scalf, M., Smith, L.M. and Vierstra, R.D. (2010). Affinity purification of the Arabidopsis 26 S proteasome reveals a diverse array of plant proteolytic complexes. *J. Biol. Chem.* **285:** 25554-25569.

Britt, A.B. (1996). DNA damage and repair in plants. *Annu. Rev. Plant Physiol. Plant Mol. Bio*l. **47:** 75–100.

Brown, P.B., Bellaloui, N., Wimmer, M.A., Bassil, E.S., Ruiz, J., Hu, H., Pfeffer, H., Dannel, F. and Römheld, V. (2000). Boron in plant biology. *Plant Biol*. **4:** 205–223.

Brukhin, V., Gheyselinck, J., Gagliardini, V., Genschik, P. and Grossniklaus, U. (2005). The RPN1 subunit of the 26S proteasome in Arabidopsis is essential for embryogenesis. *Plant Cell* **17:** 2723–2737.

Cabello, O.A., Eliseeva, E., He, W., Youssoufian, H., Plon, S.E., Brinkley, B.R. and Belmont, J.W. (2001). Cell cycle-dependent expression and nucleolar localization of hCAP-H. *Mol. Biol. Cell* **12:** 3527–3537.

Cakmak, I. and Marschner, H. (1993). Effect of zinc nutritional status on activities of superoxide radical and hydrogen peroxide scavenging enzymes in bean. *Plant Soil* **156:** 127–130.

Cakmak, I. and Römheld, V. (1997). Boron deficiency-induced impairments of cellular

functions in plants. *Plant Soil* **156:** 127–130.

Cakmak, I. (2000). Possible roles of zinc in protecting plant cells from damage by reactive oxygen species. *New Phytologist* **146:** 185–205.

Cervilla, L.M., Blasco, B. A., Ríos, J.J., Romero, L. and Ruiz, J.M. (2007). Oxidative stress and antioxidants in tomato (*Solanum lycopersicum*) plants subjected to boron toxicity. *Ann. Bot.* **100:** 747–756.

Cervilla, L.M., Blasco, B. A., Ríos, J.J., Rosales, M.A., Rubio-Wilhelmi, M.M., Sánchez-Rodríguez, E., Romero, L. and Ruiz, J.M. (2009). Response to nitrogen metabolism to boron toxicity in tomato plants. *Plant Biol.* **11:** 671–677.

Chen, E., Sutani, T. and Yanagida, M. (2004). Cti1/C1D interacts with condensin SMC hinge and supports the DNA repair function of condensin. *Proc. Natl. Acad. Sci. USA* **101:** 8078–8083.

Clough, S.J. and Bent, A.F. (1998). Floral dip: A simplified method for Agrobacterium-mediated transformation of Arabidopsis thaliana. *Plant J.* **16:** 735–743.

Cobbe, N., Savvidou, E. and Heck. M.M.S. (2003). Diverse Mitotic and Interphase Functions of Condensins in Drosophila. *Genetics* **172:** 991–1008.

Colls, T. and De Veylder, L. (2009). DNA stress checkpoint control and plant development. *Curr. Opin. Plant Biol.* **12:** 23–28.

Culligan, K., Tissier, A. and Britt, A. (2004). ATR Regulates a G2-Phase Cell-Cycle Checkpoint in *Arabidopsis thaliana*. *Plant Cell* **16:** 1091–1104,

Culligan, K.M., Robertson, C.E., Foreman, J., Doerner, P. and Britt, A.B. (2006). ATR and ATM play both distinct and additive roles in response to ionizing radiation. *Plant J.* **48:** 947–961.

Curtis, M. and Grossniklaus, U. (2003). A Gateway cloning vector set for high-throughput functional analysis of genes in plants. *Plant Physiol*. **133:** 462–469.

Deveaux, Y., Alonso, B., Pierrugues, O., Godon, C. and Kazmaier, M. (2000). Molecular cloning and developmental expression of *AtGR1*, a new growth-related Arabidopsis gene strongly induced by ionizing radiation. *Radiat. Res.* **154:** 355–364.

Dixon, D.P., Lapthorn, A. and Edward, R. (2002). Plant glutathione transferases. *Genome Biol.* **3:** 1–10.

Donnelly, P.M., Bonetta, D., Tsukaya, H., Dengler, R.E. and Dengler, N.G. (1999). Cell cycling and cell enlargement in developing leaves of *Arabidopsis*. *Dev. Biol.* **215:** 407–419.

Doucet-Chabeaud, G., Godon, C., Brutesco, C., de Murcia, G. and Kazmaier, M. (2001).

Ionising radiation induces the expression of PARP-1 and PARP-2 genes in Arabidopsis. *Mol. Genet. Genomics* **265:** 954–963.

Doutriaux, M.P., Couteau, F., Bergounioux, C. and White, C. (1998). Isolation and characterisation of the RAD51 and DMC1 homologs from *Arabidopsis thaliana. Mol. Gen. Genet.* **257:** 283–291.

Fujimoto, S., Yonemura, M., Matsunaga, S., Nakagawa, T., Uchiyama, S. and Fukui, K. (2005). Characterization and dynamic analysis of Arabidopsis condensin subunits, AtCAP-H and AtCAP-H2. *Planta* **222:** 293–300.

Fujiwara, T., Hirai, M.Y., Chino, M., Komeda, Y. and Naito, S. (1992). Effects of sulfur nutrition on expression of the soybean seed storage protein genes in transgenic petunia. *Plant Physiol.* **99:** 263–268.

Fulcher, N. and Sablowski, R. (2009). Hypersensitivity to DNA damage in plant stem cell niches. *Proc. Natl. Acad. Sci. USA* **49:** 20984–20988.

Gallois, J.L., Guyon-Debast, A., Lecureuil, A., Vezon, D., Carpentier, V., Bonhomme, S. and Guerche, P. (2009). The Arabidopsis proteasome RPT5 subunits are essential for gametophyte development and show accession-dependent redundancy. *Plant Cell* **21:** 442–459.

Garcia, V., Bruchet, H., Camescasse, D., Fabienne, G., Bouchez, D. and Tissier, A. (2003). AtATM is essential for meiosis and the somatic response to DNA damage in plants. *Plant Cell* **15:** 119–132.

Gunes, A., Soylemezoglu, G., Inal, A., Bagci, E.G., Coban, S. and Sahin, O. (2006). Antioxidant and stomatal responses of grapevine (*Vitis vinifera* L.) to boron toxicity. *Scientia Hortic*. **110:** 279–284.

Han, S., Tang, N., Jiang, H.X., Yang, L.T., Li, Y. and Chen. L.S. (2009). CO_2 assimilation, photosystem II photochemistry, carbohydrate metabolism and antioxidant system of citrus leaves in response to boron stress. *Plant Sci*. **176:** 143–153.

Hassan, M., Oldach, K., Baumann, U., Langridge, P. and Sutton, T. (2010). Genes mapping to boron tolerance QTL in barley identified by suppression subtractive hybridization. *Plant, Cell and Environ.* **33:** 188–198.

Hayes, J.E. and Reid, R.J. (2004). Boron tolerance in barley is mediated by efflux of B from the roots. *Plant Physiol.* **136:** 3376–3382.

Heale, J.T., Ball, Jr, A.R., Schmiesing, J.A., Kim, J.S., Kong, X., Zhou, S., Hudson, D.F., Earnshaw, W.C. and Yokomori, K. (2006). Condensin I interacts with the PARP-1–XRCC1 complex and functions in DNA single-strand break repair. *Mol. Cell* **21:** 837–848.

Hemerly, A., de Almeida Engler, J., Bergounioux, C., Van Montagu, M., Engler, G., Inzé,

D. and Ferriera, P. (1995). Dominant negative mutants of Cdc2 kinase uncouple cell division from iterative plant development. *EMBO J.* **14:** 3925–3936

Himanen, K., Boucheron, E. and Vanneste, S. (2002). Auxin-mediated cell cycle activation during early lateral root initiation. *Plant Cell* **14:** 2339–2351.

Hirano, T. (2005). Condensins: Organizing and Segregating the Genome. *Curr. Biol.* **15:** 265–275.

Hirota, T., Gerlich, D., Koch, B., Ellenberg, J. and Peters, J.M. (2004). Distinct functions of condensin I and II in mitotic chromosome assembly. *J. Cell Sci.* **117:** 6435–6445.

Ide, S., Miyazaki, T., Maki, H. and Kobayashi, T. (2010). Abundance of ribosomal RNA gene copies maintains genome integrity. *Science* **327:** 693–696.

Inagaki, S., Suzuki, T., Ohto, M.A., Urawa, H., Horiuchi, T., Nakamura, K. and Morikami, A. (2006). *Arabidopsis* TEBICHI, with helicase and DNA polymerase domains, is required for regulated cell division and differentiation in meristems. *Plant Cell* **18:** 879–892.

Jefferies, S., Pallotta, M., Paull, J.G., Karakousis, A., Kretschmer, J., Manning, S., Islam, A., Langridge, P. and Chalmers, K. (2000). Mapping and validation of chromosome regions conferring boron toxicity tolerance in wheat (*Triticum aestivum*). *Theor. Appl. Genet.* **101,** 767–777.

Kasajima, I. and Fujiwara, T. (2007). Identification of novel *Arabidopsis thaliana* genes which are induced by high levels of boron. *Plant Biotech*. **24:** 355–360.

Kilian, J., Whitehead, D., Horak, J., Wanke, D., Weinl, S., Batistic, O., D'Angelo, C., Bornberg-Bauer, E., Kudla, J. and Harter, K. (2007). The AtGenExpress global stress expression data set: protocols, evaluation and model data analysis of UV-B light, drought and cold stress responses. *Plant J.* **50:** 347–363.

King, R.W., Glotzer, M. and Kirschner, M.W. (1996). Mutagenic analysis of the destruction signal of mitotic cyclins and structural characterization of ubiquitinated intermediates. *Mol. Biol. Cell* **7:** 1343–1357.

Kobayashi, M., Matoh, T. and Azuma, J. (1996). Two chains of rhamnogalacturonan II are cross-linked by borate-diol ester bonds in higher plant cell walls. *Plant Physiol*. **110:** 1017–1020.

Konuk, M., Lıman, R. and Cığercı, İ.H. (2007). Determination of genotoxic effect of boron on *Allum cepa* root meristematic cells. *Pak. J. Bot*. **39:** 73–79.

Koshiba, T., Kobayashi, M. and Matoh, T. (2009). Boron nutrition of tobacco BY-2 cells. V. Oxidative damage is the major cause of cell death induced by boron deprivation. *Plant Cell Physiol.* **50:** 26–36.

Kozak, J., West, C.E., White, C., da Costa-Nunes, J.A. and Angelis, K.J. (2009). Rapid

repair of DNA double strand breaks in *Arabidopsis thaliana* is dependent on proteins involved in chromosome structure maintenance. *DNA Repair* **8:** 413–419.

Kurepa, J., Toh, E.A. and Smalle, J.A. (2008). 26S proteasome regulatory particle mutants have increased oxidative stress tolerance. *Plant J*. **53:** 102–114.

Kurepa, J., Wang, S. Li, Y., Zaitlin, D., Pierce, A.J. and Smalle, J.A. (2009). Loss of 26S proteasome function leads to increased cell size and decreased cell number in Arabidopsis shoot organs. *Plant Physiol*. **150:** 178–189.

Lafarge, S. and Montane, M.H. (2003). Characterization of *Arabidopsis thaliana* ortholog of the human breast cancer susceptibility gene 1: *AtBRCA1*, strongly induced by gamma rays. *Nucleic Acids Res*. **31:**1148–1155.

Liu, D., Jiang, W., Zhang, L. and Li, L. (2000). Effects of boron Ions on root growth and cell division of broadbean (*Vicia faba* L.). *Isr. J. Plant Sci*. **48:** 47–51.

Loomis, W.D. and Durst, R.W. (1992). Chemistry and biology of boron. *BioFactors* **3:** 229–239.

López-Juez, E., Dillon, E., Magyar, Z., Khan, S., Hazeldine, S., de Jager, S.M., Murray, J.A., Beemster, G.T., Bogre, L. and Shanahan, H. (2008). Distinct light-initiated gene expression and cell cycle programs in the shoot apex and cotyledons of Arabidopsis. *Plant Cell* **20:** 947–968.

Lukaszewski, K.M., Blevins, D.G. and Randall, D.D. (1992). Asparagine and boric acid cause allantoate accumulation in soybean leaves by inhibiting manganese-dependent allantoate amidohydrolase. *Plant Physiol.* **99:** 1670–1676.

Mahajan, S., Pandey, G.K. and Tuteja, N. (2008). Calcium- and salt-stress signaling in plants: Shedding light on SOS pathway. *Arch. Biochem. Biophys.* **471:** 146–158.

Matsuoka, S., Ballif, B.A., Smogorzewska, A., McDonald, 3rd, E.R., Hurov, K.E., Luo, J., Bakalarski, C.E., Zhao, Z., Solimini, N., Lerenthal, Y., Shiloh, Y., Gygi, S.P. and Elledge, S.J. (2007). ATM and ATR substrate analysis reveals extensive protein networks responsive to DNA damage. *Science* **316:** 1160–1166.

Menges, M., de Jager, SM., Gruissem, W. and Murray, J.A. (2005). Global analysis of the core cell cycle regulators of Arabidopsis identifies novel genes, reveals multiple and highly specific profiles of expression and provides a coherent model for plant cell cycle control. *Plant J*. **41:** 546–566.

Menke, M., Chen, I., Angelis, K.J. and Schubert, I. (2001). DNA damage and repair in Arabidopsis thaliana as measured by the comet ssay after treatment with different classes of genotoxins. *Mutat. Res.* **493:** 87–93.

Miwa, K., Takano, J., Omori, H., Seki, M., Shinozaki, K. and Fujiwara, T. (2007). Plants tolerant of high boron levels. *Science* **318:** 1417.

Miwa, K. and Fujiwara, T. (2010). Boron transport in plants: co-ordinated regulation of transporters. *Ann. Bot.* **105:** 1073−1080.

Molassiotis, A., Sotiropoulos, T., Tanou, G., Diamantidis, G. and Therios, I. (2006). Boron induced oxidative damage and antioxidant and nucleolytic responses in shoot tips culture of the apple rootstock EM9 (*Malus domestica* Borkh). *Environ*. *Exper. Bot.* **56:** 54–62.

Nable, R.O., Bañuelos, G.S. and Paull, J.G. (1997). Boron toxicity. *Plant Soil.* **193:** 181–198.

Nable, R.O. (1991). Distribution of boron within barley genotypes with differing susceptibilities to boron toxicity. *J. Plant Nutr*. **14:** 453–461.

Nakajima, K., Furutani, I., Tachimoto, H., Matsubara, H. and Hashimoto, T. (2004). SPIRAL1 encodes a plant-specific microtubule-localized protein required for directional control of rapidly expanding Arabidopsis cells. *Plant Cell* **16:** 1178–1190.

Nozawa, A., Miwa, K., Kobayashi, T. and Fujiwara, T. (2006). Isolation of Arabidopsis thaliana cDNAs that confer yeast boric acid tolerance, *Biosci*. *Biotechnol*. *Biochem*. **70:** 1724–1730.

Ochiai, K., Uemura, S., Shimizu, A., Okumoto, Y. and Matoh, M. (2008). Boron toxicity in rice (*Oryza sativa* L.). I. Quantitative trait loci (QTL) analysis of tolerance to boron toxicity. *Theor. Appl. Genet.* **117:** 125−133.

Ohkama-Ohtsu, N., Kasajima, I., Fujiwara, T. and Naito, S. (2004). Isolation and characterization of an Arabidopsis mutant that overaccumulates O-acetyl-L-Ser. *Plant Physiol*. **136:** 3209–3222.

Olive, P.L., Banath, J.P. and Durand, R.E. (1996). Heterogeneity in radiation-induced DNA damage and repair in tumour and normal cells measured using the “comet” assay. *Radiat*. *Res*. **122:** 86–94.

O’Neill, M.A., Warrenfeltz, D., Kates, K., Pellerin, P., Doci, T., Darvill, A.G. and Albersheim, P. (1996). Rhamnogalacturonan-II, a pectic polysaccharide in the walls of growing plant cell, forms a dimer that is covalently cross-linked by a borate ester. *In vitro* conditions for the formation and hydrolysis of the dimer. *J. Biol. Chem.* **271:** 22923–22930.

Ono, T., Losada, A., Hirano, M., Myers, M.P., Neuwald, A.F. and Hirano, T. (2003). Differential contributions of condensin I and condensin II to mitotic chromosome architecture in vertebrate cells. *Cell* **115:** 109–121.

Ono, T., Fang, Y., Spector, D.L. and Hirano, T. (2004). Spatial and temporal regulation of condensins I and II in mitotic chromosome assembly in human cells. *Mol*. *Biol*. *Cell*

15: 3296–3308.

Pang, Y., Li, L., Ren, F., Lu, P., Wei, P., Cai, J., Xin, L., Zhang, J., Chen, J. and Wang, X. (2010). Overexpression of the tonoplast aquaporin AtTIP5;1 conferred tolerance to boron toxicity in *Arabidopsis*. *J. Genet. Genomics* **37:** 389−397.

Paull, J.G., Rathejan, A.J. and Cartwright, B. (1991). Major gene control of tolerance bread wheat (*Triticum aestivum* L.) to high concentrations of soil boron. Euphytica **55:** 217−288.

Pfleger, C.M. and Kirschner, M.W. (2000). The KEN box: an APC recognition signal distinct from the D box targeted by Cdh1. *Genes Dev.* **14:** 655−665.

Pinton, R., Cakmak, I. and Marschner, H. (1994). Zinc deficiency enhanced NAD(P)H-dependent superoxide radical production in plasma membrane vesicles isolated from roots of bean plants. *J*. *Exp*. *Bot*. **45:** 45–50.

Qian, S.B., McDonough, H., Boellmann, F., Cyr, D.M. and Patterson, C. (2006). CHIP-mediated stress recovery by sequential ubiquitination of substrates and Hsp70. *Nature* **440:** 551–555.

Qiu, J.L., Jilk, R., Marks, M.D. and Szymanski, D.B. (2002). The Arabidopsis SPIKE1 gene is required for normal cell shape control and tissue development. *Plant Cell* **14:** 101–118.

Rashid, A. and Ryan, J. (2004). Micronutrient constraints to crop production in soils with Mediterranean-type characteristics: a review. *J. Plant Nutr.* **27:** 959–975.

Reid, R.J., Hayes, J.E., Post, A., Stangoulis, J.C.R. and Graham, R.D. (2004). A critical analysis of the causes of boron toxicity in plants. *Plant Cell Environ*. **25:** 1405–1414.

Reid, R. (2007). Identification of boron transporter genes likely to be responsible for tolerance to boron toxicity in wheat and barley. *Plant Cell Physiol.* **48:** 1673−1678.

Ricaud, L., Proux, C., Renou, J.P., Pichon, O., Fochesato, S., Ortet, P. and Montane, M.H. (2007). ATM-mediated transcriptional and developmental responses to γ-rays in *Arabidopsis*. *PLoS ONE* **2:** e430.

Roessner, U., Patterson, J.H., Forbes, M.G., Fincher, G.B., Langridge, P. and Bacic, A. (2006). An investigation of boron toxicity in barley using metabolomics. *Plant Physiol*. **142:** 1087–1101.

Roldań-Arjona, T. and Ariza, R.R. (2009). Repair and tolerance of oxidative DNA damage in plants. *Mutat. Res*. **681:** 169–179.

Romero-Puertas, M.C., Palma, J.M., Gómez, M., Delrío, L.A. and Sandalio, L.M. (2002). Cadmium causes the oxidative modification of proteins in pea plants. *Plant Cell Environ*. **25:** 677–686.

Rounds, M.A. and Larsen, P.B. (2008). Aluminum-dependent root-growth inhibition in *Arabidopsis* results from AtATR-regulated cell-cycle arrest. *Curr. Biol.* **18:** 1495–1500.

Sakamoto, T., Inui-Tsujimoto, Y. and Fujiwara, T. (2009). Isolation of mutants sensitive to excess boron. *Proc. 16th Internati. Plant Nutri. Colloq. Paper* 1126.

Schnurbusch, T., Hayes, J., Hrmova, M., Baumann, U., Ramesh, S.A., Tyerman, S.D., Langridge, P. and Sutton, T. (2010). Boron toxicity tolerance in barley through reduced expression of the multifunctional aquaporin HvNIP2;1. *Plant Physiol*. **153:** 1706–1715.

Schmiesing, J.A., Gregson, H.C., Zhou, S. and Yokomori, K. (2000). A human condensin complex containing hCAP-C/hCAP-E and CNAP1, a homolog of *Xenopus* XCAP-D2, colocalizes with phosphorylated histone H3 during the early stage of mitotic chromosome condensation. *Mol. Cell Biol*. **20:** 6996–7006.

Schuermann, D., Fritsch, O., Lucht, J.M. and Hohn, B. (2009). Replication Stress Leads to Genome Instabilities in *Arabidopsis* DNA Polymerase δ Mutants. *Plant Cell* **21:** 2700–2714.

Sessions, A., et al. (2002). A high-throughput Arabidopsis reverse genetics system. *Plant Cell* **14:** 2985–2994.

Sedbrook, J.C., Ehrhardt, D.W., Fisher, S.E., Scheible, W.R. and Somerville, C.R. (2004). The Arabidopsis sku6/spiral1 gene encodes a plus end-localized microtubule-interacting protein involved in directional cell expansion. *Plant Cell* **16:** 1506–1520.

Sharma, P.N., Kumar, P. and Tewari, R.K. (2004). Early signs of oxidative stress in wheat plants subjected to zinc deficiency. *J. Plant Nutr*. **27:** 451–463.

Shaul, O., Mironov, V., Burssens, S., Van Montagu, M. and Inzé, D. (1996). Two Arabidopsis cyclin promoters mediate distinctive transcriptional oscillation in synchronized tobacco BY-2 cells. *Proc. Natl. Acad. Sci. USA* **93:** 4868–4872.

Shringarpure, R., Grune, T., Mehlhase, J. and Davies, K.J. (2003). Ubiquitin conjugation is not required for the degradation of oxidized proteins by proteasome. *J. Biol. Chem*. **278:** 311–318.

Siddiqui, N.U., Stronghill, P.E., Dengler, R.E., Hasenkampf, C.A. and Riggs, C.D. (2003). Mutations in *Arabidopsis* condensin genes disrupt embryogenesis, meristem organization and segregation of homologous chromosomes during meiosis. *Development* **130:** 3283–3295.

Smalle, J., Kurepa, J., Yang, P., Babiychuk, E., Kushnir, S., Durski, A. and Vierstra, R.D. (2002). Cytokinin growth responses in *Arabidopsis* involve the 26S proteasome

subunit RPN12a. *Plant Cell* **14:** 17–32.

Smalle, J., Kurepa, J., Yang, P., Emborg, T.J., Babyichuk, E., Kushnir, S. and Vierstra, R.D. (2003). The pleiotropic role of the 26S proteasome subunit RPN10 in *Arabidopsis thaliana* growth and development supports a substrate-specific function in abscisic acid signaling. *Plant Cell* **15:** 965–980.

Smalle, J. and Vierstra, R.D. (2004). The ubiquitin 26S proteasome proteolytic pathway. *Annu*. *Rev*. *Plant Biol*. **55:** 555–590.

Sonoda, Y., Sako, K., Maki, Y., Yamazaki, N., Yamamoto, H., Ikeda, A. and Yamaguchi, J. (2009). Regulation of leaf organ size by the Arabidopsis RPT2a 19S proteasome subunit. *Plant J*. **60:** 68–78.

Sutton, T., Baumann, U., Hayes, J., Collins, N. C., Shi, B.J., Schnurbusch, T., Hay, A., Mayo, G., Pallotta, M., Tester, M. and Langridge, P. (2007). Boron-toxicity tolerance in barley arising from efflux transporter amplification. *Science* **318:** 1446–1449.

Takeda, S., Tadele, Z., Hofmann, I., Probst, A.V., Angelis, K.J., Kaya, H., Araki, T., Mengiste, T., Scheid, O.M., Shibahara, K., Scheel, D. and Paszkowski, J. (2004). *BRU1*, a novel link between responses to DNA damage and epigenetic gene silencing in *Arabidopsis*. *Genes Dev.* **18:** 782–793.

Tanaka. M. and Fujiwara, T. (2008). Phisiological roles and transport mechanisms of boron: perspective from plants. *Pflügers Archiv. Europ. J. Physiol.* **456:** 671–677.

Tsang, C.K., Li, H. and Zheng, X.S. (2007a). Nutrient starvation promotes condensin loading to maintain rDNA stability. *EMBO J.* **26:** 448–458.

Tsang, C.K., Wei, Y. and Zheng, X.F. (2007b). Compacting DNA during the interphase: condensin maintains rDNA integrity. *Cell Cycle* **6:** 2213–2218.

Ueda, M., Matsui, K., Ishiguro, S., Sano, R., Wada, T., Paponov, I., Palme, K. and Okada, K. (2004). The *HALTED ROOT* gene encoding the 26S proteasome subunit RPT2a is essential for the maintenance of *Arabidopsis* meristems. *Development* **131:** 2101–2111.

Uraguchi, S., Kiyono, M., Sakamoto, T., Watanabe, I. and Kuno, K. (2009). Contributions of apoplasmic cadmium accumulation, antioxidative enzymes and induction of phytochelatins in cadmium tolerance of the cadmium-accumulating cultivar of black oat (*Avena strigosa* Schreb.). *Planta*. **230:** 267–276.

Verbruggen, N., Hermans, C. and Schat, H. (2009). Mechanisms to cope with arsenic or cadmium excess in plants. *Curr. Opin. Plant Biol.* **12:** 364–372.

Vierstra, R.D. (2009). The ubiquitin/26S proteasome system at the nexus of plant biology. *Nat*. *Rev*. *Mol*. *Cell Biol*. **10:** 385–397.

Wang, H. and Jin, J.Y. (2005). Photosynthetic rate, chlorophyll fluorescence parameters, and lipid peroxidation of maize leaves as affected by zinc deficiency. *Photosynthetica* **43:** 591–596

Wang, S., Kurepa, J. and Smalle, J.A. (2009). The Arabidopsis 26S proteasome subunit RPN1a is required for optimal plant growth and stress responses. *Plant Cell Physiol.* **50:** 1721–1725.

Warington, K. (1923). The effect of boric acid and borax on the broad bean and certain other plants. *Ann. Bot.* **37:** 629–672.

Wintz, H., Fox, T., Wu, Y.Y., Feng, V., Chen, W., Chang, H. S., Zhu, T. and Vulpe, C. (2003). Expression profiles of Arabidopsis thaliana in mineral deficiencies reveal novel transporters involved in metal homeostasis. *J. Biol. Chem.* **278:** 47644–47653.

Wimmer, M.A., Lochnit, G., Bassil, E., Mühling, K.H. and Goldbach, H.E. (2009). Membrane-associated, boron-interacting proteins isolated by boronate affinity chromatography. *Plant Cell Physiol*. **50:** 1292–1304.

Wood, J.L., Liang, Y., Li, K. and Chen, J. (2008). Microcephalin/MCPH1 associates with the condensin II complex to function in homologous recombination repair. *J. Biol. Chem*. **283:** 29586–29592.

Wu, W., Wang, X., Zhang, W., Reed, W., Samet, J.M., Whang, Y.E. and Ghio, A.J. (2003). Zinc-induced PTEN protein degradation through the proteasome pathway in human airway epithelial cells. *J. Biol. Chem*. **278:** 28258–28263.

Yang, X., Zhang, F. and Kudlow, J.E. (2002). O-GlcNAc modification is an endogenous inhibitor of the proteasome. *Cell* **110:** 69–80.

Yang, P.Z., Fu, H., Walker, J., Papa, C.M., Smalle, J., Ju, Y.M. and Vierstra, R.D. (2004). Purification of the *Arabidopsis* 26S proteasome -Biochemical and molecular analyses revealed the presence of multiple isoforms. *J. Biol. Chem.* **279:** 6401–6413.

Yokota, H., Van Den Engh, G., Mostert, M. and Trask, B.J. (1995). Treatment of cells with alkaline borate buffer extends the capability interphase FISH mapping. *Genomics* **25:** 485–491.

Yoshizumi, T., Tsumoto, Y., Takiguchi, T., Nagata, N., Yamamoto, Y.Y., Kawashima, M., Ichikawa, T., Nakazawa, M., Yamamoto, N. and Matsui, M. (2006). INCREASED LEVEL OF POLYPLOIDY1, a conserved repressor of *CYCLINA2* transcription, controls endoreduplication in *Arabidopsis*. *Plant Cell*. **18:** 2452–2468.

Yu, Q. and Rengel, Z. (1999). Micronutrient deficiency influences plant growth and activities of superoxide dismutases in narrow-leafed Lupins. *Ann. Bot.* **83:** 175–182.

Zhu, Y., Dong, A., Meyer, D., Pichon, O., Renou, J.P., Cao, K. and Shena, W.H. (2006). *Arabidopsis NRP1* and *NRP2* encode histone chaperones and are required for maintaining postembryonic root growth. *Plant Cell.* **18:** 2879–2892.

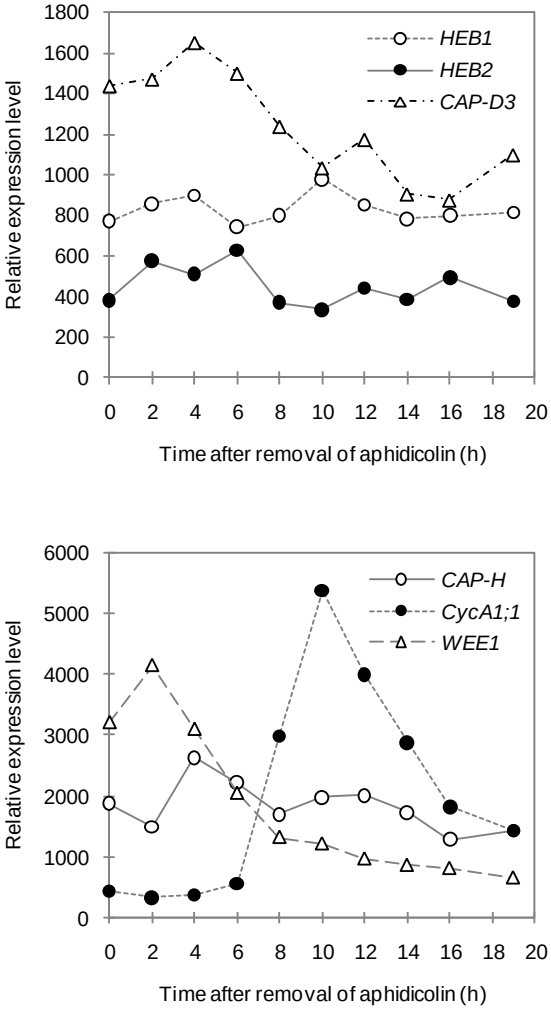

Appendix Figure 1-1 The expression of genes of condensin complex during the mitotic cell cycle.
The microarray data set conducted by Menges et al (2005) using the aphidicolin-synchronized *A. thaliana* cell culture experiments was obtained from database (http://www.arabidopsis.org/info/expression/ATGenExpress.jsp) (AtGenExpress). The expression of *HEB2* does not have an evident peak throughout the mitotic cell cycle, whereas *CAP-D3* and *CAP-H* show a peak at 4h and small peak of *HEB2* at 6h after the removal of aphidicolin. These peaks are between the peak of S phase marker *WEE1* and G2/M marker *CYCA1;1*.

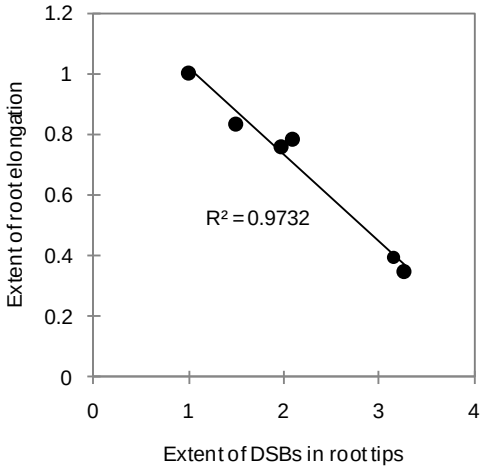

Appendix Figure 1-2 Relationship between DSBs level and root elongation property in *A. thaliana.*
Using the two factors, DSBs level in root tips determined by comet assay and the root elongation in Col-0, *heb1-1* and *heb2-1* grown exposed to the normal and excess B, the impact of DSBs level on root elongation was elucidated. It was revealed that there is a negative correlation between DSBs level and the root elongation property in *A. thaliana*.

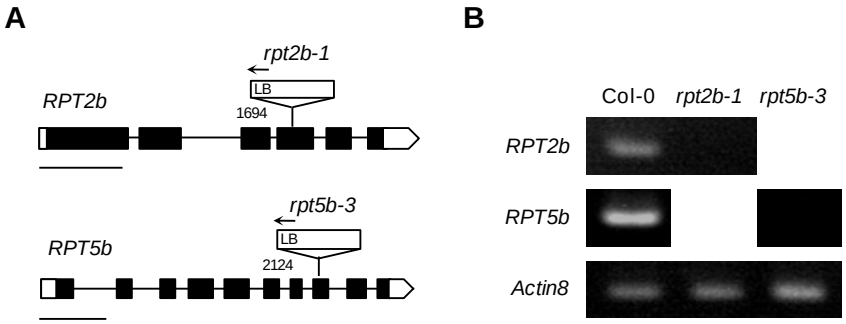

Appendix Figure 3-1 A T-DNA inserted mutant of *RPT2b* and *RPT5b*.
(A) Genomic structure of *RPT2b* and *RPT5b* and location of T-DNA insertions. Open and closed boxes indicate UTRs and coding sequences, respectively. Position of T-DNA insertion in the *rpt* mutants were represented by the relative nucleotide positions of left border (LB) from the first base of the coding sequence. Bars, 500 bp. (B) Expression of *RPT2b* and *RPT5b* in Col-0, *rpt2b-1* and *rpt5b-3*. RNA was extracted from shoots of 14d-old-seedlings grown on medium with or without Zn supply. The transcripts were detected by semi-quantitative RT-PCR. *RPT2b* (23 cycles) and *RPT5b* (30 cycles) and *Actin8* (28 cycles) were PCR amplified from cDNA. Gels were stained with ethidium bromide.

ACKNOWLEDGMENTS

I would like to thank Dr. Anne Britt for providing *atr-2* mutant. I would also thank ABRC for providing SALK and SAIL T-DNA tagged line. I would like to appreciate to Ms. Kaori Sako for establishing T-DNA homozygous lines of RPT mutants.

I would like to thank Dr. Takeshi Yoshizumi for helping the cell polidy analysis, Dr. Yoichiro Fukao and Dr. Masayuki Fujiwara for performing LC-MS/MS analysis, Dr. Mutsumi Yamagami for telling me how to make Zn deficient condition on agar medium, and Dr. Sachihiro Matsunaga, Dr. Masaaki Umeda, Dr. Junji Yamaguchi, and Dr. Kiichi Fukui for technical advice and discussion.

I would like to give my great appreciation to Dr. Toru Fujiwara for guiding and supporting me throughout the research. I would like to give my great thankful to Dr. Yayoi Tsujimoto Inui for guiding me when I started this research and technical assistance. I would like to thank great technical assistance of Ms. Yuko Kawara, Ms, Emi Yokota, and Mao Sugasawa.

I would like to acknowledge all the member of the Toru Fujiwara laboratory for constant encouragement and a variety of supports for this research and my research life.